

**NEDERLANDSE COMMISSIE voor STRALINGSDOSIMETRIE**  
**Netherlands Commission on Radiation Dosimetry**

**PROCEEDINGS of the SYMPOSIUM on**  
**THERMOLUMINESCENCE DOSIMETRY**

Bilthoven, 30th March 1988

Editors:

A.H.L. Aalbers  
A.J.J. Bos  
B.J. Mijnheer

**NCS REPORT 3**  
October 1988

# **PROCEEDINGS of the SYMPOSIUM on THERMOLUMINESCENCE DOSIMETRY**

Organizers:

**NEDERLANDSE VERENIGING voor STRALINGSHYGIENE**  
(Netherlands Society for Radiological Protection)

**NEDERLANDSE VERENIGING voor KLINISCHE FYSICA**  
(Dutch Federation of Clinical Physics)

**KRING STRALINGSFYSICA van de VERENIGING voor BIOFYSICA**  
(Netherlands Group of Radiation Physicists)

all members of the

**NEDERLANDSE COMMISSIE voor STRALINGSDOSIMETRIE**  
(Netherlands Commission on Radiation Dosimetry)

in co-operation with the

**BELGISCHE VERENIGING van ZIEKENHUISFYSICI**  
(Belgian Association of Hospital Physicists)

en

**BELGISCHE VERENIGING voor STRALINGSBESCHERMING**  
(Belgian Association of Radiation Protection)

October 1988

Further copies of this report may be obtained from A.H.L. Aalbers, Secretary, NCS,  
P.O. Box 1, NL 3720 BA, Bilthoven, The Netherlands

### **Programme committee**

|                         |   |
|-------------------------|---|
| A.H.L. Aalbers          | National Institute of Public Health and Environmental Protection, Bilthoven |
| A.J.J. Bos              | Interfaculty Reactor Institute, Delft                                       |
| J. van Dam              | University Hospital St. Raphaël, Leuven                                     |
| H.W. Julius             | Radiological Service TNO, Arnhem  |
| A.S. Keeverling Buisman | Netherlands Energy Research Foundation (ECN), Petten                        |
| B.J. Mijnheer           | The Netherlands Cancer Institute, Amsterdam                                 |
| J. Zoetelief            | Radiobiological Institute TNO, Rijswijk                                     |

### **Organizing committee**

|                |   |
|----------------|---|
| A.H.L. Aalbers | National Institute of Public Health and Environmental Protection, Bilthoven |
| A.J.J. Bos     | Interfaculty Reactor Institute, Delft                                       |
| B.J. Mijnheer  | The Netherlands Cancer Institute, Amsterdam                                 |

### **Local organizing committee**

|                |   |
|----------------|---|
| A.H.L. Aalbers | National Institute of Public Health and Environmental Protection, Bilthoven |
| F.J.M. Bader   |   |
| K. Brolsma     |   |

### **Technical Exhibitors**

Canberra Positronica BV (Harshaw Chemie BV)  
Intechmij BV (Vinten Instruments Ltd)  
Intequip Nuclear BV  
Pechiney World Trade  
Veenstra Instrumenten BV (Alnor Oy)

|                     |  |
|---------------------|--|
| <b>Lay-out</b>      | : J.B. Dielhof, Interfaculty Reactor Institute, Delft  |
| <b>Reproduction</b> | : J.J. Winters and co-workers, National Institute of Public Health and Environmental Protection, Bilthoven |

## CONTENTS

|  |    |
|--|----|
| <b>PREFACE</b> . . . . .   | 1  |
| <b>GENERAL ASPECTS OF TLD</b> . . . . .  | 3  |
| Mechanisms of Thermoluminescence Production in LiF:Mg,Ti (TLD-100) . . . . .<br><i>A.J.J. Bos</i>  | 5  |
| Some Experimental Observations on the Supralinearity of the Response<br>of TLD-100 for Radiotherapeutical Applications . . . . .<br><i>B.J. Mijneer and J. Weeda</i>         | 17 |
| Supralinearity and Dependence on Energy of LiF 700 Powder Response<br>for Photons and Electrons . . . . .<br><i>J.P.A. Marijnissen and B. Göbel</i>                          | 25 |
| Computerized Analysis of Glow Curves from LiF:Mg,Ti (TLD-100) . . . . .<br><i>W. de Vries, J.E. Hoogenboom, J.B. Dielhof and A.J.J. Bos</i>                                  | 31 |
| Carbon Loaded Dosimeters for the Measure of the Shallow Dose<br>Equivalent due to Beta Radiation. . . . .<br><i>H. Preston</i>   | 37 |
| Does the Most Sensitive Thermoluminescent Material come from China?<br>Some Characteristics of LiF:Mg,Cu,P (GR-200) TL chips . . . . .<br><i>A.J.J. Bos and J.D. Dielhof</i> | 43 |
| <b>TLD IN HEALTH PHYSICS</b> . . . . .   | 49 |
| The TNO Individual Monitoring Service based on<br>TLD Concept and Methodology. . . . .<br><i>H.W. Julius, F. Busscher and C.W. Verhoef</i>                                   | 51 |
| The Philips Personnel Dosimetry System . . . . .<br><i>H. Pauw and C.J.H. Wittenberds</i>  | 61 |
| The ECN-Neutron-Beta-Gamma Dosimeter; Theory and Practice . . . . .<br><i>A.S. Keverling Buisman</i>   | 65 |
| Environmental Radiation Monitoring using Thermoluminescence Dosimeters . . . . .<br><i>A.H.L. Aalbers, F.J.M. Bader, A.P.P.A. van Lunenburg and C.R. ter Kuile</i>           | 71 |
| Thermoluminescence Dosimetry at Eindhoven University of Technology . . . . .<br><i>J.T.G.M. Hemelaar, P.J.H. Kicken and Chr. J. Huyskens</i>                                 | 79 |
| Environmental and Calamity TLD-Systems around<br>Dutch Nuclear Power Stations . . . . .<br><i>L.P.M. van Velzen</i>  | 85 |

|  |           |
|--|-----------|
| <b>TLD IN RADIOTHERAPY AND RADIOBIOLOGY . . . . .</b>  | <b>93</b> |
| <br>   |           |
| Experience with in Vivo Thermoluminescent Dosimetry for<br>Total Body Radiation . . . . .  | 95        |
| <i>J. van Dam and A. Rijnders</i>  |           |
| <br>   |           |
| TL - Dosimetry in Clinical Practice . . . . .  | 101       |
| <i>D. Bakker, M.A. Crommelin and W.J.F. Dries</i>  |           |
| <br>   |           |
| Application of TLD for Determinations of Dose Distributions<br>for Photon Irradiations in Radiobiology. . . . .  | 109       |
| <i>J. Zoetelief and N.J.P. de Wit</i>  |           |
| <br>   |           |
| Response of <sup>7</sup> LiF Thermoluminescent Dosimeters to Clinical Neutron<br>Beams with Energies Ranging from d(14)+Be to p(75)+Be . . . . .       | 115       |
| <i>S. Vynckier, B. Hocini and A. Wambersie</i>   |           |
| <br>   |           |
| Dosimetry in a Mixed (14.8 MeV neutron, gamma) Radiation Field<br>with CaF <sub>2</sub> :Tm (TLD-300) . . . . .  | 121       |
| <i>J.B. Dielhof, A.J.J. Bos, J. Zoetelief and J.J. Broerse</i>   |           |
| <br>   |           |
| TLD using LiF Powder applied in Radiotherapy:<br>Practical Aspects and Results. . . . .  | 129       |
| <i>J.P.A. Marijnissen and B. Göbel</i>   |           |
| <br>   |           |
| Eighteen Months of Clinical TLD-dosimetry: Equipment, Calibration- and<br>Annealing Procedures, Reproducibility and Applications in Radiotherapy . . . | 135       |
| <i>R. Van Loon, B. Schaeken, L. Coppens, M. Van Lancker and C. Goor</i>  |           |
| <br>   |           |
| List of participants . . . . .   | 141       |
| Technical Exhibitors. . . . .  | 146       |
| <br>   |           |
| Index of Authors . . . . .   | 147       |



## PREFACE

Thermoluminescence Dosimetry (TLD) has found its application in a large variety of fields such as environmental monitoring, personal dosimetry, radiobiology, diagnostic radiology and radiation therapy. Although there are a number of good reference books and conference proceedings on TLD available, the need was felt for exchange of information between people working in these fields. A one day meeting on Thermoluminescence Dosimetry was organized by several Dutch organizations on radiation protection and clinical physics in co-operation with the Belgian sister organizations. The purpose of the meeting was to discuss a number of theoretical and practical aspects of TLD. The meeting was held in Bilthoven (The Netherlands) on 30 March 1988 and was attended by 105 participants.

Although during the Symposium the manuscripts as submitted by the authors were available, it was decided to edit the papers of that meeting in a more uniform format. Also comments and discussions following the presentation that day have been included by the authors in their final drafts. In this report no distinction is made between papers presented orally or as posters.

Our thanks are due to the authors for submitting their manuscripts in time and to the members of the Programme Committee for undertaking the task of reviewing the papers presented at the Symposium. Finally we like to thank the companies for demonstrating their equipment.

A.H.L. Aalbers, A.J.J. Bos, B.J. Mijnheer  
Delft, October 1988





# **General Aspects of Thermoluminescence Dosimetry**



## MECHANISMS OF THERMOLUMINESCENCE PRODUCTION IN LiF:Mg,Ti (TLD-100)

A.J.J. Bos

Interfaculty Reactor Institute, Delft University of Technology  
Mekelweg 15, NL 2629 JB Delft, The Netherlands

### INTRODUCTION

Lithium fluoride doped with magnesium and titanium and available under the trade name TLD-100, is one of the most popular thermoluminescent (TL) materials used in radiation dosimetry. Its popularity stems from properties such as tissue equivalence, adequate sensitivity for personnel dosimetry and the possibility to manufacture the material with acceptable reproducibility. The mechanism of TL production is, however, very complex. Some of this complexity is demonstrated by the effects of differences in heat treatment, such as annealing. One of the recommended annealing procedures<sup>1</sup> comprises of 1 h at 400 °C followed by 20 h at 80 °C. Such a procedure is necessary to maintain the stability of properties as sensitivity, low background and fading characteristics. Although users of TLD-100 do not need extensive knowledge of the solid state physics aspects in order to perform reliable dose measurements, there is a need for at least a broad understanding why the procedures are as they are. The purpose of this review is to describe the mechanism of TL production in TLD-100 from the viewpoint of the user of this material in dosimetry. The purpose will be didactic, without claim of originality. The solid state physicist will not find new ideas, the radiation physicist, hopefully, some background knowledge about the precepts he follows. The contents of this review is mainly based on reviews<sup>2, 3, 4</sup> and some recent books on thermoluminescence<sup>5, 6, 7</sup>. In particular the book by McKeever<sup>7</sup> is cited frequently. In order not to hamper the reader the citations are not indicated explicitly. The reader is referred to the reviews for more detailed information.

### WHAT IS THERMOLUMINESCENCE?

Thermoluminescence is the thermally stimulated emission of light from an insulator or semiconductor following previous absorption of radiant energy. In this definition the three essential ingredients necessary for the production of thermoluminescence can be found. Firstly, the material must be an insulator or semiconductor: metals do not exhibit luminescent properties. Secondly, the material must at some time have absorbed energy during

exposure to radiation. This property is distinctly different from the spontaneous emission of light from a substance when heated to candescence. Thirdly, the light emission is triggered by heating the material. During the heating the light intensity increases, reaches a maximum and decreases subsequently. In order to re-exhibit the luminescence phenomenon the material has to be re-exposed to radiation, whereupon raising the temperature will once again produce light emission.

#### A SIMPLE MODEL (QUALITATIVE)

An explanation of the observed thermoluminescence properties can be obtained from the energy band theory of solids. In an ideal crystalline semiconductor or insulator most of the electrons stay in the valence band. The next highest band where electrons may stay is the conduction band, separated from the valence band by a so-called forbidden gap  $E_g$  (see Fig. 1). However, whenever structural defects occur in a crystal, or if impurities are built into the lattice, there is a possibility for electrons to possess energies which are forbidden in the perfect crystal. In a simple TL model two levels are assumed, one situated below the bottom of the conduction band and the other situated just above the top of the valence band (see fig. 1). The highest level (Tr) is situated above the equilibrium Fermi level ( $E_f$ ) and will be empty in the equilibrium state i.e. before the absorption of radiation. It is therefore a potential electron trap. The other level is a potential hole trap and can function as a recombination centre (R). The absorption of radiant energy  $(h\nu)_0 > E_g$  results in excitation of valence electrons, producing free electrons in the conduction band and free holes in the valence band (transition 1). The free charge carriers may either recombine or become trapped. The phenomenon of immediate ( $< 10^{-8}$  s)

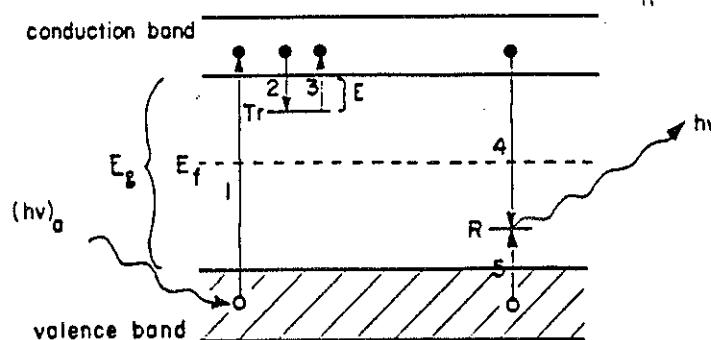


Fig 1. Simple two-level model for thermoluminescence. Allowed transitions: (1) ionization through absorption of radiant energy; (2) en (5) trapping; (3) thermal release; (4) radiative recombination and the emission of light.

recombination of free electrons and holes and subsequent emission of light is called fluorescence. This phenomenon usually is independent of the temperature. In semiconductors and insulators it is more likely that the charge carriers are trapped: the electrons at Tr (transition 2) and the holes at R (transitions 5, see Fig. 1). Recombination will therefore be delayed, depending on by the mean time  $\tau$  the electrons spend in the trap at temperature T, given by the Arrhenius equation:

$$p = \tau^{-1} = s \exp(-E/kT) \quad (1)$$

Here p is defined as the probability per unit time of release of an electron from the trap. The term s is the 'frequency factor'. In the simple model s is considered as a constant with a value in the order of the lattice vibration frequency,  $10^{12} - 10^{14} \text{ s}^{-1}$ . E is called the trap depth or activation energy, the energy needed to release an electron from the trap into the conduction band, k = Boltzmann's constant and T the absolute temperature. If the trap depth  $E \gg kT_0$ , with  $T_0$  the temperature at irradiation, then any electron which becomes trapped will remain so for a long period of time, so that after termination of the irradiation there will exist a population of trapped electrons. Furthermore, because the free electrons and holes are created and annihilated in pairs, there must exist an equal population of trapped holes at level R. Because the normal equilibrium Fermi level  $E_f$  is situated below Tr and above R, these populations of trapped electrons and holes represent a non equilibrium state. The reaction path for return to equilibrium is always open, but because the perturbation from equilibrium (i.e. irradiation) was performed at low temperature (compared with  $E/k$ ), the relaxation rate,  $\tau^{-1}$ , as determined by equation (1), is very slow. Thus, the non-equilibrium state is metastable and will exist for an indefinite period, governed by the rate parameters E and s.

The return to equilibrium can be speeded up by raising the temperature of the TL material above  $T_0$  such that  $kT \geq E$ . This in turn will increase the probability of detrapping and the electrons will now be released from the trap into the conduction band. Thermoluminescence now results when the free electrons recombine with the trapped holes. The intensity of thermoluminescence  $I(t)$  at any time during the heating is proportional to the rate of recombination of holes and electrons at level R. If  $n_h$  is the concentration of trapped holes then:

$$I(t) = -dn_h/dt \quad (2)$$

The relationship between  $I(t)$  and  $n_h$  is shown schematically in figure 2. As the temperature rises the electrons are released and recombination takes

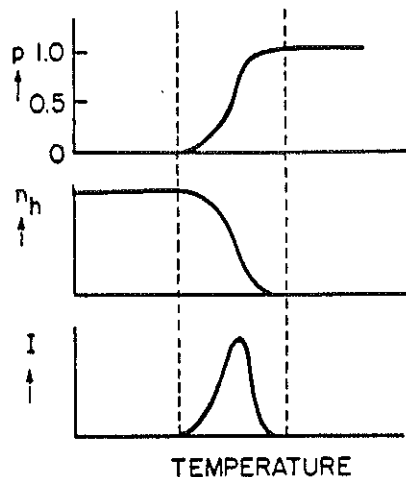


Fig. 2 Relationship between probability  $p$  to escape from a trap, the number of trapped holes  $n_h$  at the recombination centres and the thermoluminescence intensity  $I(t)$ .

place reducing the concentration of trapped holes and increasing the thermoluminescence intensity. As the electron traps are progressively emptied the rate of recombination decreases and thus the thermoluminescence intensity decreases accordingly. This produces the characteristic thermoluminescence peak.

A SIMPLE MODEL (QUANTITATIVE)

The first quantitative description of the thermoluminescence intensity as a function of temperature or time, the so-called glow curve, is given by Randall and Wilkins<sup>8</sup>. They start from the two level model and assumed that a) the concentration of free carriers in the conduction band ( $n_c$ ) is always very much less than the concentration of trapped carriers ( $n$ ) and b) once released from a trap the electron will undergo recombination rather than retrapping. These assumptions imply that the luminescence intensity will be proportional to the number of released electrons. This number will be equal to  $pn$ . Furthermore they assumed that c) the rate of change of the free carrier concentration is always very much less than the rate of change of the trapped carrier concentration, i.e.  $dn_c/dt \ll dn/dt$ . From this assumption it follows that  $I(t) = -dn_h/dt = -dn/dt$ , so that  $I(t)$  can be written as

$$I(t) = -dn/dt = cpn \tag{3}$$

with  $c$  a thermoluminescence efficiency. Without loss of generality  $c$  may be set equal to 1. Applying expression (1) to equation (3) yields

$$I(t) = -dn/dt = sn \exp(-E/kT) \Rightarrow \int \frac{dn}{n} = \int s \exp(-E/kT) \tag{4}$$

$$\ln \frac{n}{n_0} = \int s \exp(-E/kT) dt$$

$$n = n_0 \int s \exp(-E/kT) dt$$

This differential equation describes the charge transport in the lattice as a first order process and glow peaks calculated from this equation are called first order glow peaks. Solving the differential equation (1) yields

$$I(t) = -dn/dt = n_0 s \exp(-E/kT) \exp\left[-s \int_0^t \exp(-E/kT(t')) dt'\right] \quad (5)$$

where  $n_0$  is the total number of trapped electrons at time  $t = 0$ . Usually the temperature is raised as a linear function of time according to

$$T = T_0 + \beta t \quad (6)$$

where  $\beta$  is the heating rate. In figure 3 some glow peaks computed from Eq. 5

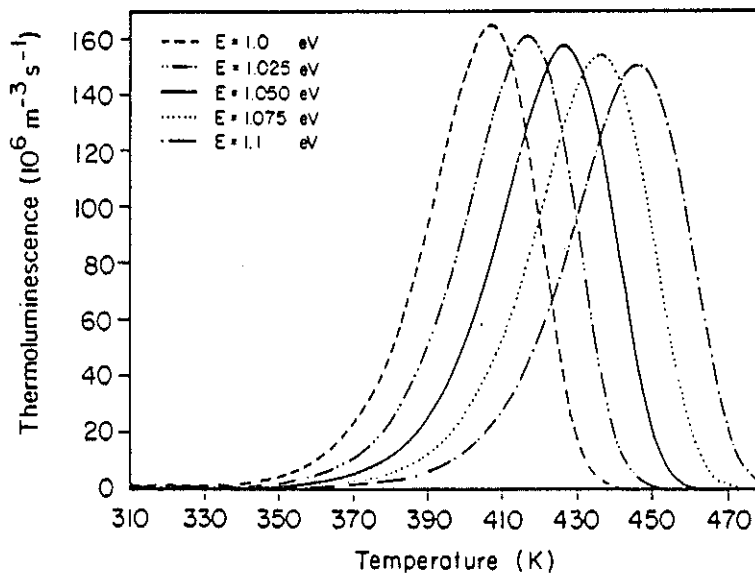


Fig. 3 Glow peaks calculated from eq. (5), assuming first order kinetics and linear heating with the activation energy E as parameter. ( $s = 10^{12} \text{ s}^{-1}$ ,  $\beta = 6 \text{ }^\circ\text{C s}^{-1}$  and  $n_0 = 10^9 \text{ m}^{-3}$ ).

are shown. The peak shows a characteristic asymmetric shape. The temperature at the maximum,  $T_m$ , can be found when the derivative of  $\ln I(t)$  is set to zero. This yields

$$\beta E / (kT_m^2) = s \exp(-E/kT_m) \quad (7)$$

From this equation it can be derived that  $T_m$  increases with increasing E (see also figure 3) according to the physical picture that for deeper traps more energy and consequently a higher temperature is needed to free the electrons. Equation (7) also reveals that  $T_m$  increases with increasing heating rate  $\beta$ . From the viewpoint of solid state physics only the parameters E and s are of interest. In dosimetry, however,  $n_0$  is the parameter of paramount importance since this parameter is associated with the absorbed



dose. It is simple to see that the area under the glow peak is equal to  $n_0$  since

$$\int_0^{\infty} I(\tau) dt = - \int_0^{\infty} (dn/dt) dt = - \int_{n_0}^{n_{\infty}} dn = n_0 - n_{\infty} \quad (8)$$

and  $n_{\infty}$  is zero for  $t \rightarrow \infty$ .

WHAT DO(N'T) WE LEARN FROM THE SIMPLE MODEL?

The simple model can explain, at least qualitatively, all the fundamental features of thermoluminescence production. The model teaches that the

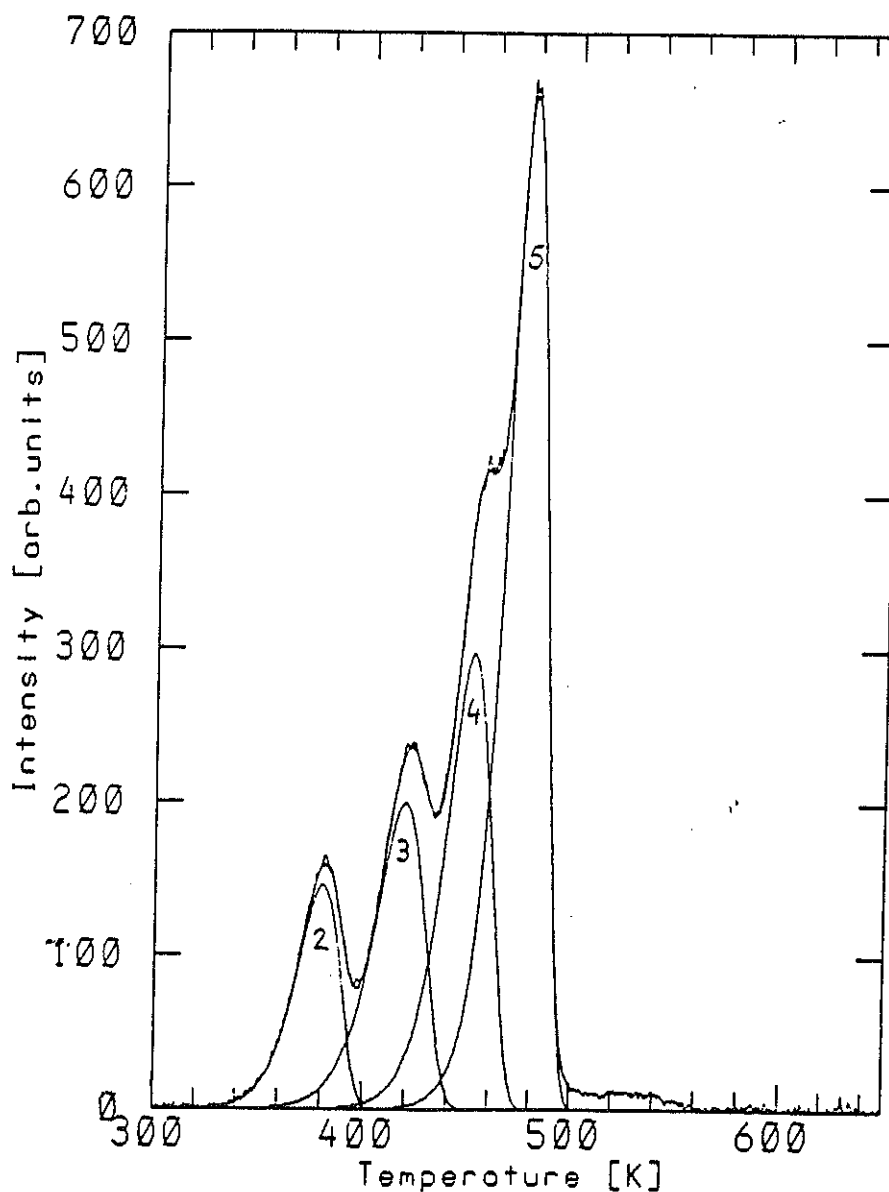


Fig.4 Glow curve of TLD-100 after a pre-irradiation annealing of 1 h 400 °C and fast cooling and irradiation with  $^{60}\text{Co}$  gamma rays. The measured glow curve is fitted with four first order peaks with a fitting procedure described elsewhere<sup>9</sup>.

presence of traps is essential for TL production. Thus, (ideal) metals where no traps are present, do not show thermoluminescence. The absorption of radiant energy is needed to fill the traps and heating is necessary to release the charge carriers from the traps. The model gives insight into how radiant energy is stored. Loss of trapped charge before readout (fading) is undesirable in dosimetry. The model explains that glow peaks at lower temperatures, corresponding to shallower traps, are more sensitive to fading.

In figure 4 a glow curve of TLD-100 is shown. The measured glow curve has been fitted with a superposition of four peaks each described by equation (5). It is seen that a very good fit is obtained. The measured activation energies agree with values reported by other investigators (see table 1).

Table 1. Activation energies and half-lives of some peaks in TLD-100.

| Peak no | McKeever <sup>10</sup> | Activation energy (eV)          |                               |               | Half life                      |                            |
|---------|------------------------|---------------------------------|-------------------------------|---------------|--------------------------------|----------------------------|
|         |                        | Taylor and Lilley <sup>11</sup> | Fairchild et al <sup>12</sup> | Present study | Calculated from fit parameters | Measured by other authors* |
| 2       | 1.13±0.01              | 1.11±0.02                       | 1.07                          | 1.10±0.03     | 26 h                           | 10 h                       |
| 3       | 1.23±0.01              | 1.27±0.03                       | 1.05                          | 1.23±0.02     | 0.45 a                         | 0.5 a                      |
| 4       | 1.54±0.01              | 1.60±0.07                       | 1.54                          | 1.63±0.05     | 6.5 10 <sup>2</sup> a          | 7 a                        |
| 5       | 2.17±0.01              | 2.06±0.11                       | 2.20                          | 1.92±0.04     | 4.8 10 <sup>5</sup> a          | 7 - 14 a                   |

\* Peak 2,3 and 4 Zimmerman et al.<sup>13</sup> and peak 5 McKeever<sup>4</sup>

The half-life  $T_{1/2} = \ln 2/p$  of each peak, which can be derived from the fitting parameters and equation (1), however, does not correspond to the fading rate during storage observed by others, especially for peak 5, the main TL dosimetry peak. The discrepancy must be sought in the nature of the traps. The type of model presented here is phenomenological. The traps are described by two parameters (E and s) but this does not reveal the true characterization of the defect structure of TLD-100. A detailed understanding of the defect structure is a necessity in order to interpret the observed TL behaviour and to improve the reliability of the thermoluminescence dosimetry. Measurement of the glow curve is of limited value to study the defects since thermoluminescence requires two principal defect types: a trap and a luminescent centre. In measuring the glow curve it is not known which one, or what kind of combination, is monitored.

TRAPPING AND RECOMBINATION/LUMINESCENT CENTRES

The ability of TLD-100 to luminescence is related to the impurity atoms Mg and Ti present in small proportions (approximately 170 and 10 mole ppm, respectively). Despite much research there is relatively little understanding of the relation between the defect state of Mg and Ti in the LiF lattice and the TL response. The intention of this section is to give an idea of the complexity of this relation rather than to review all proposed models.

Magnesium as  $Mg^{2+}$  has an ionic radius (72 pm) close to that of lithium in the LiF lattice (76 pm) and can therefore easily substitute the latter. This has two consequences:

- (i) It favours the creation of electron traps.
- (ii) It favours the creation of electron holes, because in compensating the excess positive charge of the  $Mg^{2+}$  ions substituting the  $Li^+$  ions,  $Li^+$  ion vacancies (V) appear in the crystal lattice.

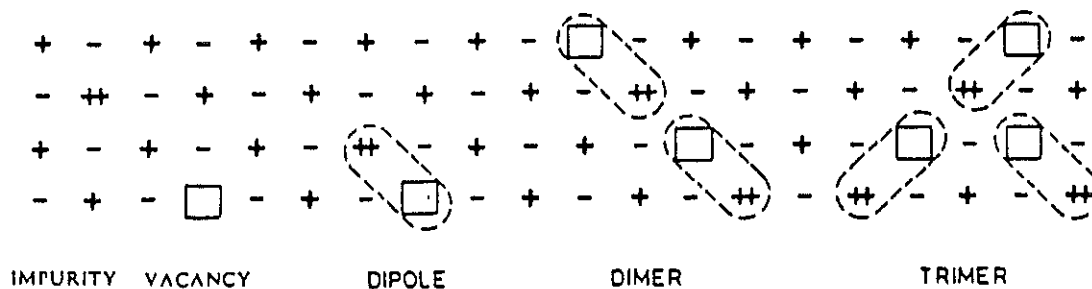


Fig.5 Divalent cation impurity (++) and host cation vacancy (□) in the LiF lattice showing the four possible configurations: free impurities and vacancies, association to a dipole and clustering to a dimer or trimer.

The divalent impurity ( $Mg^{2+}$ ) and the cation vacancy (V) have opposite charge and the coulombic attraction between them results in the formation of associated impurity-vacancy ( $Mg^{2+}-V$ ) pairs or dipoles. It has been shown that this association occurs at low temperatures. Between the dipoles further clustering reactions may occur. The most probable reaction sequence is the clustering of two pairs to form a linear dimer (see figure 5) followed by the addition of a third pair to form the stable trimer. Even the formation of some Mg precipitates ( $6LiF.MgF_2$ ) is possible. The investigation of point defect reactions by Strutt and Lilley<sup>14</sup> has led to the following picture of clustering and precipitation:

free  $Mg^{2+}$  + vacancies = dipole = dimers = trimers = precipitates (9)

The usual preirradiation annealing procedure involves an isothermal anneal at 400 °C for 1 h. This has the effect of dispersing all Mg impurities in dipole form, i.e. it pushes reaction (9) to the left. Subsequent low temperature annealing for 20 h at 80 °C results in the clustering of the dipoles into trimers, i.e. forcing reaction (9) to the right. An important, often ignored, effect on the defect concentration is the cooling rate between the high (400 °C) and low (80°C) temperature annealing. Quenching the TL material has the effect of freezing in the defect structure while a slow cooling will stimulate clustering. The effects of the cooling rate on the TL response is easy to measure but difficult to interpret because reaction (9) also takes place during TL readout. Thus the initial effect during irradiation is not being maintained during TL readout.

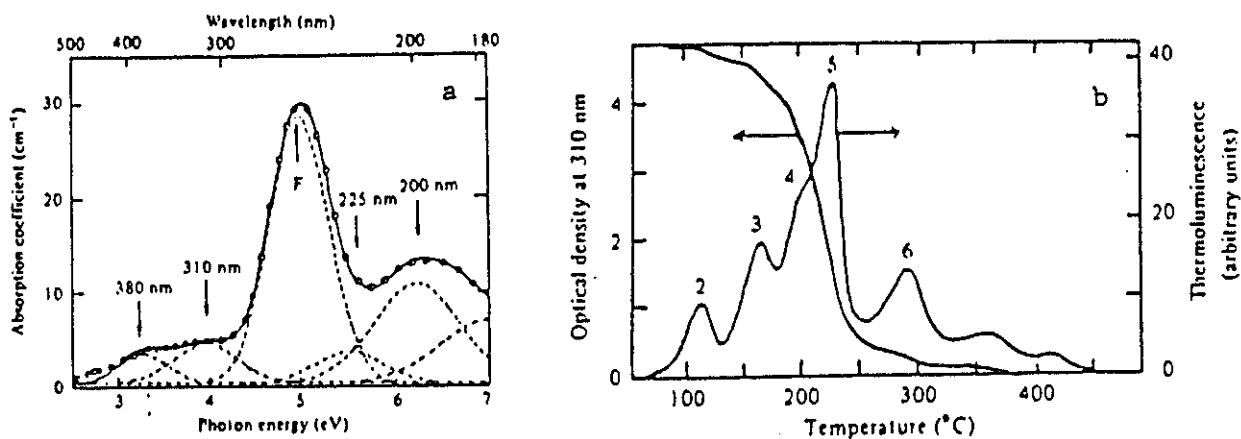


Fig. 6 a. Absorption spectrum for irradiated TLD-100. Dashed lines: calculated Gaussian absorption bands.  
 b. Thermoluminescence and annealing of the 310 nm absorption band in TLD-100 irradiated to  $10^3$  Gy (Adopted from McKeever<sup>7</sup>)

Other information about the defect structure is obtained by studying optical absorption. Pure LiF crystals are transparent throughout the visible region of the spectrum. The crystal may be coloured by irradiation. A colour center is a lattice defect which absorbs visible light. The simplest colour center is an F center (a negative ion vacancy with one excess electron bound at the vacancy). The name comes from the German word for colour, Farbe. The optical absorption versus wavelength in irradiated pure LiF shows a peak around 5 eV, the so called F - band. The absorption spectrum for irradiated LiF:Mg,Ti shows apart from the F - band some other peaks (see figure 6a). The 310 nm band has been studied as function of temperature in conjunction

with the thermoluminescence (see fig 6b). From these experiments it is concluded that absorption at 310 nm is closely associated with TL peak 5. When combined with dielectric relaxation measurements the results indicate that the defects responsible for peak 5 and for the 310 nm absorption band are related to trimer complexes of Mg.

The other impurity in TLD-100, notably Ti, is still undiscussed. Optical absorption and photoluminescence work<sup>4</sup> has shown that the luminescence centre is related to this impurity. Measurements of the emission spectra of TLD-100 during thermoluminescence<sup>15</sup> show that each peak in the glow curve emits at a slightly different wavelength, although the main emission band lies between 400 - 430 nm (i.e. blue) region. The exact wavelength at which peak emission occurs is dependent upon the aggregation state of Mg. This indicates a close, spatial correspondence between the Mg defects and the luminescence activators. One may therefore conclude that the major defect responsible for peak 5 is a Mg-trimer/Ti complex<sup>15,16</sup> wherein the trapping and recombination sites are combined. Accepting this picture of the defect structure involved in the TL production of the main dosimetry peak 5, the importance of reproducible annealing and read out procedures in TL dosimetry become clear. Any change in this procedure (i.e. any change in the temperature - time schedule) will alter the number of trimers according to reaction (9) and with that both the number of traps and luminescent centres. Some of this complexity is illustrated in the work of Julius and De Planque<sup>17</sup>. These investigators found that at low storage temperatures the decrease in the TL signal obtained from samples stored for varying periods before irradiation was similar to the signal loss obtained from those samples stored for the same periods but after irradiation. This observation can only be understood assuming that the defect structure itself is altered during the storage period.

#### CONCLUSIONS

The fundamental features of the thermoluminescence production in LiF:Mg,Ti (TLD-100) can be understood with a simple model. However, this model is only a phenomenological description. The precise relation between the observed thermoluminescence and the defect structure in the LiF lattice (i.e. the role of the impurities) is very complex and a detailed understanding is lacking. As long as the knowledge of the defects involved in the TL production is missing no precise recommendations regarding manufacturing or dosimetry methodology can be expected.

There is experimental evidence that the main peak in the glow curve (peak 5) is related to Mg-trimer/Ti complexes i.e. trapping and luminescent centres are closely connected. It is also shown that the number of Mg-trimers strongly depends on temperature. Therefore, every step in the time-temperature schedule (including annealing, irradiation, storage and readout) will influence TL response. For accurate dosimetry this emphasizes the need for very reproducible procedures.

#### REFERENCES

1. C.M.H. Driscoll, J.R. Barthe, M.Oberhofer, G. Busuoli and C. Hickman, Annealing procedures for commonly used radiothermoluminescent material, *Radiat. Prot. Dosim.* 14 (1986) 17-32
2. V.K. Jain, Thermoluminescence of Lithium Fluoride, *Radiat. Prot. Dosim.* 2(3) 1982) 141-168
3. S.W.S. McKeever, Thermoluminescence in the Alkali Halides, *Radiat. Prot. Dosim.* 8(1/2) (1984) 3-23
4. S.W.S. McKeever, Mechanisms of thermoluminescence production in materials for radiation dosimetry, 17 (1986) 431-435
5. R. Chen and Y. Kirsh, Analysis of Thermally Stimulated Processes, Pergamon Press, Oxford, UK, 1981
6. Yigal. S. Horowitz (Editor), Thermoluminescence and Thermoluminescent Dosimetry, Volumes I, II and III, CRC Press, Inc. Boca Raton, Florida, USA 1984
7. S.W.S. McKeever, Thermoluminescence of Solids, Cambridge University Press, Cambridge, UK, 1985
8. J.T. Randall and M.H.F. Wilkins, Phosphorescence and electron traps, I. The Study of trap distributions. *Proc. Royal Soc. A*(184) (1945) 366-389
9. J.E. Hoogenboom, W. de Vries, J.B. Dielhof and A.J.J. Bos, Computerized analysis of glow curves from thermally activated processes, *J. Appl. Phys.* 64(6) (1988) 3193-3200
10. S.W.S. McKeever, Thermoluminescence in LiF: Analysis of the glow-curves, *Nucl. Instr. Meth.* 175 (1980) 19-20
11. G.C. Taylor and E. Lilley, The analysis of thermoluminescent glow peaks in LiF (TLD-100), *J. Phys. D: Appl. Phys.* 11 (1978) 567-580
12. R.G. Fairchild, P.L. Mattern, K. Langweiler and P.W. Levy, Thermoluminescence of LiF (TLD-100): Glow Curve Kinetics, *J. Appl. Phys.*, 49 (1978) 4523-4533
13. D.W. Zimmerman, C.R. Rhyner and J.R. Cameron, Thermal annealing effects on Thermoluminescence of LiF, *Health Physics* 12 (1966) 525-531
14. J.E. Strutt and E. Lilley, Structural Aspects of Clustering Reactions In Alkali Halides Doped with Divalent Impurities, *Phys. Stat. Sol.(a)* 33 (1976) 229-239
15. P.D. Townsend, K. Ahmed, P.J. Chandler, S.W.S. McKeever and H.J. Whitlow, Measurements of the Emission Spectra of LiF during Thermoluminescence, *Rad. Effects* 72 (1983) 245-257
16. S.W.S. McKeever, Optical Absorption and Luminescence in Lithium Fluoride TLD-100, *J. Appl. Phys.* 56(10) (1984) 2883-2889
17. H.W. Julius and G. de Planque, Influence of Annealing and Readout Procedures on Fading and Sensitivity Changes in LiF for Temperatures and Humidities Typical for Environmental and Personnel Dosimetry, *Radiat. Prot. Dosim.* 6 (1984) 253-256



SOME EXPERIMENTAL OBSERVATIONS ON THE SUPRALINEARITY OF THE RESPONSE OF  
TLD-100 IN THE RADIOTHERAPEUTIC DOSE RANGE

B.J. Mijnheer and J. Weeda\*

The Netherlands Cancer Institute (Antoni van Leeuwenhoek Huis),  
Plesmanlaan 121, 1066 CX Amsterdam, the Netherlands

INTRODUCTION

From the presently available information on the steepness of dose-effect curves for local tumour control and normal tissue damage, several authors<sup>1,2,3</sup> have proposed a requirement for the accuracy in the delivery of the dose to the dose specification point in a patient of 3.5%, one standard deviation. Such a high accuracy is especially important if clinical data from different centres have to be compared. For other points in the target volume an accuracy requirement of 5%, one standard deviation, might be a better compromise between the clinical demand and what can be technically achieved<sup>4</sup>.

In order to obtain such a high degree of accuracy when using TLD in the clinic, a number of tests are required, as discussed, for instance by Marshall<sup>5</sup>. One of these tests refers to the relationship between dose and TLD reading. As has been observed by various authors, supralinearity in the response of several TLD materials occurs at doses above a few Gy, as summarized by Horowitz<sup>6</sup>. For LiF TLD-100, onset values of TL supralinearity varying from 1 to 10 Gy have been reported<sup>6,7,8</sup>. Because this dose range coincides with that applied in radiotherapy, it seemed worthwhile to investigate the necessity of correcting for supralinearity. It was the purpose of this study to describe the results of measurements of supralinearity for the response of TLD-100 at doses below 5 Gy using different read-out and different annealing procedures. No attempt has been made up till now to systematically study the different factors influencing supralinearity nor to correlate our findings with the various models<sup>9</sup>.

\* Present address: Clinical Oncology Department, Academic Hospital Leiden, Rijnsburgerweg 10, 2333 AA Leiden



## MATERIALS AND METHODS

Different production batches of TLD-100, both rods (diameter 1 mm, length 6 mm) and ribbons (3.2 mm x 3.2 mm x 0.9 mm), were studied. These batches were purchased from the same manufacturer, (Harshaw Chemical Company, Cleveland, Ohio, USA), over a time period of several years and therefore had a different irradiation history. Each batch was divided into sub-groups having a standard deviation in their calibration factor of about one percent. Generally, six TL detectors were irradiated for each dose value, which ranged from 0.25 Gy to 5 Gy. Such a series of experiments was repeated at least twice. Most results were obtained with Co-60 gamma rays but similar data were observed for 8MV X rays.

The read-out was performed with standard equipment (Harshaw model 2000-A/B). Several read-out procedures were applied. The initial measurements were performed using the read-out procedure recommended by Harshaw: a preheat temperature of 100° C followed by a linear increase in temperature from 100° C to 260° C in 25 s, with an additional 5 s at 260° C. In order to study other read-out procedures, the temperature of the planchet was externally controlled by a computer (PDP 11/44). Glow curves were obtained by increasing the temperature linearly between 100° C and 300° C in 60 s. Because our equipment did not have the capability of varying the integration boundary, the light output of the reader was sampled and stored in the same computer. Generally, glow curves consisting of 300 points were sampled and analysed. The contribution of background radiation to the total signal was less than 0.2% in all situations.

For practical reasons, the anneal period applied in our Department (one hour from room temperature to 400° C followed by a slow cooling period to room temperature in 16 h in the same furnace) deviates from that recommended by the manufacturer (one hour at 400° C followed by a fast cooling to 80° which temperature is held during 24 hours). It can be expected that the reproducibility of our anneal procedure is good due to the simplicity and consistency of the applied heating and cooling method.

## RESULTS

In the initial experiments, using the read-out procedure recommended by Harshaw, supralinearity was studied for TLD-100 rods under a variety of experimental conditions. The response, defined as the reading divided by the dose, is presented in figure 1. The data are normalized at a dose value of 100 cGy. As can be seen from this figure, the onset of supralinearity could already be observed, under all circumstances, at doses of 25 cGy. This unexpected result prompted us to study in somewhat more detail the possible reasons for this relatively large supralinearity effect by looking at the supralinearity of the individual glow peaks, the different TLD batches and the anneal procedure.

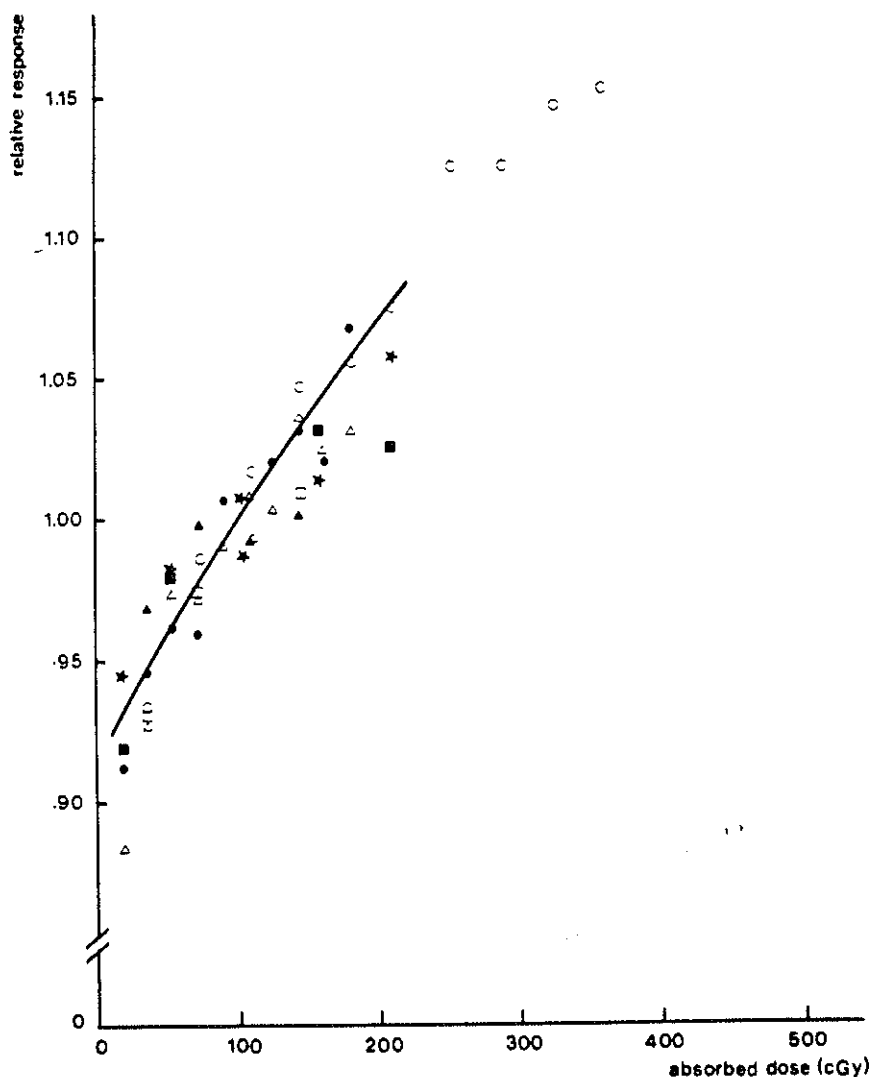


Fig. 1 Supralinearity of the response of LiF TLD-100 rods as a function of absorbed dose. The different symbols indicate different series of experiments employing different read-out and anneal procedures using equipment from different institutions.

A quantitative expression for the supralinearity of the various peaks can be obtained from a glow curve analysis. In order to obtain the area under the different peaks, a first-order kinetics<sup>10,11</sup> and a more simple Gaussian fit (see Fig. 2) were applied. Although first-order kinetics gives a better description of the charge transport in the lattice, the resulting shape of the final glow curve will also be determined by other factors, such as the characteristics of the read-out equipment, which will influence the success of the fitting procedure. The Gaussian fit yielded a slightly better accuracy with respect to the reconstruction of the total glow curve from the individual peaks and was therefore used in further analyses.

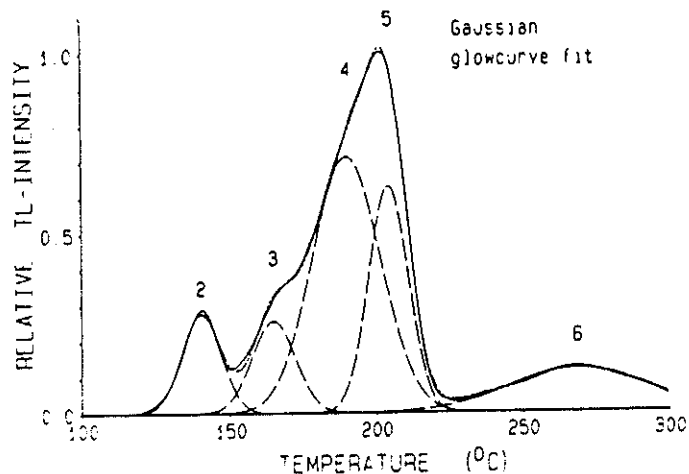


Fig. 2 Gaussian fit of glow curve of TLD-100 rod showing the individual Gaussians, the combined fitted curve (---) and the original measured curve (—)

By calculating the area under the different peaks of the TL detectors, irradiated at different dose levels, it was possible to assess the supralinearity of the individual glow peaks. Due to the small distance between peaks 4 and 5, these peaks were combined, whereas peak 2 was not considered due to its rapid fading. All results could be represented by the equation  $R = aD + bD^2$  where  $R$  is the TL reading observed for each peak,  $D$  is the

absorbed dose (to water) and  $a$  and  $b$  are constants. A useful way to express the supralinearity of the TL response  $R/D$  is by the magnitude of the coefficient  $b$ , the slope of the curve  $R/D$  versus  $D$ .  $b$  is given as percent per 100 cGy (see Fig. 1). Values for the supralinearity of the different peaks that could be derived from the results of all TLD-100 rod experiments are:  $0 \pm 1\%$  (peak 3);  $2.8 \pm 0.6\%$  (peak 4 + 5) and  $35 \pm 2\%$  (peak 6) per 100 cGy increase in dose, i.e. an increase in supralinearity with glow peak temperature. It would be of interest to perform a more extensive set of measurements of the supralinearity of the individual peaks in order to ascertain its variation for the various batches.

Careful analysis of the results of different batches of rods as well as of ribbons, showed significant differences in their supralinear behaviour. Glow curves of different batches, normalized to the highest peak (peak 5), are presented in Fig. 3. The figure shows that the relative heights of the different peaks vary considerably between the different batches. By counting the total area under peaks 3 + 4 + 5, values of 1.2, 1.5 and 2.9% per 100 cGy could be derived for the supralinearity of the upper, middle and lower curve of figure 3, respectively. These values are qualitatively in agreement with the relative contribution of peak 3 to the total peak area.

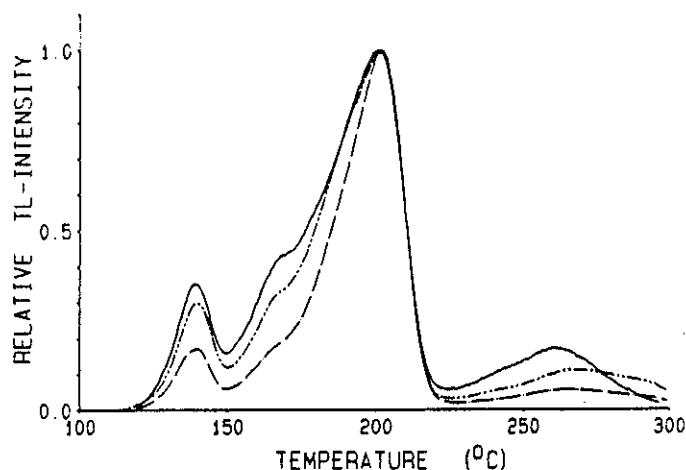
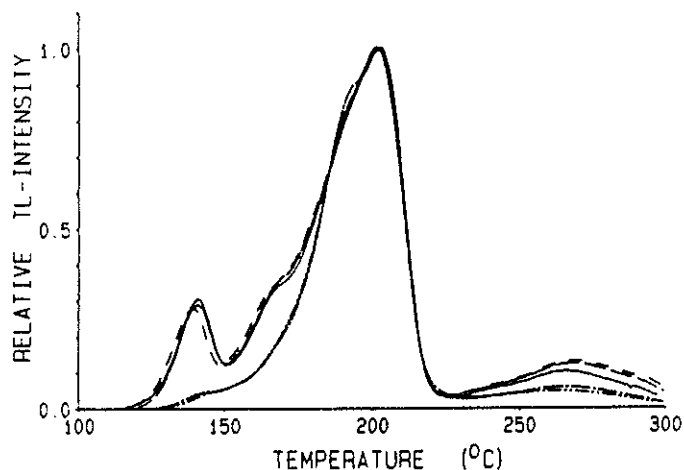


Fig. 3 Glow curves of three different batches of TLD-100 rods irradiated with a dose of 100 cGy

The results for ribbons also showed small but significant differences in shape of the glow curves. Values for the supralinearity of peaks 3 + 4 + 5 of  $1.7 \pm 0.5\%$  and  $2.6 \pm 0.2\%$  per 100 cGy were observed in two different batches. A remarkable difference was also seen in the value of the supralinearity of peak 6: about 12% for the ribbons compared with 35% for the rods.

The influence of the different methods of annealing on the shape of the glow curve is illustrated in figure 4. The immediate cooling to 80° C instead of the slow cooling to room temperature, obviously results in less contribution of peak 6 relative to peaks 4 + 5. Additional experiments are required to determine whether in addition to this difference in shape of the glow curves also the supralinearity of the individual peaks is dependent on the method of annealing.



**Fig. 4** Glow curves of TLD-100 rods for two different methods of annealing. Upper three curves: one hour at 400° followed by a slow cooling period to room temperature in 16 h; lower two curves: one hour at 400° C followed by an immediate cooling to 80°. The absence of peak 2 in the lower two curves is due to the larger waiting period between the irradiations and the read-out.

## DISCUSSION AND CONCLUSIONS

Our measurements showed that an increase in glow peak temperature is correlated with an increase in supralinearity, which is in agreement with observations by other groups<sup>6</sup>. In particular, peak 6 shows a large supralinearity. If part of this peak is included in the read-out cycle, which occurs during the procedure recommended by Harshaw, and if the contribution of peak 6 relative to peaks 4 + 5 is large, which results from our method of annealing, then a large supralinearity can be expected: about 8% per 100 cGy (see Fig. 1).

One method to reduce supralinearity effects is to apply a glow curve analysis and to count only the area under peaks 3 + 4 + 5. The remaining values for supralinearity vary between about 1% and 3% per 100 cGy for the different batches of rods and ribbons. Those differences might be caused by the dependence of supralinearity on impurity composition<sup>6</sup>, thus yielding different contributions of peaks 3, 4 and 5 to the total reading.

A simpler method for routine dosimetry would be to stop the integration in the valley between peaks 5 and 6. A pre-read-out anneal of 18 s at 135°, followed by a linear temperature increase to 210° C in 25 s with an additional 5 s at 210° C, is now applied in our institution. The supralinearity observed under these circumstances is identical to that found with glow curve analysis, while, in addition, no difference in precision of the resulting dose values could be observed between the two methods.

A supralinearity of at least 1 to 3% per 100 cGy will always be present during the clinical use of TLD-100. Only by careful measurements can such small changes in response be observed and considered meaningful. The magnitude of the effect probably explains the different values for the onset of supralinearity as observed by various authors. For accurate measurements in the clinic, corrections for supralinearity will therefore always be necessary. These corrections will have to be determined for each batch of TLD-100 for the read-out and anneal procedure applied in a particular institution.

#### ACKNOWLEDGEMENTS

The authors greatly appreciate the cooperation with J.P.A. Marijnissen from the Daniel den Hoed Clinic (Rotterdam) and P.J.H. Kicken from the Technical University (Eindhoven) during the initial stage of this investigation.

#### REFERENCES

1. M. Goitein, Nonstandard deviations, Med. Phys. 10 (1983) 709-711
2. A. Brahme, Dosimetric precision requirements in radiation therapy, (Acta Radiol. Oncol. 23 (1984) 379-391
3. B.J. Mijnheer, J.J. Battermann and A. Wambersie, What degree of accuracy is required and can be achieved in photon and neutron therapy?, Radiother. Oncol. 8 (1987) 237-252
4. ICRU (International Commission on Radiation Units and Measurements), Determination of Absorbed Dose in a Patient irradiated by Beams of X- or Gamma Rays in Radiotherapy Procedures, Report 24, ICRU Publications, Bethesda, Maryland, USA, 1976
5. T.O. Marshall, Accuracy and precision in thermoluminescence dosimetry, in: Practical Aspects of Thermoluminescence Dosimetry, Hospital Physicists Association Report CRS 43, pp 12-22, HPA Publications, London, UK, 1984
6. Y.S. Horowitz, TL dose response, in: Thermoluminescence and Thermoluminescent Dosimetry, Vol. II, pp 2-36, CRC Press, Boca Raton, Florida, USA, 1984
7. H.D. Strüter, Eigenschaften von LiF-Thermolumineszenzdetektoren bei der Dosimetrie energiereicher Strahlen, Strahlentherapie 142 (1971) 174-182
8. B. Planskoy, Quality control of LiF TLD-100 for radiotherapy dosimetry, in: Practical Aspects of Thermoluminescence Dosimetry, Hospital Physicists Association Report CRS 43, pp 74-82, HPA Publications, London, UK, 1984
9. Y.S. Horowitz, Recent models for TL supralinearity, Radiat. Prot. Dosim. 6 (1984) 17-20
10. N. Vana and G. Ritzinger, Analysis of TL glow curves in differently doped LiF: Mg, Ti, Radiat. Prot. Dos. 6 (1984) 29-32
11. M. Moscovitch, Y.S. Horowitz and J. Oduko, LiF thermoluminescence dosimetry via computerized first order kinetics glow curve analysis, Rad. Prot. Dosim. 6 (1984) 157-159

SUPRALINEARITY AND DEPENDENCE ON ENERGY OF LiF 700 POWDER RESPONSE  
FOR PHOTONS AND ELECTRONS.

J.P.A. Marijnissen and B. Göbel.

Dr Daniel den Hoed Cancer Centre,  
Groene Hilledijk 301, 3075 EA Rotterdam, The Netherlands.

INTRODUCTION.

Thermoluminescence dosimetry (TLD) using LiF 700 powder is applied in the Dr Daniel den Hoed Cancer Centre for the measurement of dose distributions in phantoms as well as in patients. The radiotherapy department utilizes I-125, Ir-192 and Cs-137 sources, a 50 kV superficial and 120-250 kV deep X-ray therapy machine, 4-25 MV photons and 4-32 MeV electrons of linear accelerator therapy machines. TLD is applied in this full range of radiation qualities except 50 kV. The LiF powder is calibrated against a 0.6 cm<sup>3</sup> thimble ionization chamber in a 4 MV photon beam at a reference test dose of 1 Gy. The TL-response/unit dose is considered as the calibration factor for this particular dose and radiation quality. TL-response to dose conversion for TLD measurements at other radiation qualities and doses requires adequate knowledge of the TL properties of the TL-material, i.e. the supralinearity and dependence on energy of the LiF 700 response. Supralinearity and energy dependence for average photon energies of 45 keV-12 MeV and for electrons with initial energies of 4-32 MeV have been studied. In this paper preliminary results are given with emphasis on the difference in response in high energy electrons and high energy photon beams.

MATERIALS AND METHODS.

Samples of Harshaw LiF 700 powder from batch 1KTU and B701 were encapsulated in polyethylene tubing with 0.25 mm wall thickness and 1.6 mm inner diameter. Each capsule contained 30 mg LiF powder, adequate for 5 independent read-outs of 6 mg LiF each. The TL response was measured with a Pitman model 654 TLD-reader. For each TLD-read-out the mass of the powder together with the TLD reader planchet was determined by a Mettler M5 analytical balance. Subsequently the mass of the LiF was calculated by subtracting the known mass of the planchet. The precision obtained by this method is discussed elsewhere in these proceedings<sup>1</sup>. After each annealing (1.5 h at 400°C - 16 h at 80°C) the LiF is calibrated in a 4 MV photon beam. TLD capsules are positioned in a perspex phantom (30x30x25 cm) at depth of maximum build-up as well as at a reference depth of 5 gcm<sup>-2</sup>. At both depths the doses are calibrated against an ionization



chamber (NE 2505/3A) traceable to a secondary standard. The 4 MV beam is used for convenience, because irradiations at our Co-60 teletherapy unit take too much time for routine calibrations. However, TL-reponse for 4 MV photons relative to Co-60 photons has been compared at both depths for perspex and water and appeared to be identical. All TLD capsules were located at ionization chamber depth corrected for displacement of the effective measuring point appropriate for the phantom material. Irradiation of TLD capsules at all high energy photon and electron beams have been performed in perspex phantoms. The electron beam doses have been measured with a NACP ionization chamber using the NACP protocol<sup>2,3</sup>

## RESULTS

Supralinearity. It has often been reported that LiF 700 has a linear dose-response characteristic over a  $10^{-4}$  - 10 Gy range. However the observed response of the LiF 700 already deviates from proportionality at a dose level of about 0.01 Gy (Co-60 photons)<sup>1,4</sup>. Supralinearity can be quantified by a supralinearity ratio  $F_s$  :

$$F_s = \frac{(R/D) \{D=10\}}{(R/D) \{D=1\}} \quad (1)$$

where  $R/D$  is the TL-reponse per mg LiF per unit dose to LiF [Gy].

The response per unit dose in the denominator is the response per Gy at a dose of 1 Gy, which is the reference test dose. The response per unit dose in the numerator is determined for a dose of 10 Gy. Because the dose measurements for most of the TLD applications in radiotherapy range between 0.1 to 20 Gy, the supralinearity ratio  $F_s$  is an appropriate quantity for this range. It has been reported that supralinearity is dependent on the LiF composition<sup>4</sup> and sensitive to the annealing procedure and grain size<sup>5</sup>. Consequently a check on the supralinearity ratio after each annealing is performed. For the 4 MV reference beam the supralinearity ratio  $F_s$  is  $1.21 \pm 0.01$ . Because the LiF is used over a wide range of energies, the dependence of supralinearity on radiation quality should be checked. In Table 1 the results of measurements on  $F_s$  are summarized for various beam qualities. From Table 1 it is clear that the supralinearity is independent of the energy spectrum above 100 keV mean energy. Recently LiF powder manufactured by Vinten (LiF 700 powder batch 118) became available for evaluation. The supralinearity for the 4 MV beam turned out to be  $1.18 \pm 0.02$ .

Energy response to high energy photons. Analogous to the definition of  $F_s$  an energy factor  $F_x$  is defined :

$$F_x = \frac{(R/D) \{D, x\}}{(R/D) \{D, \text{ref}\}} \tag{2}$$

where the index x stands for p (photons) or e (electrons) and ref. for the 4 MV reference beam. TL-response per unit dose has been determined for the same dose D to avoid corrections for supralinearity.

Table 1. Supralinearity ratio Fs of LiF 700 powder.

| Initial energy       | Average energy | Fs          |
|----------------------|----------------|-------------|
| Photons              |                |             |
| 120 kV - 4.0 Al      | 45 keV         | 1.11 ± 0.03 |
| 250 kV - Thoraesus-I | 130 keV        | 1.18 ± 0.03 |
| Co-60                | 1.3 MeV        | 1.21 ± 0.02 |
| 4 MV                 | 1.5 MeV        | 1.21 ± 0.01 |
| 25 MV                | 12 MeV         | 1.24 ± 0.03 |
| Electrons            |                |             |
| 4 MeV                | 2.4 MeV        | 1.20 ± 0.01 |
| 7 MeV                | 4.2 MeV        | 1.23 ± 0.02 |
| 10 MeV               | 7 MeV          | 1.21 ± 0.01 |
| 28 MeV               | 23 MeV         | 1.23 ± 0.02 |

In figure 1 the results of the measurements of Fp are shown. The energy dependence is flat from about Co-60 to at least 12 MeV mean energy. However there is an unexpected increase in Fp observed at Cs-137 and Ir-192. The I-125 data point has been taken from literature<sup>6</sup> and demonstrates that Fp tends to increase more rapidly than expected from calculations based on the increase in the mass absorption coefficient.

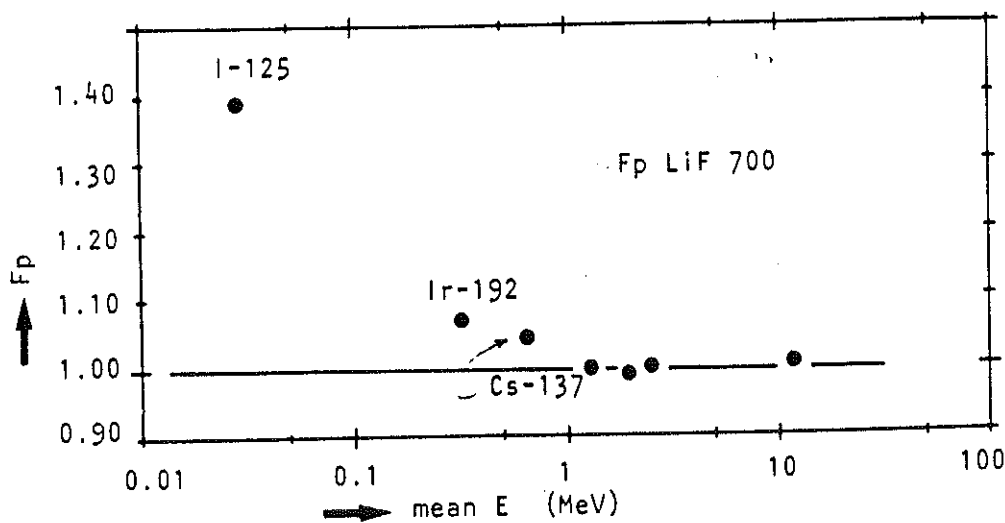


Fig. 1. Measured response of LiF 700 powder relative to 4 MV. The characteristic has been extended to lower energies, demonstrating the rapid increase at energies below about 1 MeV.

Energy response to high energy electrons. The results of the measurements of Fe (see eq. 2) are presented in figure 2. Electron doses to the LiF in the perspex phantom were determined with the NACP parallel plate ionization chamber. Symbols indicate Fe values based on NACP dose measurements. All LiF capsules have been irradiated at the depth of the effective measuring point of the ionization chamber. At selected points the measurements have been repeated with LiF capsules of 1.0 mm instead of 1.6 mm inner diameter. Within the experimental error the same values for Fe were observed. From cavity theory and the discussions about this subject in the literature it became clear that cavity sizes of the order of about a millimeter are hard to manage theoretically. New measurements have been carried out at 19 MeV using 0.1 mm thick (12.7 mm diam.) LiF 700 PTFE disks. This experiment yielded an Fe value of  $0.89 \pm 0.02$ , being far from the theoretical value 0.99 - 1.00 for thin LiF TLD elements. Subsequently, measurements have been performed using LiF powder distributed over a thin layer of 0.1 - 0.2 mm thickness. In this case a value of  $0.93 \pm 0.03$  was obtained. This slightly higher value has a larger uncertainty because the experimental conditions of the loose powder in the solid phantom were less favorable.

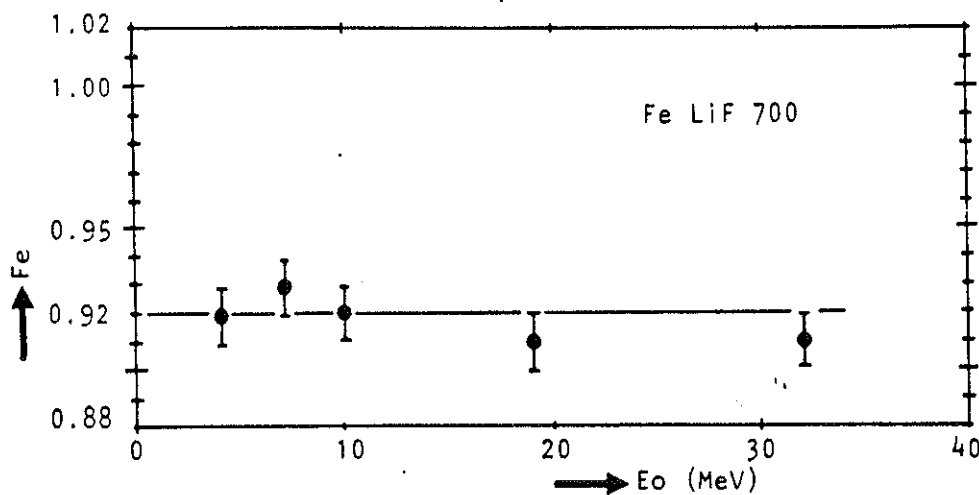


Fig. 2. Results of Fe measured with LiF 700 powder. Symbols are Fe determined using the NACP parallel-plate ionization chamber.

#### DISCUSSION

As shown, supralinearity is independent of the radiation quality for average photon energies above about 100 keV. There is a small difference in the magnitude of supralinearity observed in batches obtained from different manufacturers, possibly due to small differences in dopants. The supralinearity ratio  $F_s$  remains stable after repeated annealing procedures. It should be

realized that the results may be highly dependent on the annealing and read-out procedures. Analysis of differences in energy response of LiF or other TLD materials to high energy photons and electrons is based on cavity theory. Cavity theory has been applied to calculate the absorbed dose in the LiF cavity in a medium of different material. In the comparison of the TL response of LiF per unit dose of photons or electrons, the dose actually absorbed by the LiF determines the response. Cavity theory relates the ratio of absorbed dose in the medium  $D_m$  to the dose in the cavity  $D_c$  by:

$$f = D_c/D_m \quad (3)$$

The ratio  $f$  appears in the calculation of the absorbed dose in the LiF relative to the dose to the medium for the reference radiation quality as well as for the radiation quality considered.

The ratio of the response to electrons relative to the reference photon radiation quality (Co-60 or 4 MV) is:

$$F_e = \frac{D_c/D_m \text{ (electrons)}}{D_c/D_m \text{ (ref. photons)}} \quad (4)$$

For the exact formulation of the cavity theory, the reader is referred to the literature<sup>7</sup>. For this study the formulations of Ogunleye and Fregene<sup>8</sup> and a more recent modification by Horowitz and Dubi<sup>9</sup> are applied. The observed  $F_e$  value of the capsules for electrons is 0.92. However, theory predicts  $F = 0.98 \pm 0.01$ . Modifications of cavity theory did not significantly affect this result. A problem in getting reliable  $F_e$  values for the loose powder is its airy structure. Therefore, the experimental results of the PTFE discs and the thin LiF powder layer, which give similar results, are surprising. Theory predicts  $F_e$  values very close to unity. The electron fluence disturbance due to inhomogeneity by introducing the LiF powder capsule is negligible<sup>10</sup>. Also the disturbance by the PTFE/LiF discs is negligible because its small thickness and density comparable to LiF.

## CONCLUSION

Supralinearity may affect the accuracy of TLD. A number of sources and explanations have been reported in the literature for the phenomenon of supralinearity. However, the actual supralinearity of the LiF depends on its composition, (thermal) history and read-out procedure etc.. Therefore the actual supralinearity should repeatedly be checked for the TL-material in use.

The measured supralinearity ratio  $F_s$  for Harshaw LiF 700 powder is  $1.21 \pm 0.02$  for most of the radiation qualities in use for radiotherapy. There is an indication of a decrease in supralinearity for soft X-ray qualities, which is in agreement with the literature.

The energy dependence of the LiF 700 for high energy photons and electrons has been assessed. TL-response for photon energies  $E_m > 1.3$  MeV relative to the 4 MV photon beam is unity. However the TL-response to high energy electrons ( $4 < E_e < 28$  MeV) is systematically  $8 \pm 1\%$  lower compared to the 4 MV reference beam. These results are valid for 1.6 mm inner diameter LiF capsules. Measurements using 0.1 mm thick PTFE LiF 700 disks as well as 0.1 - 0.2 mm thick layers of LiF 700 powder yielded a relative response of  $0.89 \pm 0.02$  and  $0.93 \pm 0.03$  respectively. Contrary to expectation the results of the thin discs are in disagreement with cavity theory, which predicts  $F_c = 1$  for thin cavities. Cavity theories applied to the dimensions ( $\phi$  1.0 - 1.6 mm) and consistency of the LiF in the capsules (airy powder) are not yet in accordance with experimental results. A 5 per cent discrepancy remains between the experimental  $F_c$  values and the  $F_c$  values predicted by cavity theory. The simple TL-response to dose conversion as derived for the 4 MV reference beam<sup>1</sup> is applicable to high energy photons and electrons, taking into account a  $0.92^{-1}$  correction to the electron response.

#### REFERENCES

1. J.P.A. Marijnissen and B. Göbel, TLD using LiF 700 powder applied in radiotherapy: Practical aspects and results, Proceedings TLD-symposium Bilthoven, The Netherlands, 1988.
2. Procedures in external radiation dosimetry with electron and photon beams with maximum energies between 1 and 50 MeV, Acta Rad.Oncology 19 (1980) 55-79.
3. -, Acta Rad.Oncology 20 (1981) 401-415.
4. V.K. Jain, S.P. Kathuria and A.K. Ganguly, Supralinearity and sensitisation in LiF TLD phosphor, J.Phys.C:Solid State Phys. 7 (1974) 3810-3816.
5. A. Shiragai, Effects of grain size and initial trap density on supralinearity of LiF-TLD, Health Phys. 18 (1970) 728-729.
6. K.A. Weaver, Response of LiF to  $^{125}\text{I}$  photons. Med.Phys. 11 (1984) 850-854.
7. T.E. Burlin, A general theory of cavity ionization, Br. J. Radiol. 39 (1966) 727.
8. O.T. Ogunleye and A.O. Fregene, Application of cavity theories to high energy response of LiF dosimeters, Radiat.Res. 87 (1981) 251-264.
9. Y.S. Horowitz and A. Dubi, A proposed modification of Burlin's general cavity theory for photons, Phys.Med.Biol. 6 (1982) 867-870.
10. M. Goitein, A technique for calculation the influence of thin inhomogeneities on charged particle beams, Med. Phys. 5 (1978) 258-264.

COMPUTERIZED ANALYSIS OF GLOW CURVES FROM LiF:Mg,Ti (TLD-100)

W. de Vries, J.E. Hoogenboom, J.B. Dielhof and A.J.J. Bos

Interfaculty Reactor Institute, Delft University of Technology  
Mekelweg 15, NL 2629 JB Delft, The NetherlandsINTRODUCTION

Computerized glow curve analysis is an advanced technique used to study various parameters associated with the charge transfer that occurs during thermoluminescence emission. Recently a computer program has been developed<sup>1</sup> to analyze complex glow curves, based on a non-linear least-squares program FATAL<sup>2</sup>. The program decomposes a measured glow curve into a number (up to ten) different glow peaks, each of them described by four physical parameters of the TL-process involved: 1) the order of kinetics of the process 2) the trap depth 3) a frequency factor and 4) the number of traps.

In this study the applicability of this computer program for analyzing glow curves of LiF:Mg,Ti (TLD-100) in routine dosimetry is investigated. Glow curve analysis by decomposing the measured glow curve into individual peaks has a number of advantages over the method of integrating part of the glow curve (currently used in routine dosimetry). Firstly it makes time consuming low temperature annealing (24h at 80°C) redundant. Secondly, dose evaluation becomes much more independent of fading of the low temperature peaks. Low temperature peaks can even be used for determining the elapsed time since irradiation<sup>3,4</sup>. Finally, the technique may lead to an improved precision in dose measurement and a lower detection limit<sup>5</sup>.

However, a prerequisite using computerized glow curve analysis in routine TL dosimetry is a model of the TL-process that describes the shape of the glow curve exclusively in terms of the dose, i.e. a model which is independent of the experimental and/or radiation field parameters. In this investigation we study the constancy of the various model parameters for different radiation types, energies and doses.

THEORY

A common description of the TL-process is given by the differential equation

$$\frac{dn}{dt} = -s' n^p(t) e^{-E/kT} \quad (1)$$

where  $n(t)$  is the number of trapped electrons as a function of time  $t$ ,  $E$  the

energy needed to release an electron from a trap,  $s'$  a parameter proportional to the frequency of occurrence,  $p$  the order of the process,  $k$  Boltzmann's constant and  $T$  the absolute temperature.

With initial condition  $n(t=0)=n_0$  and

$$s = s' n^{p-1} \quad (2)$$

the rate of release of electrons from a single trap  $I(t)=-dn/dt$  can be solved from differential equation (1). As  $I(t)$  is measured with some efficiency  $\epsilon$  the measured intensity  $J(t)=\epsilon I(t)$  can be written as

$$J(t)=\epsilon I(t)=m_0 s e^{-E/kT} \left(1 + (p-1) \int_0^t e^{-E/kT'} dt'\right)^{-\frac{p}{p-1}} \quad (3)$$

with  $m_0 = \epsilon n_0$ .

The limit for a first order process ( $p=1$ ) becomes

$$J(t) = m_0 s e^{-E/kT} \exp\left(-s \int_0^t e^{-E/kT'} dt'\right) \quad (4)$$

The computer program fits a number of glow peaks to the measured glow curve by minimizing the function

$$S = \sum_i w_i \left( J(t_i) - \sum_{n=1}^N J_n(t_i) \right)^2 \quad (5)$$

with  $J(t_i)$  the measured glow curve for time  $t_i$ ,  $J_n(t_i)$  the theoretical value of glow peak  $n$  for time  $t_i$ ,  $w_i$  a weight factor (currently set to 1 for all times  $t_i$ ) and  $N$  the number of single peaks in the glow curve.

The process order  $p$  for each peak has to be predetermined, the parameters  $m_0$ ,  $E$  and  $s$  will be fitted by the program.

### EXPERIMENTAL

The TLD-100 chips use in the experiments were selected from a batch of LiF:Mg,Ti chips (Harshaw) with dimensions  $3.2 \times 3.2 \times 0.38$  mm<sup>3</sup>. Before irradiation the chips were annealed at 400°C for 1 hour, followed by rapid cooling to room temperature ( $360$  °C min<sup>-1</sup>). <sup>60</sup>Co irradiation was performed with a local irradiation facility, X irradiation with a 250 kV X-ray apparatus, provided with a standard filter set<sup>6</sup>. For  $\beta$ -irradiations a 93 MBq <sup>90</sup>Sr/<sup>90</sup>Y source was used, for  $\alpha$ -irradiations a 500 Bq <sup>244</sup>Cm source.  $\gamma$  and X irradiations were performed in 4.0 and 0.5 mm thick phantoms of A-150 plastic,

respectively. For  $\alpha$  and  $\beta$  irradiations no phantom was used.

A modified Harshaw TL-reader in combination with a microprocessor<sup>7</sup> was used for readout of the dosimeters. The readout took place within 10 hours from irradiation, at a linear heating rate of  $1.00 \text{ }^\circ\text{C s}^{-1}$ . The maximum readout temperature was  $360 \text{ }^\circ\text{C}$ . The resulting glow curve consists of 512 pairs of temperature and light output, recorded at a time interval of 0.75 seconds. Every readout from a dosimeter was followed by a second one, used for subtraction of background and infra red light output.

Analysis of the glow curves of the dosimeters was performed on a VAX-11/750 computer.

## RESULTS

At present it is accepted that the most important glow peaks in TLD-100, peaks 2-5, follow first order kinetics<sup>8,9,10</sup>. This is confirmed by the value of the fit parameter  $S$  from Eq.(5), which increases strongly when the process order of one or more peaks is set to a value not equal 1. For this reason analysis was performed with four first order peaks in the temperature range from 355 K to 495 K (figure 1.). The results of the analysis for different radiation types and energies are given in table 1. Each value listed is the average of four chips.

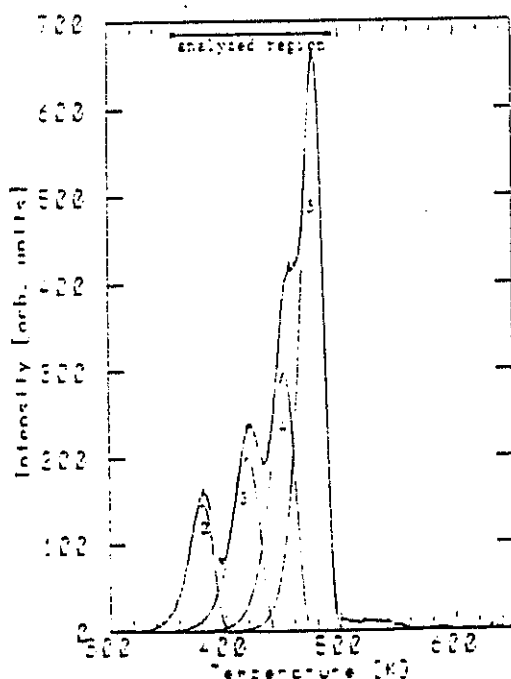


Figure 1  
Measured and fitted TLD-100 glow curve obtained after  $\beta$ -irradiation. The numbers indicate the component glow peaks analyzed.

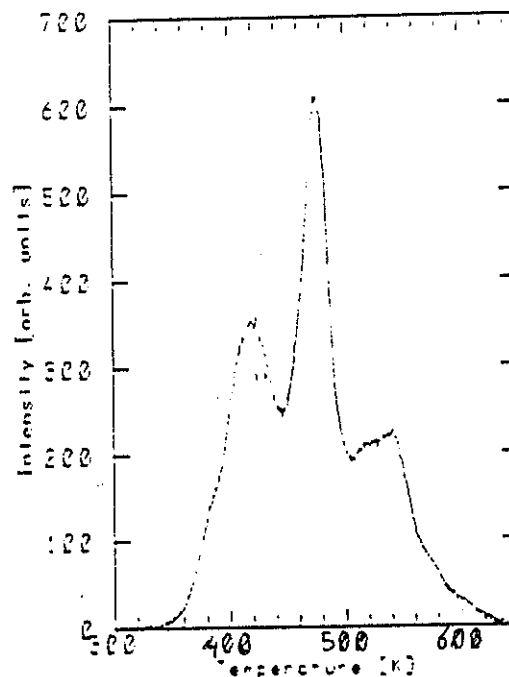


Figure 2  
TLD-100 glow curve obtained after  $\alpha$ -irradiation.



Table 1. Results of the analysis for different radiation types and energies

| Radiation type | Radiation energy [MeV] | parameter             | peak 2              | peak 3              | peak 4              | peak 5              |
|----------------|------------------------|-----------------------|---------------------|---------------------|---------------------|---------------------|
| $\gamma$       | $^{60}\text{Co}$       | E [eV]                | 1.22                | 1.28                | 1.64                | 2.00                |
|                |                        | s [ $\text{s}^{-1}$ ] | $1.3 \cdot 10^{15}$ | $1.8 \cdot 10^{14}$ | $1.5 \cdot 10^{17}$ | $1.1 \cdot 10^{20}$ |
|                |                        | $T_m$ [K]             | 380.5               | 420.5               | 452.7               | 479.4               |
| X              | 0.029                  | E                     | 1.23                | 1.27                | 1.64                | 2.03                |
|                |                        | s                     | $2.1 \cdot 10^{15}$ | $8.0 \cdot 10^{13}$ | $2.0 \cdot 10^{17}$ | $2.4 \cdot 10^{20}$ |
|                |                        | $T_m$                 | 380.5               | 419.6               | 451.7               | 478.3               |
| X              | 0.048                  | E                     | 1.21                | 1.25                | 1.64                | 1.99                |
|                |                        | s                     | $1.2 \cdot 10^{15}$ | $9.7 \cdot 10^{13}$ | $2.0 \cdot 10^{17}$ | $9.8 \cdot 10^{19}$ |
|                |                        | $T_m$                 | 378.8               | 418.1               | 450.3               | 477.2               |
| X              | 0.065                  | E                     | 1.22                | 1.25                | 1.61                | 1.98                |
|                |                        | s                     | $1.5 \cdot 10^{15}$ | $1.1 \cdot 10^{14}$ | $8.9 \cdot 10^{16}$ | $7.6 \cdot 10^{19}$ |
|                |                        | $T_m$                 | 379.2               | 418.4               | 450.4               | 477.4               |
| X              | 0.083                  | E                     | 1.21                | 1.26                | 1.61                | 1.98                |
|                |                        | s                     | $1.2 \cdot 10^{15}$ | $1.4 \cdot 10^{14}$ | $9.1 \cdot 10^{16}$ | $7.6 \cdot 10^{19}$ |
|                |                        | $T_m$                 | 379.0               | 418.2               | 450.2               | 477.2               |
| X              | 0.100                  | E                     | 1.22                | 1.26                | 1.63                | 2.00                |
|                |                        | s                     | $1.2 \cdot 10^{15}$ | $1.1 \cdot 10^{14}$ | $1.4 \cdot 10^{17}$ | $1.1 \cdot 10^{20}$ |
|                |                        | $T_m$                 | 380.9               | 420.5               | 452.6               | 479.6               |
| X              | 0.118                  | E                     | 1.21                | 1.29                | 1.60                | 2.01                |
|                |                        | s                     | $1.1 \cdot 10^{15}$ | $3.0 \cdot 10^{14}$ | $1.0 \cdot 10^{17}$ | $1.8 \cdot 10^{20}$ |
|                |                        | $T_m$                 | 379.5               | 418.7               | 450.9               | 477.6               |
| X              | 0.161                  | E                     | 1.21                | 1.26                | 1.63                | 1.97                |
|                |                        | s                     | $1.5 \cdot 10^{15}$ | $1.4 \cdot 10^{14}$ | $1.6 \cdot 10^{17}$ | $6.9 \cdot 10^{19}$ |
|                |                        | $T_m$                 | 378.5               | 417.8               | 449.8               | 476.8               |
| X              | 0.205                  | E                     | 1.21                | 1.27                | 1.60                | 1.98                |
|                |                        | s                     | $1.2 \cdot 10^{15}$ | $1.8 \cdot 10^{14}$ | $7.7 \cdot 10^{16}$ | $9.3 \cdot 10^{19}$ |
|                |                        | $T_m$                 | 378.4               | 417.6               | 449.8               | 476.7               |
| $\beta$        | 0.55 max.              | E                     | 1.22                | 1.27                | 1.63                | 2.01                |
|                |                        | s                     | $1.4 \cdot 10^{15}$ | $1.5 \cdot 10^{14}$ | $1.4 \cdot 10^{17}$ | $1.5 \cdot 10^{20}$ |
|                |                        | $T_m$                 | 379.7               | 419.0               | 451.2               | 477.9               |

The glow curve obtained after  $\alpha$ -irradiation shows a much more complex structure (see figure 2.). It appears that this glow curve cannot be fitted with the parameters of table 1. A best fit to the measured curve required a minimum of twelve peaks.

The results of the analysis for different dose values are given in table 2. The values of the parameters in table 2 show considerably more aberrations than those in table 1. For the lowest dose values this is due to the poor statistics (the maximum channel content for the lowest dose value is 14 counts). For high dose values the high temperature part of the glow curve (following peak 5) becomes much more expressive. As can be seen from figure 3 this part of the glow curve grows more than proportional to the low temperature part. Especially at the highest dose (600 Gy) it can be seen from figure 3 that there is a peak at the high temperature wing of peak 5 (a peak marked as peak 5a by Fairchild<sup>8</sup>, but not detected by Horowitz<sup>11</sup>). Not fit-

Table 2. Results of the analysis for different doses

| Radiation type   | Dose [Gy] | parameter            | peak 2               | peak 3               | peak 4               | peak 5               |
|------------------|-----------|----------------------|----------------------|----------------------|----------------------|----------------------|
| <sup>60</sup> Co | 0.0005    | E [eV]               | 1.12                 | 1.23                 | 1.77                 | 2.01                 |
|                  |           | s [s <sup>-1</sup> ] | 7.2·10 <sup>13</sup> | 3.7·10 <sup>13</sup> | 6.1·10 <sup>18</sup> | 1.3·10 <sup>20</sup> |
|                  |           | T <sub>m</sub> [K]   | 379.6                | 420.5                | 452.7                | 479.4                |
| <sup>60</sup> Co | 0.005     | E                    | 1.25                 | 1.26                 | 1.63                 | 2.00                 |
|                  |           | s                    | 3.7·10 <sup>15</sup> | 1.0·10 <sup>14</sup> | 1.3·10 <sup>17</sup> | 1.0·10 <sup>20</sup> |
|                  |           | T <sub>m</sub>       | 380.5                | 420.5                | 452.7                | 479.4                |
| <sup>60</sup> Co | 0.05      | E                    | 1.22                 | 1.28                 | 1.64                 | 2.00                 |
|                  |           | s                    | 1.3·10 <sup>15</sup> | 1.8·10 <sup>14</sup> | 1.5·10 <sup>17</sup> | 1.1·10 <sup>20</sup> |
|                  |           | T <sub>m</sub>       | 380.5                | 420.5                | 452.7                | 479.4                |
| X(50 kVp)        | 0.2       | E                    | 1.18                 | 1.28                 | 1.69                 | 1.94                 |
|                  |           | s                    | 4.9·10 <sup>14</sup> | 2.0·10 <sup>14</sup> | 7.4·10 <sup>17</sup> | 2.0·10 <sup>18</sup> |
|                  |           | T <sub>m</sub>       | 380.5                | 420.5                | 452.7                | 479.4                |
| X(50 kVp)        | 2         | E                    | 1.18                 | 1.27                 | 1.67                 | 1.94                 |
|                  |           | s                    | 4.6·10 <sup>14</sup> | 1.8·10 <sup>14</sup> | 5.1·10 <sup>17</sup> | 4.3·10 <sup>18</sup> |
|                  |           | T <sub>m</sub>       | 380.5                | 420.5                | 452.7                | 479.4                |
| X(50 kVp)        | 6         | E                    | 1.19                 | 1.27                 | 1.66                 | 1.96                 |
|                  |           | s                    | 7.2·10 <sup>14</sup> | 1.4·10 <sup>14</sup> | 3.4·10 <sup>17</sup> | 4.5·10 <sup>18</sup> |
|                  |           | T <sub>m</sub>       | 380.5                | 420.5                | 452.7                | 479.4                |
| X(50 kVp)        | 60        | E                    | 1.20                 | 1.29                 | 1.68                 | 2.02                 |
|                  |           | s                    | 8.2·10 <sup>14</sup> | 2.3·10 <sup>14</sup> | 4.9·10 <sup>17</sup> | 1.9·10 <sup>20</sup> |
|                  |           | T <sub>m</sub>       | 380.5                | 420.5                | 452.7                | 479.4                |
| X(50 kVp)        | 600       | E                    | 1.29                 | 1.23                 | 1.74                 | 1.88                 |
|                  |           | s                    | 1.7·10 <sup>16</sup> | 4.2·10 <sup>13</sup> | 2.6·10 <sup>18</sup> | 7.8·10 <sup>18</sup> |
|                  |           | T <sub>m</sub>       | 380.5                | 420.5                | 452.7                | 479.4                |

ting these high temperature peaks influences the parameters of the other peaks significantly.

DISCUSSION AND CONCLUSIONS

It has been shown that the trapping parameters (activation energy E and frequency factor s) corresponding to the glow peaks 2, 3, 4 and 5 of TLD-100 found by computerized analysis of the glow curve are the same for each peak, irrespective of photon energy (within the range from 29 keV to 1.25 MeV) and photon dose (within the range from 0.0005 to 1 Gy). Glow curves induced by β's of a <sup>90</sup>Sr/<sup>90</sup>Y source also give the same values.

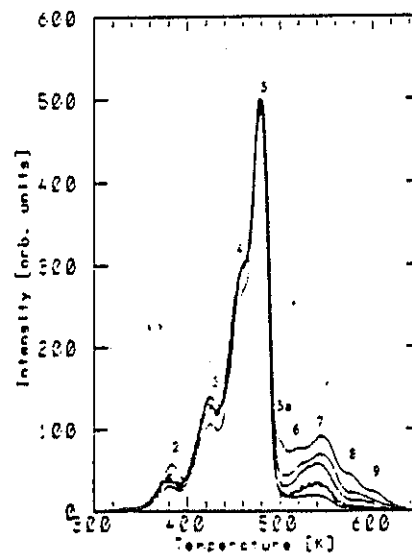


Figure 3  
Glow curves obtained after 50 kVp X-irradiation. Dose ranging from 0.2 to 600 Gy (see table 2). The numbers indicate component glow peaks. The curves are normalized on the highest channel content.

Because in the fitting procedure the quantities  $E$  and  $s$  are implemented as free parameters this result means that the model used describes the glow curve of TLD-100 (i.e. peaks 2 to 5) in a consistent way. Therefore it is justified to develop a program that just fits the values of the third parameter  $m_0$  which is proportional to the absorbed dose. The dose range for which the model has been proven to be valid is large enough to use that program in routine dosimetry for dose evaluation. An additional advantage of reducing the number of parameters from three to one per peak is the reduction of CPU-time needed per dosimeter.

For higher doses ( $D > 1$  Gy) and  $\alpha$  irradiations the glow curve becomes much more complex. More peaks are needed to get a good fit. Glow curve analysis becomes very complicated and time consuming. As long as no internal consistency for the peak parameters for different radiation fields has been found it is not justified to use computerized glow curve analysis in high dose dosimetry, e.g. for radiation therapy.

#### REFERENCES

1. J.E. Hoogenboom, W. de Vries, J.B. Dielhof and A.J.J. Bos, Computerized analysis of glow curves from thermally activated processes, *J. Appl. Phys.* 64(6) (1988) 3193-3200
2. L. Salmon and D.V. Booker, report AERE-R 7129 (1972)
3. M. Moskovitch, Automatic method for evaluating elapsed time between irradiation and readout in LiF-TLD, *Radiat. Prot. Dosim.* 17(1986) 165-169
4. C. Furetta, J.W.N. Tuyn, F. Louis, J. Azorin-Nieto, A. Gutiérrez and C.M.H. Driscoll, A method for determining simultaneously the dose and the elapsed time since irradiation using TLD's, *Appl. Radiat. Isot.* 39(1) (1988) 59-69
5. Y.S. Horowitz, M. Moskovitch and M. Wilt, Computerized glow curve deconvolution applied to ultralow dose LiF thermoluminescence dosimetry, *Nucl. Instr. and Meth.* A244 (1986) 556-564
6. International standard ISO 4037 (1983)
7. M.H. van Wijngaarden, J. Plaisier and A.J.J. Bos, A microprocessor Controlled Thermoluminescence Dosimeter Reader for Routine Use and Research, *Radiat. Prot. Dosim.* 11(3) (1985) 179-183
8. R.G. Fairchild, P.L. Mattern, K. Langweiler and P.W. Levy, Thermoluminescence of LiF TLD-100: Glow curve Kinetics, *J. Appl. Phys.* 49 (1978) 4523-4533
9. A. Delgado and J.C. Barreiro, On the Determination of the Order of Kinetics for Peak V in LiF TLD-100 by Isothermal Decay Methods, *Radiat. Prot. Dosim.* 16(4) (1986) 295-300
10. S.W.S. McKeever, *Thermoluminescence of Solids* (Cambridge University Press) (1986)
11. Y.S. Horowitz and M. Moskovitch, Computerized glow curve deconvolution applied to high dose ( $10^2 - 10^5$  Gy) TL dosimetry, *Nucl. Instr. and Meth.* A243 (1986) 207-214

CARBON LOADED DOSEMETERS FOR THE MEASURE OF THE SHALLOW DOSE  
EQUIVALENT DUE TO BETA-RADIATION

H.E. Preston

Vinten Instruments Limited, Jessamy Road,  
Weybridge, Surrey, KT13 8LE, United Kingdom

INTRODUCTION

One of the undeveloped areas in current TL dosimetry is the measurement of beta-doses, whether to the extremities or the whole body. The measurement of quantity  $H_p(0.07)$  i.e. dose equivalent at a depth of  $7 \text{ mg/cm}^2$  tissue due to beta-radiation is difficult because the large majority of available TL detectors are relatively thick, typically from  $44 \text{ mg/cm}^2$  for a 0.2 mm PTFE disc to  $\approx 200 \text{ mg/cm}^2$  for a 0.9 mm pellet. There have been many attempts to produce thin TL detectors, but to date the detectors have been largely experimental and have not been produced in quantities to satisfy large scale application. The basic problem is to produce a dosimeter which, while being physically thick for ease of handling and length of useful life, will behave to radiation as if it were thin. Developments have taken place over the past twelve months which lead us to believe that we have such a dosimeter, i.e. dosimetrically thin but physically thick.

DOSIMETRIC REQUIREMENTS

For the measurement of dose to the skin of the body or an extremity i.e. the Dose Equivalent Superficial  $H_p(0.07)$ , the recommendations of the ICRP<sup>1</sup> are that the dose to be measured is that at a depth of  $7 \text{ mg/cm}^2$  in tissue. Currently due to the inadequacies of available dosimeters, the ISO<sup>2</sup> have set down standards of performance for skin dosimeters which fall far short of the ideal. The relevant performance characteristic is as follows:

Energy response (beta-rays) in the range (EMAX) 0.5 to 3 MeV: the response shall not vary more than 30%.

There is, however, increasing pressure to adopt the  $7 \text{ mg/cm}^2$  depth even for extremity dosimeters, and therefore dosimeters for extremity use should be designed to measure this quantity.

There is a number of extremity dosimeters in use which satisfy the beta and photon response criteria. However, they are generally either experimental, in small scale use, or are based upon the ring dosimeter and cannot be used on the finger tips. Currently used dosimeters for the measurement of beta-dose,

consist of a detector of thickness from 10-200 mg/cm<sup>2</sup> and a covering layer which may vary from 3 to 12 mg/cm<sup>2</sup>. The dosimeter response of currently available dosimeters will be relatively low at low beta-energies since the normal TL dosimeter will be too thick and absorption of radiation within the detector will be high.

There are two ways of increasing the response of the TL dosimeter to soft beta-radiation (1) to reduce the thickness of the covering material and (2) to reduce the thickness of the dosimeter. Ideally the covering material should be 7 mg/cm<sup>2</sup> thick and the dosimeter infinitely thin. This is clearly impossible in practice so some form of compromise is necessary. Marshall<sup>3</sup> has suggested that a detector of 5 mg/cm<sup>2</sup> under a filter of 5 mg/cm<sup>2</sup> is very close to the ideal. Calculation shows that the response of such a dosimeter at 0.2 MeV would be 0.96 x its response at 2 MeV.

#### ENHANCEMENT OF BETA-RESPONSE

However, if we consider what physical thickness is represented by 5 mg/cm<sup>2</sup> in LiF we find it is of the order of 23 μm, which if we assume LiF is a body centred cubic crystal, represents a grain size of 40 μm. At very low grain sizes the thermoluminescent output is considerably reduced and reasonable sensitivity with low background is not achievable at grain sizes much less than 90 μm. The effective thickness therefore of the thinnest dosimeter is of the order of 10 mg/cm<sup>2</sup>.

The response of such a dosimeter can be improved by using a thinner covering layer. However, this layer should preferably be light tight and capable of resisting quite harsh usage. At present we have not found a material satisfying these requirements at less than 3-4 mg/cm<sup>2</sup>.

#### PRACTICAL REALISATION OF THE 'BEST' DOSEMETER

For purely extremity dosimetry there is already a dosimeter whose response is close to the ideal. This is the extremity tape, which when fitted with the 3.4 mg/cm<sup>2</sup> covering has a response at 0.2 MeV of 0.83 its response at 2 MeV. (The extremity tape consists of a thin layer LiF powder, mounted on adhesive high temperature Kapton tape). However, the dosimeter is disposable and cannot easily be used for the measurement of whole body skin dose.

Generally dosimeters to measure low penetrating radiation have been produced by bonding thin layers of TL material onto more substantial substrates such as aluminium plates or thick PTFE, and have proved difficult to produce in

commercial quantities. In principle the simplest method for reducing the effective thickness of a dosimeter is to prevent the light from all depths of the dosimeter except the surface layer from escaping from the detector. This effect can be achieved by mixing an optically opaque substance into the TL matrix. The most obvious substance being graphite (carbon) since it is black and has properties close to tissue, i.e. low Z number. The technique is not new and has been attempted by Harshaw Bøter-Jensen<sup>4</sup> and others. However, no one has to date succeeded in preparing these materials in large quantities and they are still not in general use.

The two main forms of TL dosimeter in common use are the PTFE discs and the chip or pellet. We have attempted to produce carbon loaded dosimeters based upon both these forms but to date we have concentrated on the PTFE disc form. The following will particularly deal with the properties of the carbon loaded disc as we feel that this dosimeter is ready for production, whereas the work on the carbon loaded pellet is not yet completed.

The introduction of carbon into the PTFE matrix of a 0.4 mm thick disc will obviously effect a number of properties of the disc, i.e.

- (1) Sensitivity.
- (2) Reading from unirradiated dosimeter after anneal.
- (3) Minimum detectable dose.
- (4) Soft  $\beta$ -response which can be quantified in terms of the response to Pm relative to Sr/Y or Cs-137.

#### PROPERTIES OF THE CARBON LOADED DISC

These quantities will vary with the percentage of carbon introduced and the variation with loading are shown in Figs. 1, 2 and 3. It can be seen from Fig. 1 that the sensitivity falls very rapidly for percentages of carbon up to 5% when the sensitivity levels off. From Fig. 2 we can see that both background and Minimum Detectable Levels (MDL) rise with carbon percentage. Figure 3 shows the variation in the Pm/Sr response with carbon content and we can see that from 5 to 10% loading the response to soft beta-radiation is constant. Table 1 summarizes relative response of carbon loaded disc to normal disc.

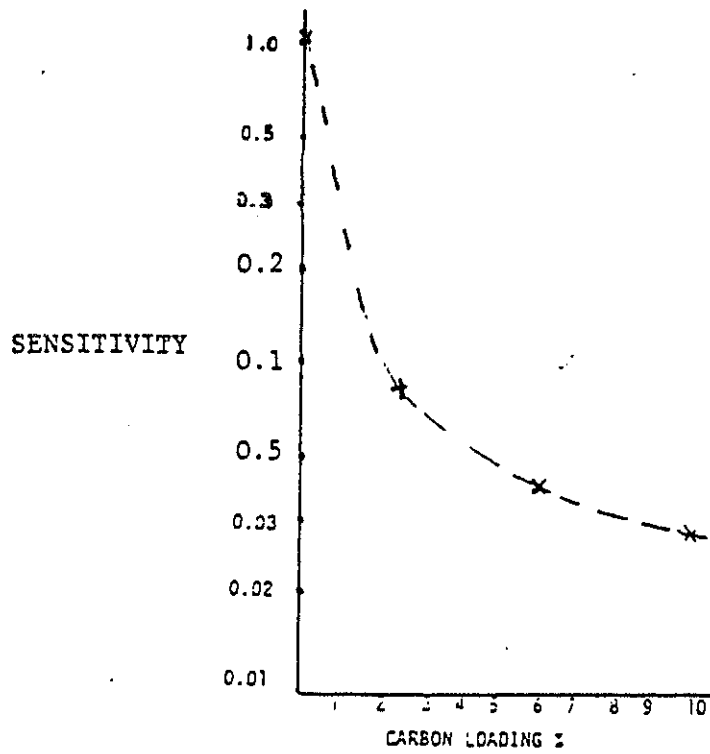


Fig. 1. Variation in sensitivity of disc with carbon loading (% by weight)

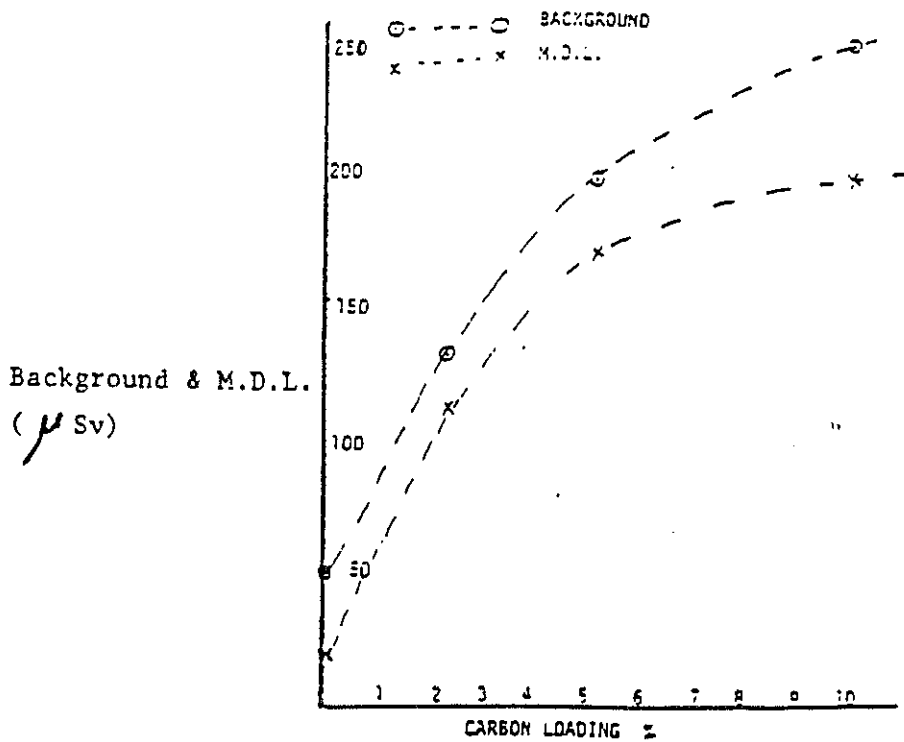


Fig. 2. Variation of background and MDL with carbon loading

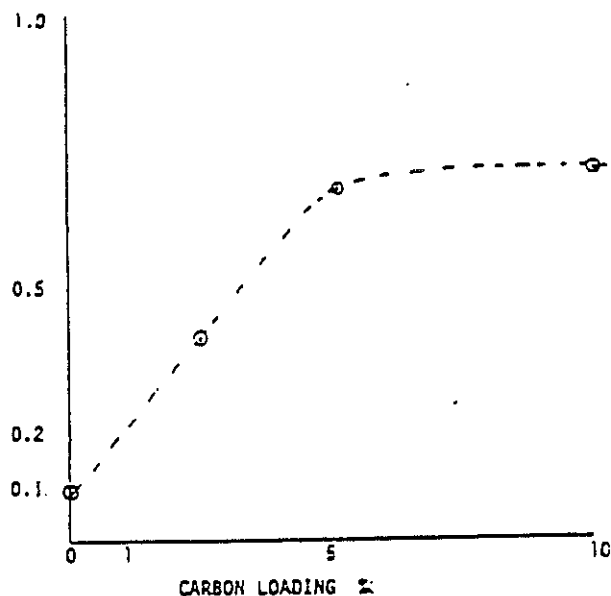


Fig. 3. Variation in Pm/Sr ratio with carbon loading (6 mg/cm<sup>2</sup> polythene)

Table 1. Comparison of some properties of normal and carbon loaded discs.

| Property                 | Normal disc   | Carbon disc   |
|--------------------------|---------------|---------------|
| Sensitivity              | 1.0 ± 7%      | 0.02 ± 9%     |
| Background               | 100 μSv ± 20% | 240 μSv ± 20% |
| Minimum Detectable Level | 60 μSv        | 140 μSv       |
| Pm/Sr response           | 0.07          | 0.82          |

DISCUSSION AND CONCLUSIONS

It is possible to produce a dosimeter which response is close to the ideal beta dosimeter by introducing carbon into the dosimeter matrix. The measurement of the dose equivalent superficial as defined by the ICRU (H<sub>s</sub>(0.07)) for finger tips is covered by the extremity tape currently produced, with improved response characteristics, when covered by the 3-4 mg/cm<sup>2</sup> bilaminar material. However, the nature of the extremity tape means that it is a non-reusable dosimeter and some users prefer to reuse their dosimeters for technical and/or economic reasons. In which case the carbon-loaded dosimeter, which can be used many time, in a thin sachet will satisfy their requirements.



The measurement of  $H_s(0.07)$  to the whole body is currently very badly performed for soft beat radiations using 0.2 mm PTFE discs under a covering of  $\approx 12 \text{ mg/cm}^2$  Melinex. Considerable improvement in the measurement of this quantity can be achieved by using a carbon loaded disc in the standard card and replacing the Melinex front covering by the  $3\text{-}4 \text{ mg/cm}^2$  bilaminar plastic.

Work is in progress which will result in a carbon loaded pellet, having similar response characteristics and this will be available in the near future.

#### REFERENCES

1. ICRP (International Commission on Radiological Protection), Recommendations of the ICRP, Publication 26, Pergamon Press, Oxford, UK, 1977
2. ISO (International Organization for Standardization), Standard Thermoluminescent Dosimetry for Personal and Environmental Monitoring, Draft August 13, 1986
3. P. Christensen, Y. Herbout, T.O. Marshall, Personal monitoring for external sources of beta and low energy photon radiations, Radiat. Prot. Dosim. 18 (4) (1987) 241-260
4. Graphite mixed non transparent  $\text{LiF-7 Li}_2\text{B}_4\text{O}_7:\text{Mn}$  TL dosimeters with a two-side readings system for beta-gamma dosimetry, In: Proc. 4th Int. Conf. on Luminescence Dosimetry, Institute of Nuclear Physics, Krakov, 1974.

DOES THE MOST SENSITIVE THERMOLUMINESCENT MATERIAL COME FROM CHINA?Some characteristics of LiF:Mg,Cu,P (GR-200) TL chips

A.J.J. Bos and J.B. Dielhof

Interfaculty Reactor Institute, Delft University of technology,  
Mekelweg 15, 2629 JB Delft, The NetherlandsINTRODUCTION

In 1978 Nakajima et al.<sup>1</sup> reported about a new highly sensitive thermoluminescence (TL) material. The TL material was a LiF phosphor activated with Mg, Cu and P, available in powder form. Dosimetric properties of that new TL material have also been investigated by others<sup>2,3,4</sup>. The TL sensitivity (measured by light integration) to gamma rays was found to be 23 to 38 times higher than that of LiF:Mg,Ti (TLD-100). All investigators reported a decrease in sensitivity after repeated use. It was also reported that the sensitivity strongly depends on the temperature and duration of the annealing procedure<sup>2</sup>. A main drawback of the TL material was the powder form, implicating a relatively high background, inconvenience in handling and poor repeatability. This drawback has been overcome with the production of solid LiF:Mg,Cu,P (GR-200) chips<sup>5</sup>, developed with the aid of a special technology in the Central Research Laboratory, Beijing in China. The producers claim both the advantages of the outstanding characteristics of the material in powder form and further superiorities as: lower detection threshold, simplification in re-use and convenience in handling. The aim of the present investigation is to study some dosimetric characteristics of the GR-200 chips in order to verify the claims of the manufacturer.

MATERIALS

For reasons of comparison some other TL materials were studied as well. Relevant data regarding the investigated TL materials are summarized in

Table 1. Investigated TL Materials

| Material   | Trade name    | Manufacturer                    | Country |
|--|---------------|---------------------------------|---------|
| LiF:Mg,Ti  | TLD-100       | Harshaw Chem. Co., Ohio         | USA     |
| LiF:Mg,Na  | PTL-710       | Desmarquest & CEC, Evreux       | France  |
| LiF:Mg,Cu,P  | GR-200        | Beijing Shiyang Rad. Det. Works | China   |
| CaF <sub>2</sub> :Dy                                 | TLD-200       | Harshaw Chem. Co., Ohio         | USA     |
| Li <sub>2</sub> B <sub>4</sub> O <sub>7</sub> :Mn,Si | LiB           | Alnor, Turku                    | Finland |
| Al <sub>2</sub> O <sub>3</sub>                       | AL            | Desmarquest & CEC, Evreux       | France  |
| BeO  | Thermalox 995 | Brush Beryll Co., Ohio          | USA     |

Table 2. Dimensions, mass and applied annealing cycle of the investigated TL materials

| Material | $Z_{eff}$ | Dimensions (mm)        | Mass* (mg) | Annealing procedure** |
|----------|-----------|------------------------|------------|-----------------------|
| TLD-100  | 8.14      | 3.2 x 3.2 x 0.9        | 23.9 ± 0.3 | 1h 400 °C, 21 h 80 °C |
| PTL-710  | 8.14      | diam. 4.5; thick 0.85  | 34.4 ± 0.4 | 0.5 h 500 °C          |
| GR-200   | 8.14      | 4 x 4 x 0.8            | 33.9 ± 0.8 | 10 min 240 °C         |
| TLD-200  | 16.3      | 3.2 x 3.2 x 0.9        | 28.6 ± 0.2 | 1h 400 °C             |
| LiB      | 7.4       | diam. 4.6; thick 0.8   | 27.7 ± 0.6 | 1h 300 °C             |
| AL       | 10.2      | diam. 5.8; thick 0.9   | 46.7 ± 5.4 | 0.5 h 750 °C          |
| T-995    | 7.13      | diam. 4.95; thick 1.02 | 56.2 ± 0.2 | 15 min 400 °C         |

\* Average and standard deviation of 15 chips

\*\* Every procedure was ended with a fast cooling

Tables 1 and 2. Measurements on GR-200 have been made on 40 samples taken from one production batch. For sensitivity measurements only fifteen samples were used. The TL response and glow curves were measured in a  $N_2$  atmosphere using a modified microprocessor controlled Harshaw 2000 TL reader described elsewhere<sup>6</sup>. Before every irradiation the ribbons were annealed in a specially designed microprocessor controlled annealing oven (Norhof, Vianen, The Netherlands). The oven provides highly reproducible annealing cycles in heating and cooling. In this study the following standard annealing procedure was applied to the GR-200 chips:  $240 \pm 0.5$  °C for 10 minutes in a nitrogen atmosphere with controlled fast cooling to room temperature at a rate of  $235$  °C  $min^{-1}$ .

## RESULTS

### TL glow curve and readout cycle

Figure 1 shows the glow curves of TLD-100 and GR-200 measured at a constant

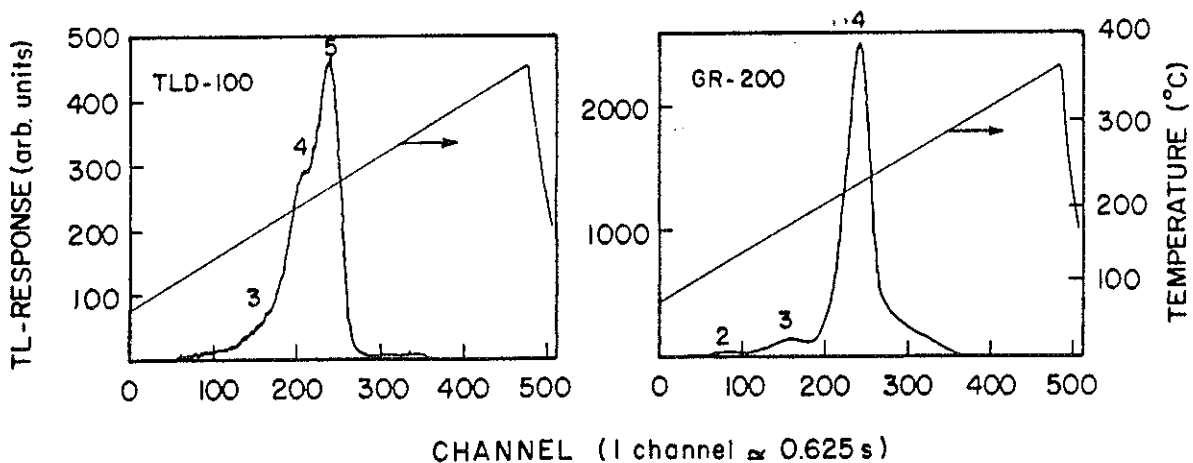


Fig.1 Glow curves of TLD-100 (10 mGy  $^{60}Co$  gamma rays) and GR-200 (1 mGy  $^{60}Co$  gamma rays) read out under the same procedure ( $1$  °C  $s^{-1}$ ). Note the difference in scale of the TL response and the difference in dose.

## Does the Most Sensitive Thermoluminescent Material come from China?

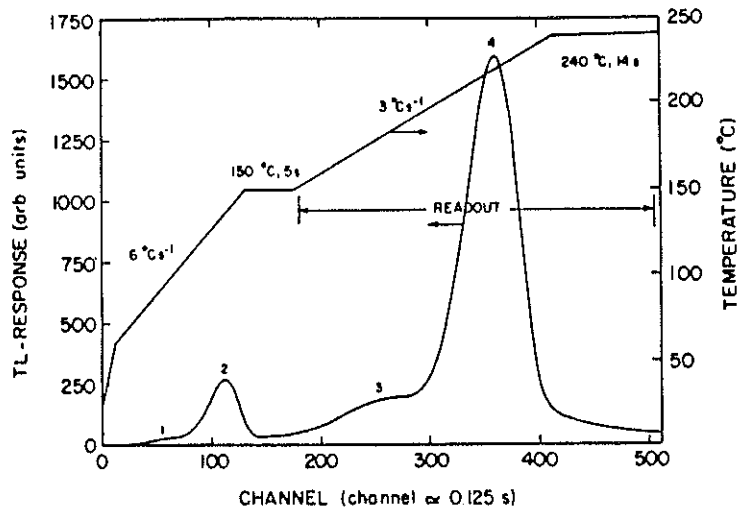


Fig.2 Glow curve of GR-200 and standard heating cycle used in this study.

heating rate of  $1\text{ }^{\circ}\text{C s}^{-1}$ . The main peak of both materials occurs at the same temperature ( $210\text{ }^{\circ}\text{C}$ ). The shape of the GR-200 glow curve is similar to that shown by Shoushan et al<sup>5</sup>. The peak positions, however, appear shifted to the high temperature side by approximately  $6\text{ }^{\circ}\text{C}$ . The recommended heating cycle during readout<sup>5</sup> comprises: heating rate:  $6\text{ }^{\circ}\text{C s}^{-1}$ , preread annealing at constant temperature:  $150\text{ }^{\circ}\text{C}$  for 5 s, constant temperature for reading:  $240\text{ }^{\circ}\text{C}$  for 10 s. This heating cycle, however, does not appear to be the most optimized one in our reader (resulting in a high residual signal) as a consequence of the higher measured temperature of the main peak. Since the maximum temperature must be kept below  $240\text{ }^{\circ}\text{C}$  (a higher temperature will lead to poorer re-usability) it was decided to lower the heating rate to  $3\text{ }^{\circ}\text{C s}^{-1}$  and to extend the maximum readout temperature plateau to 14 s. This resulted in a residual signal of 2.4%. The standard heating cycle used in this study and the corresponding glow curve are shown in fig. 2.

#### Sensitivity, zero dose and detection threshold

Fifteen samples of each TL material were irradiated to an absorbed soft tissue dose of 10 mGy originating from  $^{60}\text{Co}$  gamma rays (in case of GR-200 to 1 mGy). The samples were read out within 1 h after irradiation. The TL response was corrected for zero dose using the readout of the same but unirradiated samples after annealing. The sensitivities of the investigated TL materials were determined by light integration over the main peak in the glow curve (see fig. 2). After repeated use the sensitivity of GR-200 showed a significant reduction (see fig. 3). After nine cycles, however, no reduction could be observed within the experimental error. No change in the glow curve pattern could be observed during the 12 cycles. Detection thresholds were determined at the 95% confidence limit using the standard

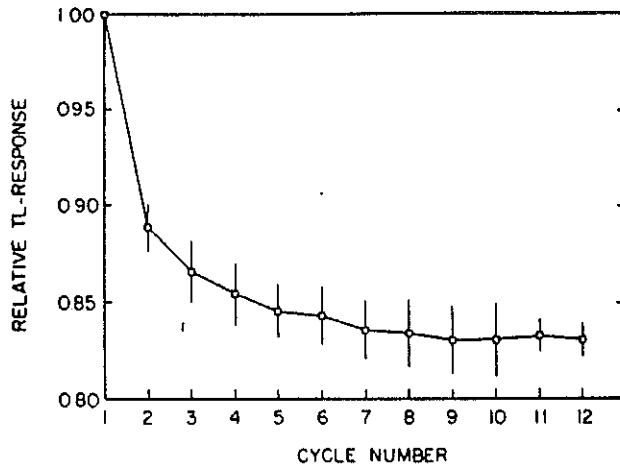


Fig.3 Change in sensitivity of GR-200 after repeated use. Every cycle involves annealing (10 min at 240 °C followed by a fast cooling i.e. 235 °C min<sup>-1</sup>), irradiation (1 mGy <sup>60</sup>Co gamma rays) and standard readout. Every point is the average ± standard deviation of 15 chips.

deviation of the zero readings and the measured sensitivities. The results are summarized in table 3.

Table 3. Sensitivity, Zero Dose and Detection Threshold of the investigated TL materials

| Material |  | Sensitivity to <sup>60</sup> Co γ rays<br>(nC mg <sup>-1</sup> mGy <sup>-1</sup> ) | (relative to TLD-100<br>per unit mass) | Zero Dose*<br>(μGy) | Detection Threshold**<br>(μGy) |
|----------|--|--|--|---------------------|--------------------------------|
| USA      | LiF:Mg,Ti  | 1.30   | (1)                                    | 7                   | 3.5                            |
| France   | LiF:Mg,Na  | 1.33   | 1.0                                    | 70                  | 32                             |
| China    | LiF:Mg,Cu,P  | 35.6   | 27***                                  | 0.1                 | 0.1                            |
| USA      | CaF <sub>2</sub> :Dy                                 | 37.2   | 29                                     | 0.8                 | 0.4                            |
| Finland  | Li <sub>2</sub> B <sub>4</sub> O <sub>7</sub> :Mn,Si | 0.37   | 0.28                                   | 52                  | 30                             |
| France   | Al <sub>2</sub> O <sub>3</sub>                       | 0.63   | 0.48                                   | 37                  | 40                             |
| USA      | BeO  | 0.056  | 0.04                                   | 1.2·10 <sup>2</sup> | 1·10 <sup>2</sup>              |

\* The corresponding dose of an unirradiated, annealed TL material corrected for reader background

\*\* At 95% confidence level

\*\*\* After 12 cycles of repeated use

**DISCUSSION**

The results of the present study are compared with values published by other investigators in table 4. There is good agreement in the relative sensitivity found by the manufacturers<sup>5,7</sup> and the presently measured value. The value found by Driscoll et al.<sup>8</sup> is significantly higher but they reported the value measured after first use while here the sensitivity after 9 cycles is given. The fact that the (net) zero dose and the detection threshold are equal indicates a relatively high contribution of the reader background to

Table 4. Comparison of some measured properties of LiF:Mg,Cu,P (GR-200)

| Property  | Shoushan et al. <sup>5,7</sup> | Driscoll et al. <sup>8</sup> | Present Study |
|---|--------------------------------|------------------------------|---------------|
| Sensitivity (by light integration relative to the same mass of TLD-100) | 29                             | 40*                          | 27**          |
| Batch homogeneity (rel. stand. dev. in %)                               | 3                              | -                            | 5.3           |
| Zero dose ( $\mu\text{Gy}$ )  | 0.06                           | -                            | 0.1           |
| Detection threshold ( $\mu\text{Gy}$ )                                  | 0.06                           | 0.2                          | 0.1           |
| Sensitivity loss after 5 cycles*** (%)                                  | $\approx 0$                    | 20****                       | 15            |

- \* Reduced to 32 after 5 cycles of repeated use including oven annealing
- \*\* Measured after 9 cycles of repeated use including oven annealing
- \*\*\* One cycle comprises oven annealing, irradiation (1 mGy) and readout
- \*\*\*\*  $\approx 0$  (within 10%) with reader annealing

the detection threshold. The background differences of the different readers used by the investigators mentioned in table 4 may explain the differences in the observed detection thresholds.

The sensitivity reduces 17% after 9 repeated cycles. The curve in fig. 3 indicates a stabilization of the defect structure distribution. It is not clear whether this effect is caused by the annealing or readout procedure (or a combination of both).

The influence of the method of annealing (in the reader or in an oven) on the re-usability found by Driscoll et al.<sup>7</sup> was the reason for us to look into the influence of the cooling rate (see fig. 4) which can be adjusted in our oven very reproducibly. A low cooling rate changes the glow curve drastically but the glow curve pattern is completely restored after applying the standard annealing cycle (for samples with a 12 cycles history). This result

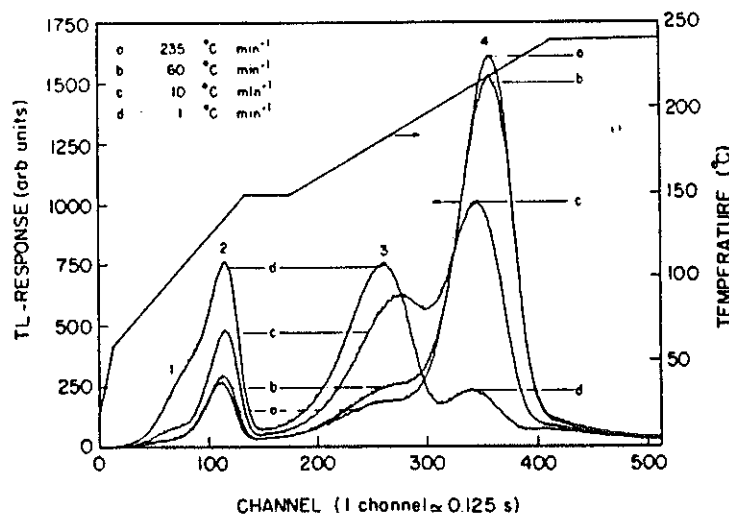


Fig.4 Change in glow curve pattern of GR-200 for different cooling rates in the annealing procedure starting at 240 °C for 10 min. Glow curves originate of the same chip irradiated to the same dose level (1 mGy).

indicates that a fast and reproducible cooling rate in the annealing procedure is very important. Probably the cooling rate influences the number of cycles needed before a constant sensitivity is reached.

### CONCLUSIONS

1. Of all investigated materials (see table 3), LiF:Mg,Cu,P (GR-200) is the most sensitive tissue equivalent TL material. The measured sensitivity is close to the value claimed by the manufacturer.
2. The use of GR-200 makes high demands upon the adjustment and reproducibility of both the annealing and readout cycle. This limits the applicability of this material in many cases.
3. While earlier results indicate the influence of the duration and the temperature of the annealing on the sensitivity<sup>2,7</sup>, the results of the present study reveal the importance of the cooling rate.
4. An acceptable stability of the sensitivity was reached after 9 cycles of measurements (including an oven anneal at 240 °C for 10 minutes followed by a fast cooling (235 °C min<sup>-1</sup>)). There is a lack of understanding of this behaviour. More research is needed on the influence of the annealing procedure (including the cooling rate) on the re-usability of this TL material.

### REFERENCES

1. T. Nakajima, Y. Murayama, T. Matsuzawa and A. Koyano, Development of a new highly sensitive LiF Thermoluminescence Dosimeter and its Applications, Nucl. Instr. and Meth. 157 (1978) 155-162
2. B. Chandra, A.R. Lakshmanan, R.C. Bhatt and K.G. Vohra, Annealing and Re-usability Characteristics of LiF(Mg,Cu,P) TLD Phosphor, Radiat. Prot. Dosim. 3(3) (1982) 161-167
3. Wu Da-Ke, Sun Fu-Yin and Dai Hong-Chen, A High Sensitivity LiF Thermoluminescent Dosimeter - LiF (Mg,Cu,P), Health Physics 46(5) (1984) 1063-1067
4. L.A. DeWerd, J.R. Cameron, Wu Da-Ke, T. Rapini and I.J. Das, Characteristics of a New Dosemeter Material; LiF(Mg,Cu,P), Radiat. Prot. Dosim. 6(1) (1984) 350-352
5. Wang Shoushan, Chen Guolong, Wu Fang, Li Yuanfang, Zha Ziyang and Zhu Jianhuan, Newly Developed Highly Sensitive LiF (Mg,Cu,P) TL Chips with High Signal-To Noise Ratio, Radiat. Prot. Dosim. 14(3) (1986) 223-227
6. M.H. van Wijngaarden, J. Plaisier and A.J.J. Bos, A Microprocessor Controlled Thermoluminescence Dosimeter Reader for Routine Use and Research, Radiat. Prot. Dosim. 11(3) (1985) 179-183
7. Zha Ziyang, Wang Shoushan, Wu Fang, Chen Guolong, Li Yuafang, Zhu Jianhuan, Measurements of extremely Low Dose with LiF (Mg,Cu,P) TL chips, Radiat. Prot. Dosim. 17(1-4) (1986) 415-418
8. C.M.H. Driscoll, A.F. McWhan, J.B. O'Hagan, J. Dodson, S.J. Mundy, C.D. Todd, The Characteristics of a new LiF preparations and sensitised LiF, Radiat. Prot. Dosim. 17(1-4) (1986) 367-371

**Thermoluminescence Dosimetry  
in  
Health Physics**





## THE TNO INDIVIDUAL MONITORING SERVICE BASED ON TLD CONCEPTS AND METHODOLOGY

H.W. Julius , F.A.I. Busscher , C.W. Verhoef

TNO, Netherlands Organisation for Applied Scientific Research  
Radiological Service TNO, P.O.Box 9034, 6800 ES Arnhem, The Netherlands

### INTRODUCTION

The Government approved Individual Monitoring Service, operated by the Radiological Service TNO, issues dosimeters to almost 20,000 workers in the Netherlands. An automatic TLD system, developed to replace photographic dosimetry, has been put into operation in 1984 and presently covers more than one third of the total capacity.

In the following a general description is given of the dosimetric concepts in today's Individual Monitoring on which the TNO TLD system is based. Some technical details of the TLD system itself are given.

### DOSIMETRIC CONCEPTS IN INDIVIDUAL MONITORING

The radiation quantities which should ideally be measured in individual monitoring stem from the adopted system of dose limitation. For non-stochastic effects ICRP in Publication 26<sup>1</sup> places limits on the dose equivalent to individual organs,  $H_T$ , while for stochastic effects the Commission places limits on effective dose equivalent  $H_E$ . These concepts have since been adopted by the CEC in their Basic Safety Standards<sup>2</sup> and are consequently built into the national legislation of the member states of the EC. Therefore, in principle,  $H_E$  and  $H_T$  should be measured in carrying out individual monitoring.

The effective dose equivalent is the sum of the weighted mean dose equivalents in six specified organs or tissues, each with its own weighting factor, plus the dose equivalents in five of the remaining organs receiving the highest dose equivalents, each with a weighting factor of 0.06. The specified organs and the corresponding weighting factors are given in Table 1.

$H_E$  provides an estimate of the risk to the individual of fatal cancers and serious hereditary defects in the first two generations and is formulated to take into account such factors as the variation of dose within the body and the different radiosensitivities of the various organs. The quantity is a measure of the consequences of radiation exposure in terms of the detriment to the individual, i.e., his increased risk of suffering the effects mentioned earlier.  $H_E$  is thus more meaningful than the basic

quantity, dose equivalent, from the point of view of radiation protection in general, epidemiological studies and cases of litigation concerning claims for compensation.

**Table 1** Weighting factors for specified organs and tissues

| Organ or Tissue     | Weighting factor |
|---------------------|------------------|
| Gonads (hereditary) | 0.25             |
| Breast              | 0.15             |
| Red bone marrow     | 0.12             |
| Lung                | 0.12             |
| Thyroid             | 0.03             |
| Bone surfaces       | 0.03             |
| Remainder           | 0.30             |
| WHOLE BODY          | 1.0              |

However, in practice, we cannot assess either  $H_T$  or  $H_E$  because it requires a knowledge of organ dose. To overcome this difficulty ICRU in Publication 39<sup>3</sup> recommended new practical quantities or *secondary* quantities for operational use which provide an estimate of  $H_E$  (avoiding under-estimation and excessive over-estimation) and an upper limit to the value of  $H_T$ . Two quantities are recommended for individual monitoring: individual dose equivalent, *penetrating* and individual dose equivalent, *superficial*.

*Individual dose equivalent, penetrating,  $H_p(d)$*

Individual dose equivalent, penetrating,  $H_p(d)$ , is the dose equivalent in soft tissue below a specified point on the body at a depth that is appropriate for strongly penetrating radiations. The currently recommended depth,  $d$ , for monitoring in terms of  $H_p(d)$  is 10 mm. The quantity is then written as  $H_p(10)$  and is meant to give an estimate of the effective dose equivalent  $H_E$  received by the wearer and an upper limit to the dose equivalent  $H_T$  to any single deep seated organ.  $H_p(10)$  is deemed to represent a measurement of  $H_E$  for dose record keeping purposes.

*Individual dose equivalent, superficial,  $H_s(d)$*

Individual dose equivalent, superficial,  $H_s(d)$ , is the dose equivalent in soft tissue below a specified point on the body at a depth that is appropriate for weakly penetrating radiations. The currently recommended depth,  $d$ , for monitoring in terms of  $H_s(d)$  is

0.07 mm. The quantity is then written as  $H_p(0.07)$  and is meant to give an estimate of the dose to the skin of the wearer and is of particular importance where the proportion of weakly penetrating radiations in the field is such that the skin may be the limiting organ.

Secondary quantities are essential for legislators working in the field of radiation protection and for those responsible for monitoring programmes and dosimetry services. The choice of secondary quantities also has implications for dosimeter design and for type testing of dosimeters.

Those responsible for individual monitoring programmes and those operating individual monitoring services need secondary quantities which are straightforward to use to allow them to work in an efficient and cost effective manner. What is required is an unified system of quantities which are additive so that the total dose, from whatever source of radiation, can be computed.

Moreover occasionally it is necessary to control the exposure to individuals at, or near to, the dose limits. In these circumstances it is necessary to be able to obtain a reasonably accurate assessment of effective dose equivalent. This should be possible with the scheme of secondary quantities adopted.

Qualitatively the new ICRU quantities go a long way towards satisfying the requirements of secondary quantities for individual monitoring. They have been studied extensively by ICRU and clearly have the backing of both ICRU and ICRP so their use can readily be defended. Provided we accept the ICRU suggestion that for dosimeters to be worn on the trunk the ICRU sphere is a suitable phantom on which to develop and type test personal dosimeters, the definitions do prescribe a required energy and angular response for dosimeters. Type testing of dosimeters is, in principle, straightforward. Conversion coefficients such as those published by ICRP in Publication 51<sup>4</sup> allow the conversion of intensities measured in terms of the more conventional quantities, such as air kerma for photons, to the new quantities (see, as an example, Figure 1 for photons at normal incidence). There is no need to develop primary standards for this purpose.

A major consideration is the degree of approximation of  $H_E$  afforded by the new quantity  $H_p(10)$ . The relationship for photons between  $H_p(10)$  and  $H_E$  has been calculated<sup>5</sup> for several different irradiation geometries, such as AP, lateral, rotational and isotropic. It can be seen from Figure 2 that, for photons, in the majority of cases  $H_p(10)$  overestimates  $H_E$ , apart from a large under-estimate for rotational irradiation at an energy of about 10 keV (which occurs because of the risk to the female breast).

The extent of the overall overestimation is acceptable where doses are low, which is usually the case when applying the ALARA principle. However, where there is a need for worker's doses to be controlled at or near the dose limits, the use of  $H_p(10)$  as an estimate of effective dose equivalent may be over restrictive. In such cases it may be worthwhile characterising the radiation field in sufficient detail to get a better estimate of  $H_E$ .

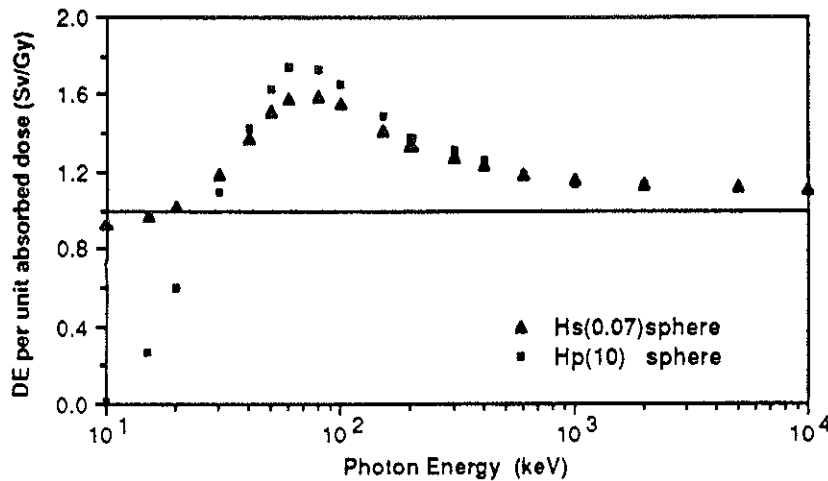


Fig. 1. Dose equivalents at 0.07 and 10 mm depths on the principal axis of the ICRU sphere per unit absorbed dose to air in free air for photons incident in a plane parallel beam<sup>4</sup>.

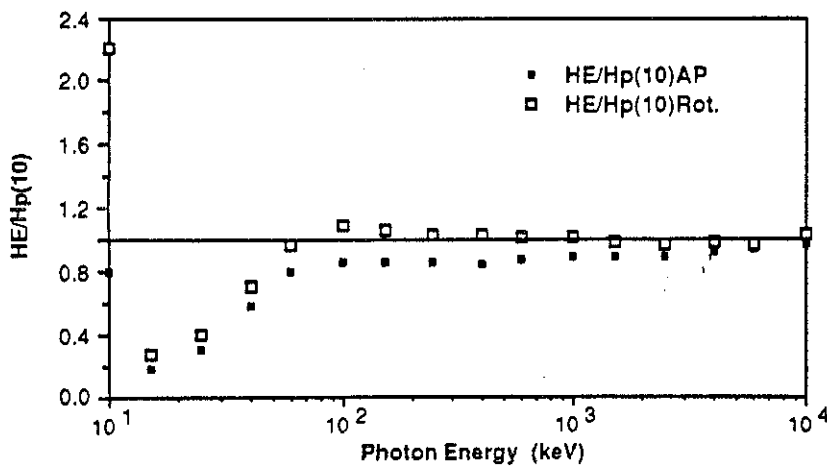


Fig. 2. The relationship between  $H_p(10)$  and  $H_E$  for AP and for rotational irradiation geometries (photons)<sup>5</sup>.

As mentioned above, ICRU state that a suitable phantom for typetesting dosimeters, intended to be worn on the trunk, would be the ICRU sphere<sup>3</sup>. For typetesting, dosimeters should therefore be exposed on the sphere, or its equivalent. The evaluated

dose of the dosimeter should be tested against (i.e. compared with) the conventionally true value, being the dose equivalent at the appropriate depth in the sphere (i.e.  $H_p(10)$  or  $H_s(0.07)$ ). For testing the photon energy response of dosimeters,  $H_p(10)$  and  $H_s(0.07)$  are determined by multiplying the intensities of the calibration beam, e.g. expressed in terms of absorbed dose to air, by the appropriate conversion coefficients (see Fig. 1).

## THE TNO TLD SYSTEM

The TLD system developed by TNO essentially comprises of a personal dosimeter and the corresponding readout equipment. The latter is micro-processor controlled and hooked up to the computerised dose record keeping system, which will serve as the National Dose Register system in the near future.

### 1. The TLD dosimeter

In the past, personal dosimeters have been based on the use of photographic film as the sensitive medium. Because of the high atomic number,  $Z$ , of AgBr the variation of response with photon energy is significant. To overcome this problem, most film dosimeters are designed with an arrangement of filters of various composition and thickness beneath which the response of the film is modified. As a result, the irradiated and developed film exhibits a pattern of optical densities from which the radiation dose can be determined and, incidentally, additional information such as radiation energy can be obtained. Therefore film dosimeters, by nature, are "discriminating dosimeters" <sup>6,7</sup>.

Thermoluminescence dosimetry, where lower  $Z$  materials are available for which the response as a function of radiation energy is close to directly proportional to the energy deposition in tissue, allows for dosimeters of basically simpler design. A dosimeter, containing two elements of near tissue equivalent TL material, covered by filters of appropriate compositions and thicknesses to measure  $H_p(10)$  and  $H_s(0.07)$ , satisfies the needs for the majority of radiation workers. Such dosimeters are usually called "basic dosimeters", because they do not provide any information additional to the measurement of the basic quantities. With extra detectors and a filtersystem, thermoluminescent dosimeters can also be designed to provide information on radiation energy and hence to some extent become discriminating dosimeters. These tend to be more expensive both in manufacturing and processing.

TNO, anticipating the use of both types of dosimeter, decided to develop one single "multipurpose" TLD badge-holder in order to avoid the development of two different dosimeters and possibly two different processing devices. The distinction between the simple "basic" and the more complicated "discriminating" dosimeter can be made by

loading the holder with the appropriate number and, if necessary, different types of detectors and filters. The resulting TLD badge, shown in Figure 3, is highly versatile and can be adopted to various dosimetric needs. It essentially may accommodate 6 elements, 4 of which can be processed automatically. These 4 detectors can be covered by:

- A. an open window, the thickness of which may be chosen between 4 and 35 mg cm<sup>-2</sup>
- B. a plastic filter (340 mg cm<sup>-2</sup>)
- C. a metal filter of any material and of thickness up to a maximum of 2 mm
- D. as in C, usually chosen as 2 mm aluminium



**Fig. 3.** The TNO TLD dosemeter, with and without the wearer's label, showing the individual's name, number and issuing period

The basic dosemeter contains two TLD-100 (LiF) detectors for the measurement of  $H_s(0.07)$  and  $H_p(10)$  respectively. The relative response (defined as the ratio between the measured and the conventionally true value, e.g. for the dose equivalent, penetrating:  $H_p(10)_{\text{measured}} / H_p(10)_{\text{given}}$ ) for photons at normal incidence of the TNO TLD badge is shown in Figures 4 and 5. Measurements have been made using the X-ray ISO wide spectrum series for photons below 200 keV.

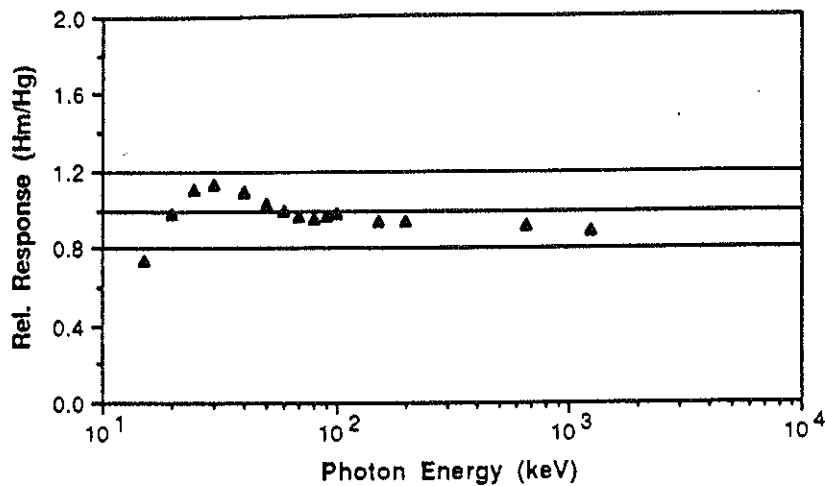


Fig. 4. Relative response for dose equivalent, superficial, of the TNO TLD badge

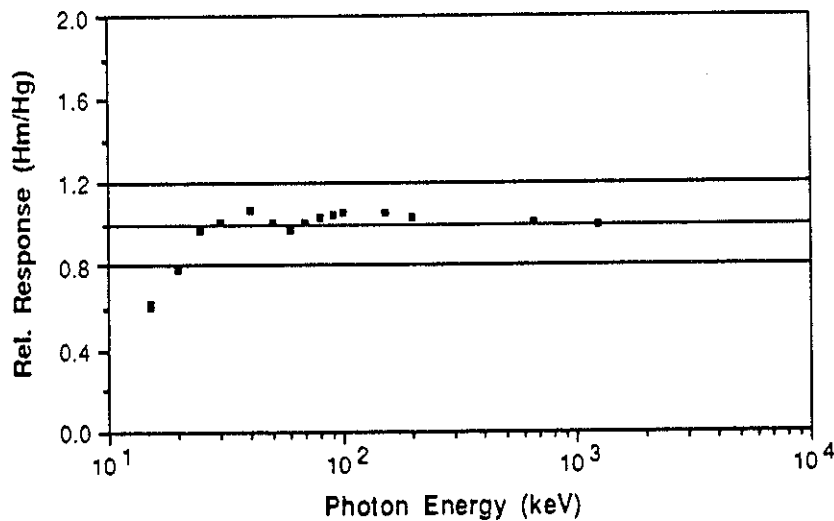


Fig. 5. Relative response for dose equivalent, penetrating, of the TNO TLD badge

There is a slight under-estimation at photon energies below 20 keV which, for  $H_p(10)$ , provides compensation for the over-estimation of this quantity with respect to the effective dose equivalent (see Figure 2).

The basic dosimeter as described above is suitable for photon radiation. For beta radiation a third detector needs to be introduced. For this purpose the dosimeter will be equipped with a carbon loaded TL-detector of either LiF or  $MgB_4O_7$  which will be



covered by a titanium coated mylar foil of  $4 \text{ mg cm}^{-2}$ . The carbon loaded material – which, from a dosimetric point of view, effectively behaves as a TLD of only a few  $\text{mg cm}^{-2}$  because the luminescent light from only the very top layer can leave the detector – is presently the most promising material for beta dosimetry. Preliminary investigations have demonstrated that its response (see Figure 6) to even very low beta energies (even at various angles of incidence<sup>8</sup>) is excellent. This dosimeter is planned to be available within a few months.

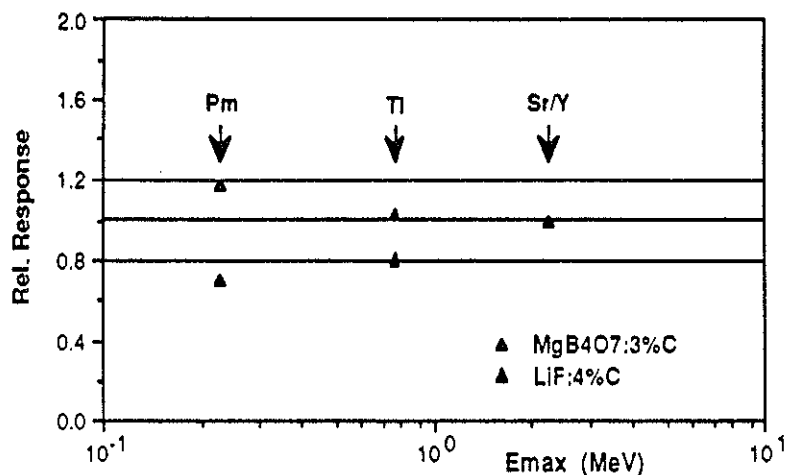


Fig. 6. Relative response for  $H_s(0.07)$  to beta radiation at normal incidence of the TNO TLD equipped with carbon loaded TL-material

For routine application in individual monitoring all detectors in each – uniquely identified – dosimeter are individually calibrated. As a consequence all dosimeters may be considered interchangeable which permits random distribution among the users. Issuing of dosimeters is fully computer controlled and includes a unique link between the individual worker and the TLD badge for any particular issuing period. To this end the dosimeters are labelled with the individual's name and code as well as the number of the issuing period. The TNO dosimeter is watertight and is therefore also suitable for environmental dosimetry.

## 2. Readout equipment

The development of the automatic readout equipment used for the processing of the TNO TL-dosimeters started in the seventies. Although significant improvements have been made since, the essentials are still the same<sup>9,10</sup>. For readout the detectors are heated by three jets of hot pure nitrogen gas. This technique has proved to provide good

precision due to the excellent thermal contact between the detector and the heating medium. The system as a whole essentially consists of two parts: The TLD reader and a dosimeter handling device which automatically identifies and opens the dosimeters, feeds the TL elements to the reader and closes the badges after the readout cycle has been completed. The reader - which can be operated as a stand alone instrument for dosimetric experiments with loose detectors - uses a vacuum needle to bring the TLD into the heating cavity. Typical readout time is 11 seconds. After readout the TL elements return in their original position in the dosimeter so as to guarantee that their identity is retained.

### 3. Results

Although the detection threshold of the system as a whole (i.e. detectors plus readout equipment) is less than 0.01 mSv and the reproducibility of one single TLD, irradiated and read under laboratory conditions, is better than 1% (SD), the precision in routine operation ranges from 9% at 0.20 mSv level to 5% at 10 mSv level. These values have been determined from measurements of some 100 randomly chosen dosimeters (attributed to some 6 fake "individuals") which have been subjected to all possible steps in the routine procedure (including postal mailing), except for irradiation. The variations observed in the low dose range may, to a large extent, be due to errors introduced by subtraction of the natural background, which is determined on the basis of a fixed value (0.090  $\mu$ Sv/h) for the entire country and calculated taking into account the time interval between the last and the previous readout as stored, for each dosimeter, into the computer. Individual variations obviously level out nicely, the accuracy of the cumulative dose for each "individual" over a period of somewhat less than one year appearing to be within a total error of 5%, even at the 0.20 mSv level.

### REFERENCES

1. ICRP (International Commission on Radiological Protection), Recommendations of the International Commission on Radiological Protection, ICRP Publication 26, Pergamon Press, Oxford, UK, 1977
2. Commission of the European Communities, Council Directive of 15th July 1980 amending the Directives laying down the Basic Safety Standards for the health protection of the general public and workers against the dangers of ionising radiation. CEC, EUR 7330 (1980)
3. ICRU (International Commission on Radiation Units and Measurements), Determination of Dose Equivalents Resulting from External Radiation Sources, Report 39, Bethesda, MD, USA, 1985
4. ICRP (International Commission on Radiological Protection), Data for Use in Protection Against External Radiation, ICRP Publication 51, Pergamon Press, Oxford, UK, 1987

5. G. Williams, M. Zankel, H. Eckerl and G. Drexler, The calculations of dose from external exposures using reference human phantoms and Monte-Carlo methods, Part II, Organ doses from occupational exposures. München, Gesellschaft für Strahlen und Umweltforschung mbH, GSF Bericht S-1079 (1984)
6. T.O. Marshall, P. Christensen, H.W. Julius and J.W. Smith, The Relative Merits of Discriminating and Non-Discriminating Dosimeters, Rad. Prot. Dosim., 14 (1) (1986) 5-10
7. ICRP (International Commission on Radiological Protection), General Principles of Monitoring for Radiation Protection of Workers, ICRP Publication 35, Pergamon Press, Oxford, UK, 1982
8. P. Christensen, J. Böhm and T.M. Francis, Measurement of absorbed dose to tissue in a slab phantom for beta radiation incident at various angles, To be published
9. H.W. Julius, C.W. Verhoef and F. Busscher, A universal automatic TLD-reader for large scale radiation dosimetry, Proc. 3rd Int. IRPA Conf., Washington D.C. (1973) 563-567
10. H.W. Julius, C.W. Verhoef, F. Busscher and F. Oterman, A versatile automatic TLD system under development, Proc. 4th Int. Conf. on Lumin. Dos., Krakow, (1974) 675-689

## THE PHILIPS PERSONNEL DOSIMETRY SYSTEM

H. Pauw, and C.J.H. Wittenbernds,  
Philips Occupational Safety Department,  
Willemstraat 22a, Building ECY-4,  
5600 MD Eindhoven, The Netherlands

### INTRODUCTION

Shielding X-ray devices and the issuing of film badges to radiological workers in 1936 can be considered as the start of radiological protection in the Philips' establishments in the Netherlands.

In 1956 a Central Philips Committee for Radiological Protection was founded, which also issued in 1960 an internal licensing system in order to regulate the proper precautions to be taken: workplace design and layout, technological provisions and working procedures. An evaluation of all radiological work in 1971 showed that a stricter health surveillance programme was needed to follow up the precautions laid down in the licence.

In this way an obligatory and optimal health surveillance programme was specified for each type of radiological work. In this paper the personnel dosimetry system and its results will be described as part of the health surveillance programme.

### HEALTH SURVEILLANCE PROGRAMME

In 1972 the following 7 items were defined and recently up-dated:

1. Periodical inspection and radiation measurement of switchable sources;
2. Periodical inspection, radiation measurement and wipe test of radionuclide sources;
3. Personal dosimetry with thermoluminescent dosimeters. In special cases a neutron badge or direct reading dosimeter can be prescribed. Mandatory environmental monitoring was laid down in the licence;
4. Medical examination: prior to employment with the company and on leaving the company;
5. Periodical medical examination;
6. Periodical bio-assay analysis, mostly urine samples;
7. Periodical total or partial body counting.

The periodicity was set at a minimum of once a year. The highest frequency was for the personal dosimetry: every month.

The policy of the Central Philips Committee for Radiological Protection is that for radiological workers a dose equivalent of 500  $\mu$ Sv per month or 5 mSv per year should not be exceeded.

### THE PERSONNEL DOSIMETRY SYSTEM

Since 1978 the Philips Personnel Dosimetry System is based on the Harshaw Model 2271 Automated Personnel Monitoring TLD System.

The Harshaw System consists of the following main units:

- \* TLD cards
- \* Model 2271 Tl Detector/Dosimeter Identifier
- \* Model 2271 L Card Loader
- \* Model 2271 R Card Receiver
- \* Model 2000 B Automatic Integrating Picoammeter
- \* Nitrogen Gas Supply and Flow Regulator Meter.

The TLD card contains two solid-state thermoluminescent dosimeters of LiF in a 3.175 mm x 3.175 mm ribbon form and a 5 x 7 hole matrix system to form the card identification number in binary coded decimals (BCD code).

The dosimeters are mounted into two holes on an aluminium support plate. A plastic plate is bonded to the aluminium plate and the individual identification numbers are formed by selective covering of the matrix.

At Philips a personal dosimeter consists of two identical TLD cards (red and blue) with the same identification number. The personal dosimeters are carefully selected by Harshaw to have a reproducibility of  $\pm 10\%$  in a batch of dosimeters and/or a pair of identical dosimeters. The TLD material is TLD-100 for beta and gamma dosimetry.

Because the Harshaw System is very sensitive to dust, Philips has designed its own closed standard dosimeter badge holder with sliding lid, also in the colours red and blue. The plastic window for the TLD is 0.5 mm thick.

The holder is designed to be worn by personnel on the wrist by means of a watchstrap or on the clothes by means of a clip. The red holder has to be worn in odd months and the blue holder in even months of the year.

In addition, a grey holder is used for special purposes such as training and education.

A special set of dosimeters is used for calibrating the Harshaw system. The dosimeters are irradiated by means of a certificated Cs-137 source.

EVALUATION

Periodical checks of working conditions and of dose equivalents achieved are necessary. Incidents still occur without the knowledge of the radiological worker.

In the first 6 years after the introduction of the health surveillance programme dose equivalents exceeding 5mSv still occurred. In the same period dose equivalents exceeding 50 mSv were registered 12 times.

However, the extensive health surveillance programme made it possible to improve the safety of the radiological work. In this way the personnel dosimetry system was quite helpful in reducing the dose equivalent of the individual radiological worker. This can be shown by the statistics of the last ten years.

Table 1. Registered dose equivalent, including background, in percentage of the total number of radiological workers.

| Year | < 5 mSv | 5-15 mSv | 15-50 mSv | > 50 mSv | Total |
|------|---------|----------|-----------|----------|-------|
| 1978 | 95.5    | 1.7      | 2.8       | 0.0      | 1180  |
| 1979 | 99.7    | 0.2      | 0.1       | 0.0      | 1213  |
| 1980 | 100.0   | 0.0      | 0.0       | 0.0      | 1270  |
| 1981 | 99.9    | 0.1      | 0.0       | 0.0      | 1247  |
| 1982 | 99.9    | 0.1      | 0.0       | 0.0      | 1276  |
| 1983 | 99.9    | 0.1      | 0.0       | 0.0      | 1504  |
| 1984 | 100.0   | 0.0      | 0.0       | 0.0      | 1501  |
| 1985 | 100.0   | 0.0      | 0.0       | 0.0      | 1609  |
| 1986 | 100.0   | 0.0      | 0.0       | 0.0      | 1642  |
| 1987 | 100.0   | 0.0      | 0.0       | 0.0      | 1633  |

In recent years a subdivision has been made in the lowest dose equivalent area (< 5 mSv) in order to trace small incidents further.

The statistics are shown in Table 2:

Table 2. Registered dose equivalent, including background, in percentage of the total number of radiological workers.

| Year | 0-1 mSv | 1-2 mSv | 2-3 mSv | 3-4 mSv | 4-5 mSv | Total |
|------|---------|---------|---------|---------|---------|-------|
| 1984 | 59.76   | 39.70   | 0.40    | 0.07    | 0.07    | 1501  |
| 1985 | 61.28   | 38.29   | 0.37    | 0.06    | 0.00    | 1609  |
| 1986 | 52.68   | 46.83   | 0.49    | 0.00    | 0.00    | 1642  |
| 1987 | 60.08   | 39.50   | 0.24    | 0.18    | 0.00    | 1633  |

In recent years, the preset dose equivalent limit of 500  $\mu$ Sv in a month has been exceeded about ten times a year.

Investigation shows that most of the time the dosimeter is deliberately irradiated, without irradiating the radiological worker. About three times a year the registered dose equivalent is due to a leakage of an X-ray device or careless handling of a radioactive source.

The investigation always led to the issuing of additional safety instructions to the radiological worker or to a group of radiological workers, above the standard instructions.

#### CONCLUSIONS

Classification of types of radiological work and an appropriate health surveillance programme has proven to be effective in view of the substantial reduction in the dose equivalent. The contribution of the personnel dosimetry system was most effective.

THE ECN-NEUTRON-BETA-GAMMA DOSIMETER  
THEORY AND PRACTICE

A.S. Keverling Buisman

Netherlands Energy Research Foundation (ECN)  
P.O. Box 1, NL-1755 ZG PETTEN, The Netherlands

INTRODUCTION

The Netherlands Energy Research Foundation operates a government licensed personnel dosimetry service. Of the dosimeters used one type is sensitive to neutron, beta and gamma radiation. This dosimeter is presently used by about 800 persons throughout the country. These persons are employed by universities, research institutes, oil companies, construction works and road building companies. The neutron sources involved range from reactors to those applied in moisture detectors. The ECN-Dosimetry service gradually replaced the formerly used film dosimeter starting July 1987. The new dosimeter is based upon thermoluminescent techniques. Apart from a better sensitivity this technique allows full automatization of readout and storage of dosimetric results. This paper concentrates on the theory and practice of the dosimeter.

MEASURING PRINCIPLES

The neutron sensitivity of TLD-material is based upon the (n, $\alpha$ )-reaction. The phosphor used is lithiumborate ( $\text{Li}_2\text{B}_4\text{O}_{10}$ ), in which both enriched lithium and boron is employed. The relevant reactions are  ${}^6\text{Li}(n,\alpha){}^3\text{H}$  ( $\sigma_{n,\alpha} = 940 \text{ b}$ ) and  ${}^{10}\text{B}(n,\alpha){}^7\text{Li}$  ( $\sigma_{n,\alpha} = 3836 \text{ b}$ ). These reactions make the  ${}^6\text{Li}_2{}^{10}\text{B}_4\text{O}_{10}$ -phosphor extremely sensitive to thermal neutrons. Medium energy and fast neutrons do not interact appreciably with this material. A practical dosimeter therefore must either itself attenuate the incident neutrons to approximately thermal energies or moderating material should be added. In this latter respect nature is helpful: the human body is a very effective neutron moderator, as it contains 10% hydrogen by weight. Neutrons that are back-scattered from a body are called albedo neutrons. As explained above these neutrons may be readily detected by the enriched lithiumborate phosphor.



In theory an albedo neutron dosimeter could consist of a  ${}^6\text{Li}_2, {}^{10}\text{B}_4\text{O}_{10}$ -element in a thermal neutron capturing box with a hole in the backside. Such a dosimeter, however, would not be practicable as its response would be dependent on the incident neutron energy spectrum, apart from the unavoidable gamma-ray sensitivity.

One way to tackle this problem is to measure the thermal component of the incident neutron spectrum. This requires a second neutron sensitive TLD-element, open to the beam but shielded from albedo neutrons.

The ratio of the direct and the albedo TLD-signals gives an indication of the thermal neutron component. Unfortunately, this ratio is not fully independent of the type of neutron source. For a given neutron source, however, this ratio is a measure of the amount of moderation.

A practical dosimeter must also take into account the gamma-ray sensitivity. A simple solution is the use of a neutron insensitive phosphor: in this case  ${}^7\text{Li}_2, {}^{11}\text{B}_4\text{O}_{10}$  is the obvious material. A pair of lithiumborate elements, one neutron sensitive and one neutron insensitive, gives the gamma and neutron contribution of the incident radiation field by simple subtraction of the readout values. The complete dosimeter therefore consists of two such TLD-pairs, one measuring the albedo neutrons and the other the thermal component of the incident neutron fluence. As explained in the next section the four TLD-signals also yield the shallow dose equivalent, i.e. the skin dose due to beta rays.

#### CONSTRUCTION OF THE DOSIMETER

In figure 1 the construction of the complete dosimeter is shown. It consists of a B,C-box with two windows: one in the back side (for the detection of albedo neutrons) and one in the front side (for the detection of the thermal component). The front window is only  $20 \text{ mg/cm}^2$  thick and therefore allows beta rays to enter the TLD-phosphor pair. The TLD-elements are listed in table 1.

#### TLD-phosphors in the ECN-dosimeter

Table 1

| Number * | Phosphor  | Sensitive to                     |
|----------|---|----------------------------------|
| 1        | ${}^6\text{Li}_2, {}^{10}\text{B}_4\text{O}_{10} : \text{Cu}$ | $n_{\text{th}} + \beta + \gamma$ |
| 2        | ${}^7\text{Li}_2, {}^{11}\text{B}_4\text{O}_{10} : \text{Cu}$ | $\beta + \gamma$                 |
| 3        | ${}^7\text{Li}_2, {}^{11}\text{B}_4\text{O}_{10} : \text{Cu}$ | $\gamma$                         |
| 4        | ${}^6\text{Li}_2, {}^{10}\text{B}_4\text{O}_{10} : \text{Cu}$ | $n_{\text{alb}} + \gamma$        |

\* refers to fig. 1

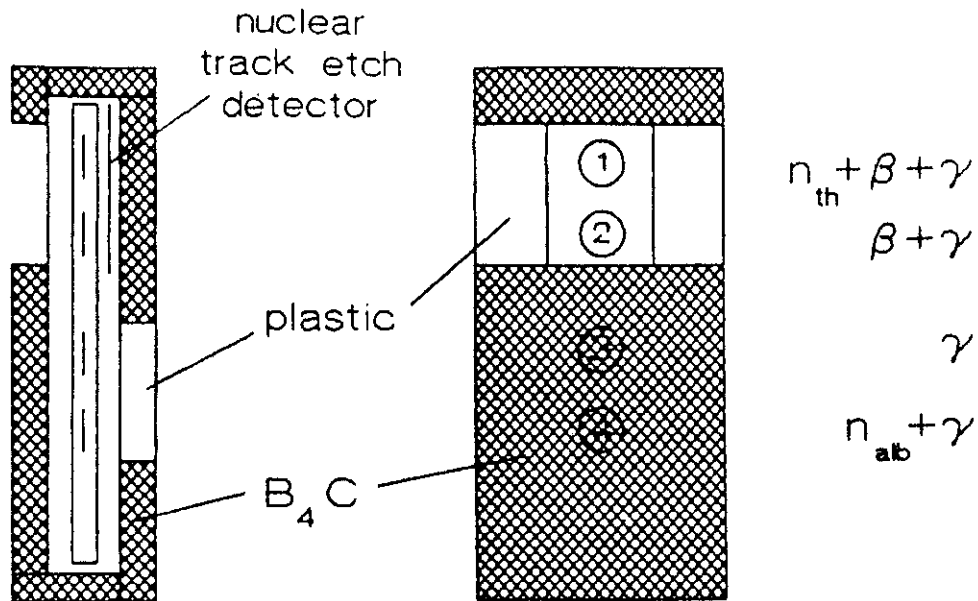


Figure 1. Construction of the dosimeter

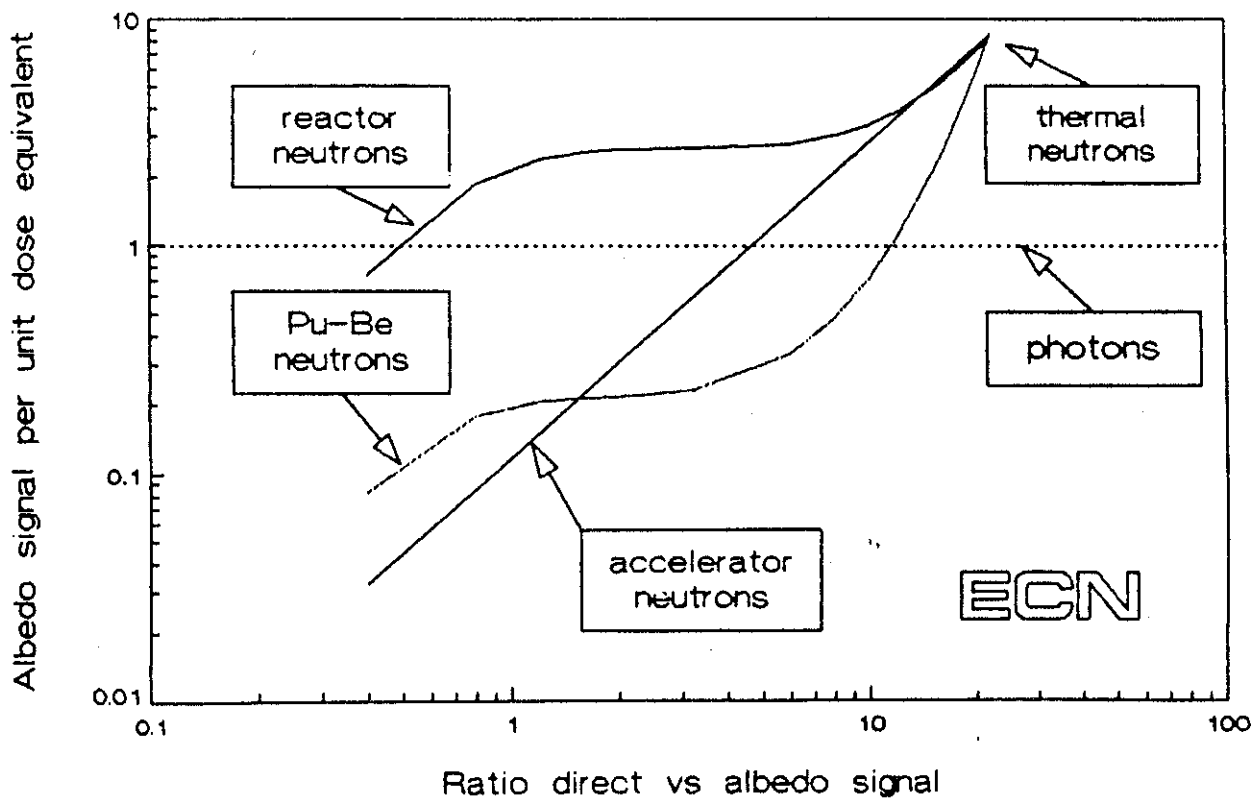


Figure 2. Neutron response to different sources

From figure 1 and table 1 the dose calculation may be anticipated: Element 3 gives the  $\gamma$ -ray dose equivalent, while the difference between elements 4 and 3 indicates the albedo neutron fluence. The difference between elements 1 and 2 yields the incident thermal neutron component and the difference between elements 2 and 3 gives the shallow dose equivalent. As usual, all thermoluminescent signals must be calibrated against known radiation fields. The B,C-box is manufactured by Wellhöfer Kernphysik, W. Germany; the four element TLD-cassette type UD813 is made by Panasonic, Japan.

#### NEUTRON DOSE CALCULATION

As mentioned above the information on the albedo neutron fluence alone is not enough to find the neutron dose equivalent. The ratio of the incident thermal vs. the albedo fluence is necessary additional information. However, a certain dependence on the type of neutron source remains as can be seen from the calibration of the albedo signal shown in figure 2 for three different neutron sources. In all cases there is a certain dependence of the calibration factor on the ratio direct vs. albedo neutron signal. For reactor neutrons the albedo signal is fairly large. In fact it exceeds the gamma equivalent signal under normal circumstances. For accelerator neutrons the calibration factor depends strongly upon the degree of moderation, i.e. the shielding thickness. For  $(\alpha, n)$ -neutrons the calibration factor oscillates around the factor for accelerator neutrons. From figure 2 it is clear that for fast neutrons (low direct/albedo ratio) the dosimetric sensitivity is relatively poor, i.e. a factor of 10 - 30 less sensitive than for photons.

#### READOUT SYSTEM

The phosphors are permanently mounted upon a cassette. During readout the phosphors are heated by infrared radiation from a special lamp. Each cycle consists of three short flashes (100 - 500 ms): preheating, readout and annealing, consecutively. The phosphors are not mechanically moved and remain fixed to the cassette. This procedure ensures both reproducibility and identification. The complete readout takes approximately 30 seconds. The system used is the Panasonic UD-702E semi-automatic TLD-reader coupled to a 640k Tulip-XT personal computer. This system is programmed to calculate and store individual dose equivalents of about 2000 persons.

## EXPERIENCE

As may readily be deduced from figure 2 the dosimetry around reactors is expected to proceed without problems. In practice a neutron detection limit of 20  $\mu\text{Sv}$  is easily achievable, even in presence of photons.

Experiments with dosimeters mounted on phantoms have shown an excellent correspondence between remcounter readings and dosimetric results. In the observed population of radiation workers around research reactors the fraction of nonzero neutron dose equivalents varies from 5 to 25%. The actual values of the dose equivalents are usually low (ranging from 20 - 100  $\mu\text{Sv}$ ), in all cases only a fraction of the corresponding gamma doses.

Dosimetry around accelerators is less sensitive as may be seen from figure 2. However, the monitored individuals usually remain outside of the shielding structures. This shielding material significantly increases the relative contribution of thermal neutrons in the neutron field. This improves the sensitivity considerably with respect to the unshielded situation. In practice, therefore, the dosimetry around fixed fast neutron sources hardly poses any problems. The practical dose equivalent limit is about 400  $\mu\text{Sv}$ . A different situation is encountered when portable ( $\alpha, n$ )-sources are used. Here the shielding is often minimal. This increases the detection limit in extreme cases to values exceeding 400  $\mu\text{Sv}$ . The source strength, however, limits the dose equivalent rates considerably during normal operation. The purpose of the dosimeter in these cases is shifted more towards accident dosimetry.

In case of an appreciable dose equivalent due to fast neutrons an extra source of dosimetric information is available: each dosimeter contains a polycarbonate nuclear track etch foil. The detection limit of this system lies around 300  $\mu\text{Sv}$ .

In general the albedo dosimeter served its purpose very well. The detection of individual dose equivalents is more sensitive and more certain than for the formerly used film dosimeter. The previous uncertainty regarding the detection of epithermal neutron is absent in the TLD-system. Both from a dosimetric and from an administrative point of view the TLD-system has proved to be a major improvement over the film dosimeters previously used.



## ENVIRONMENTAL RADIATION MONITORING USING THERMOLUMINESCENCE DOSEMETERS

A.H.L. Aalbers, F.J.M. Bader, A.P.P.A. van Lunenburg and C.R. ter Kuile

National Institute of Public Health and Environmental Protection  
Bilthoven, The Netherlands

### INTRODUCTION

Thermoluminescence dosimeters are widely used by the National Institute of Public Health and Environmental Protection (RIVM) for environmental radiation measurements around nuclear installations. The main objective of the current monitoring program is the ability to measure short term fluctuations of the background radiation, which may be due to contributions from nuclear power stations under surveillance. Since short monitoring periods (1 to 3 months) are required, a sensitive thermoluminescence material such as calcium fluoride is applied. Although multi-element dosimeters containing  $\text{CaF}_2:\text{Dy}$  are mainly used in the current program, a pilot study is undertaken to investigate the performance of  $\text{LiF}:\text{Mg,Ti}$  for environmental dosimetry and to establish appropriate processing procedures. The RIVM has a continuing interest in the development and quality assurance aspects of thermoluminescence measurement techniques suitable for routine monitoring of environmental radiation levels. Therefore experimental work is undertaken directed at specific problems associated with environmental dosimetry, such as: readout technique and calibration procedures. Optimizing reader conditions and operational procedures for annealing and calibration is of vital importance for performing precise and reproducible environmental TLD measurements. The performance of TL-dosimeters under laboratory and field measurement conditions can be improved by experience gained in participating in international intercomparisons and from standardisation studies. In this paper the set up and processing of the thermoluminescence devices used in an intercomparison study is briefly described as well as some aspects of the readout technique, calibration procedure and temperature related effects. Some preliminary results from

environmental measurements performed with TL-dosemeters and a high pressure ionisation chamber are reported.

## MATERIALS AND METHODS

### The TL-dosemeters

LiF:Mg,Ti (TLD-100/700) and  $\text{CaF}_2\text{:Dy}$  (TLD-200) phosphors, in the form of ribbons ( $3.2 \times 3.2 \times 0.9 \text{ mm}^3$ ), are obtained from Harshaw Chemical Co. Six ribbons at maximum can be inserted in a plastic disc. The disc, containing the ribbons, is equipped with a cover plate and placed in a spherical or cylindrical holder, made of plastic. An exploded view of the standard RIVM dosemeter for routine monitoring, containing six ribbons, is shown in figure 1. Due to the strong energy dependence of  $\text{CaF}_2\text{:Dy}$  in the energy range below 100 keV an energy compensation filter has to be used. A spherical or cylindrical encapsulation of 2.5 mm copper instead of the plastic holder is used as an energy compensation filter. This filter does not seriously affect the results, because only a small percentage (about 6%) of the typical environmental exposure is due to photons with an energy less than 100 keV [1]. Figure 2 shows the effect of a spherical encapsulation on the energy dependence of the  $\text{CaF}_2$  dosemeter.

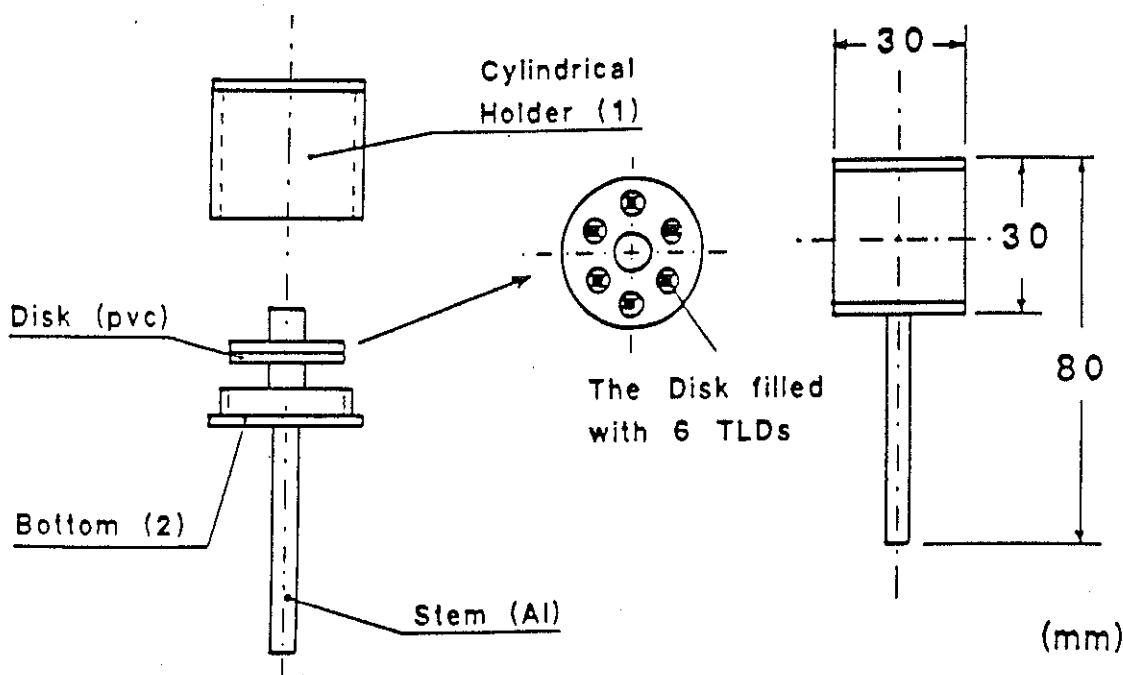


Fig. 1: Dosemeter applied for environmental monitoring at RIVM with a 2.5 mm copper cylindrical holder to provide for energy compensation. In case of LiF:Mg,Ti part 1 and 2 consist of PVC.

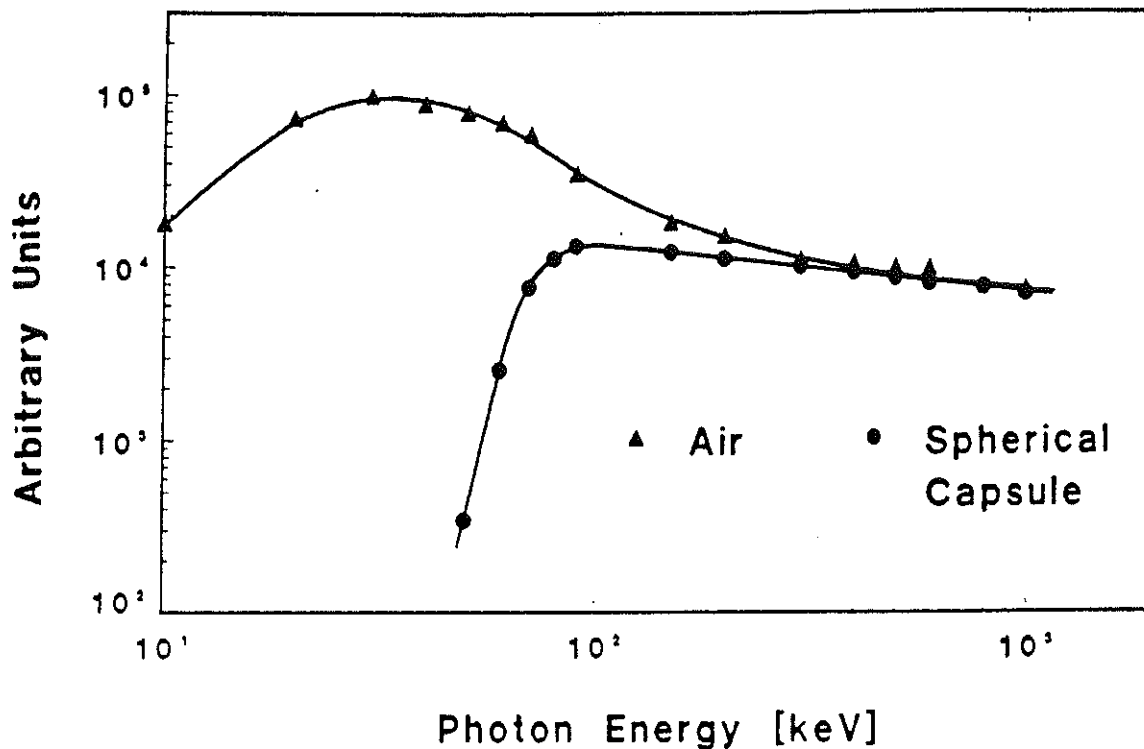


Fig. 2: Energy dependence of  $\text{CaF}_2:\text{Dy}$  (TLD-200) with spherical encapsulation of 2.5 mm copper and without an energy compensation shield.

#### Processing procedures

The ribbons are initialised by a repeated annealing and calibration procedure to stabilise the sensitivity and the zero dose response. Before and after the field exposure the thermoluminescence ribbons are individually calibrated in a collimated photon beam of  $^{137}\text{Cs}$  in case of routine monitoring. In each multi-element dosimeter at least one ribbon is given a radiation exposure to monitor fading of the thermoluminescence signal during the field period. Separate control dosimeters are used to assess radiation exposures received by the dosimeter batch during transit and storage. Further a set of control dosimeters is kept at the laboratory in an area with a low radiation exposure rate. These dosimeters can be used to detect, for instance, possible variations in reader conditions or readout parameters. After field deployment the dosimeters are returned to the laboratory and prepared for readout. Routine preparation of the TL-reader for readout includes checks on dark current, heating cycle, and the



response of the reader to an internal and external light source. The procedures to check the reader are repeated at the completion of readout. Each ribbon is read twice in succession. The value obtained during the second readout is used to correct for the background during the initial readout. After completion of the readout all ribbons are submitted to the same annealing and calibration procedure as given prior to field deployment. A simplified diagram showing the entire procedure for calibration and measurement is given in figure 3.

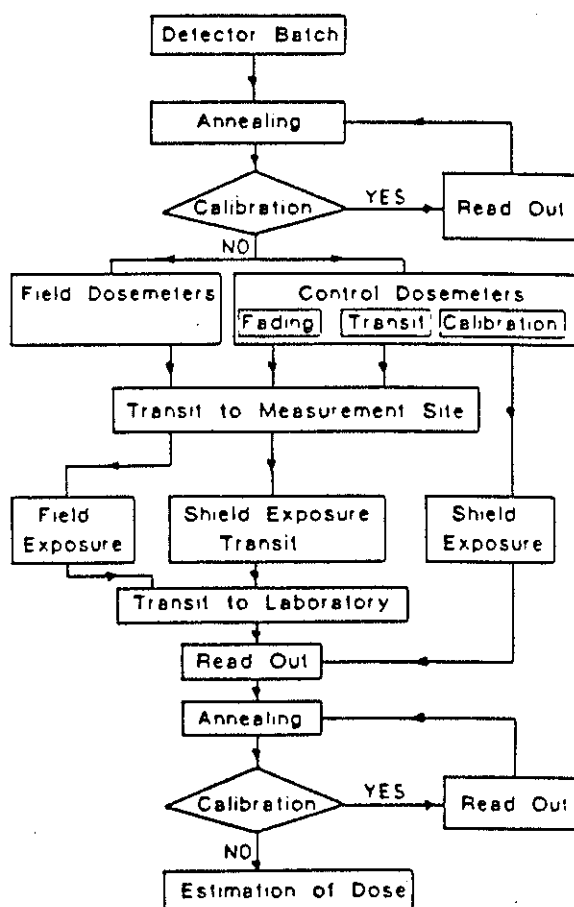


Fig. 3: Simplified diagram illustrating the measurement and calibration procedure of environmental TL-dosimeters.

## RESULTS OF AN INTERCOMPARISON STUDY

Intercomparison studies provide a very useful tool to investigate particular problems encountered in environmental radiation measurements [2,3]. Moreover intercomparisons provide an opportunity to determine the performance and the reliability of environmental dosimeter systems. By participating in intercomparisons, several parameters associated with the readout technique and calibration procedures were studied. These investigations were focussed on establishing stable (short and long-term) reader conditions and carefully controlled annealing procedures, which can be implemented in the routine monitoring programme. Some of these points may be demonstrated by the following example. During the preparation at RIVM of the  $\text{CaF}_2:\text{Dy}$  ribbons for the 7th international intercomparison of environmental dosimeters conducted by the U.S. Department of Energy [3] a repeated annealing and calibration procedure for each ribbon was introduced in order to improve the stability of the calibration factor and to reduce the fading of the dosimeters under laboratory and field conditions. The temperature profile of the annealing oven was carefully controlled to allow for a constant and reproducible cooling rate after the high temperature part of the annealing cycle. By submitting the  $\text{CaF}_2:\text{Dy}$  ribbons to a pre-readout anneal the thermal fading was reduced significantly [4]. These modified procedures were tested during the intercomparison. The design of the intercomparison was as follows: each participant was requested to send eight dosimeters (including control dosimeters) to perform field and laboratory irradiations (with two different radionuclides,  $^{137}\text{Cs}$  and  $^{60}\text{Co}$ ). The field dosimeters were deployed at the Nevada Test Site near Las Vegas. At the end of the field cycle, the field dosimeters were re-united with the laboratory and control dosimeters and returned to the participants for analysis. In figure 4 the exposures estimated by RIVM are compared with the exposure values obtained by the reference laboratory (RSEL). The results derived by RIVM were corrected for fading. The fading correction was based on the signal loss of pre-irradiated chips, which have been exposed together with the other TL-detectors at the field location. In estimating a correction factor for the fading effect uncertainties arose from lack of knowledge of the field temperature and exposure rate profiles. At the field site temperatures were expected to vary between -12 to +38 degrees celsius during the whole field period of about 3 months. The error bars given in figure 4 indicate one standard deviation.

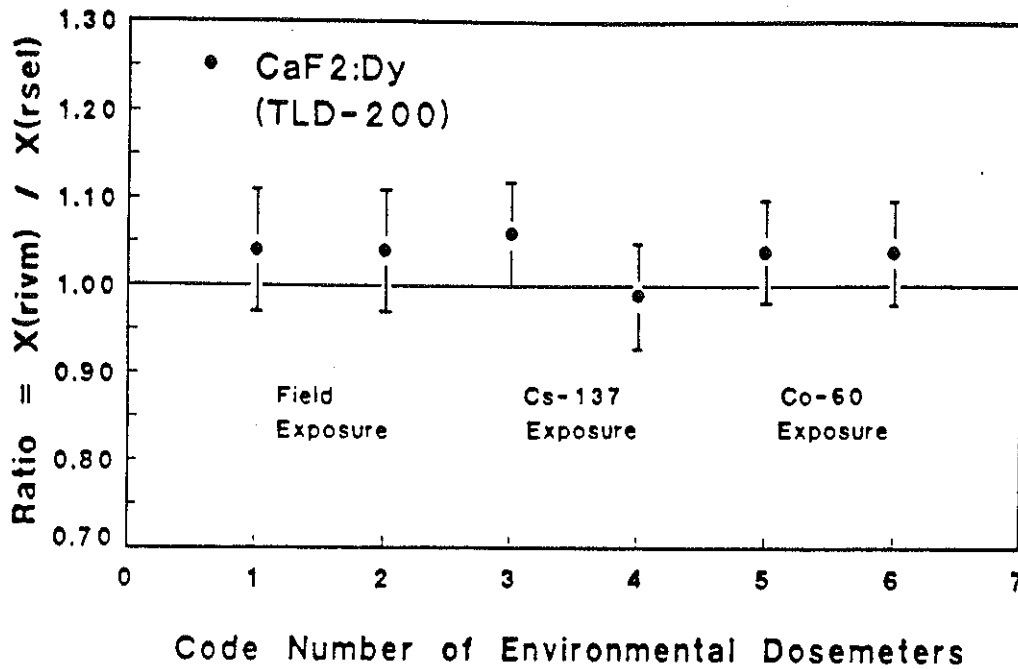


Fig. 4: Results of the 7th International Intercomparison of Environmental Dosimeters 1984. Comparison of the calculated (RIVM) exposure with the delivered test exposure. The intercomparison consisted of test exposures to laboratory sources of  $^{137}\text{Cs}$  and  $^{60}\text{Co}$  and an outdoor exposure to a mixed radiation field from natural and (old) fallout sources.

#### ENVIRONMENTAL MEASUREMENTS AROUND THE NUCLEAR POWER STATION EMSLAND

$\text{CaF}_2:\text{Dy}$  dosimeters are applied to determine environmental radiation levels at different locations in the vicinity of the nuclear power station of Emsland (FRG). During the field cycle of 6 months the Emsland power station was not in operation. It should be noted, that the calibration procedure outlined in figure 3 was not incorporated in these measurements. At the same locations the exposure rate was measured directly with a steel walled, high pressure ionization chamber (Reuter Stokes RSS-111). The ionization current was measured with an electrometer, digitised with a voltage-to-frequency converter, and integrated with a scaler. The instrument was calibrated in a collimated gamma ray beam of  $^{137}\text{Cs}$ . The results obtained with the TL-dosimeters, corrected for fading and normalized to the results of the ionization chamber, are presented in figure 5. The data suggest that

the exposure values measured by the thermoluminescence dosimeters are significantly lower than the corresponding values derived from the ionization chamber measurements. However, the correction for the actual field fading could not be made accurately enough by using pre-irradiated dosimeters at the field site.

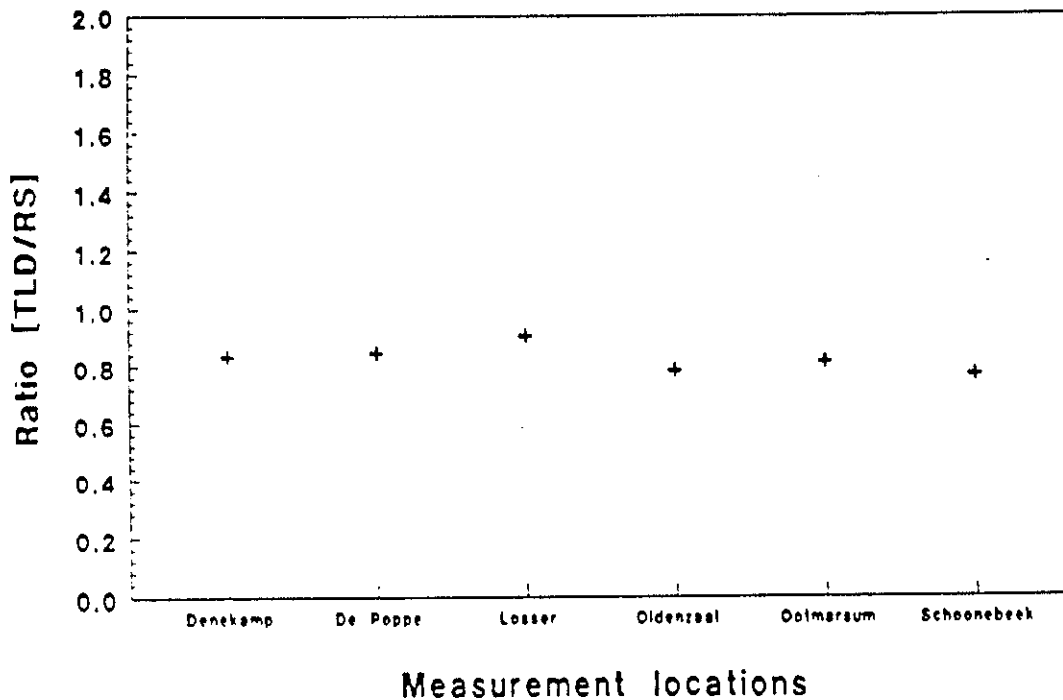


Fig. 5: Preliminary results of environmental measurements around the Emsland nuclear power plant. The results of the TLD-measurements are normalized to the results of the Reuter-Stokes high pressure ionization chamber.

#### CONCLUSIONS

As can be seen from figure 4 the results for the field and the laboratory irradiations as estimated by RIVM show good agreement with the values obtained by the reference laboratory. These findings support the recommendation that  $\text{CaF}_2:\text{Dy}$  can be used for exposure periods up to three months [4]. No conclusions can be drawn from the available data presented in figure 5. Further measurements are needed to explore the

observed difference in the TL-dosimetry and ionization chamber measurements and to assess the overall uncertainty of both methods. Participation in TLD intercomparisons is a valuable way to improve the performance and the quality of TLD systems and measurement techniques used for environmental monitoring. It is intended to apply the measurement and calibration procedure illustrated in figure 3 to the monitoring programmes around nuclear facilities (including the nuclear power station Emsland).

#### REFERENCES

1. H.L. Beck, 2nd Int.Symposium on the natural radiation environment, Houston, CONF-720805 (1975)
2. G. de Planque Burke and T.F. Gesell, Thermoluminescence Dosimetry - Environmental Applications, Int. J. Appl. Radiat. Isot. 33 (1982) 1015 - 1034.
3. G. de Planque Burke and T.F. Gesell, Environmental measurements with thermoluminescence dosimeters - Trends and issues, Radiat.Prot.Dosim. 17 (1986) 193-200
4. E.Piesch. Application of TLD systems for environmental monitoring, In Applied thermoluminescence dosimetry (Eds. M.Oberhofer and A.Scharmann), A.Hilger, Bristol(1980)197-228

## THERMOLUMINESCENCE DOSIMETRY AT EINDHOVEN UNIVERSITY OF TECHNOLOGY

Jos. T. Hemelaar, Pierre J. Kicken and Chris J. Huyskens

Eindhoven University of Technology, Health Physics Division  
P.O. Box 513, 5600 MB Eindhoven, The Netherlands

### INTRODUCTION

Over 20 years the Health Physics Division of the Eindhoven University of Technology operates an approved personal dosimetry service with filmbadge dosimeters. Approximately 200 filmbadges (type Harwell) and ca. 100 thermoluminescence dosimeters (TLD-chips) are issued every two weeks for individual monitoring.

Additionally, dosimetry studies are performed especially in the field of medical applications, for which up to 500 TLD-chips are issued per month.

In 1988 filmbadge dosimetry will be replaced by thermoluminescence techniques for the greater part. This paper gives an outline of organisational aspects and technical features of our TLD-system.

### DOSIMETRY AS A TOOL IN RADIATION PROTECTION

In general, personal dosimetry comprises the following processes:

- registration of personnel data
- registration of dosimeter data
- calibration of dosimeters
- issue of dosimeters
- "processing" of measurements (dosimeter response signal and dose calculation)
- registration of personal dose
- reporting.

Additionally to execution of personal dosimetry to demonstrate compliance with regulations on dose limitation, we strongly believe in the necessity to use personal dosimetry as a tool for good practice in operational radiation protection management.

This implicates extra requirements, particularly with respect to the last four items mentioned above:

- permanent availability of extra dosimeters for reasons of flexibility in the execution of dosimetry (additional dosimetry for body, extremities and jobs as well as ambient dosimetry)
- a short time delay between collection of issued dosimeters and the read-out process, so that dose measurements can be quickly evaluated in relation to working conditions
- a high level of automation both in process operation and management of personal data and dose data.

Individual monitoring is done by one filmbadge worn on the trunk.

For workers in Working Condition A additional dosimetry for job and extremities is carried out. The number of dosimeters, dosimeter design, length of measurement time, dosimeter position, dose evaluation etc. are dependent on working conditions.

An outline of our organisation of the dosimetry service is given in a flowchart (fig. 1). The person related functions are shown on the left and processes which are related to dosimeters at the right hand side. Interrelated processes are shown in between.

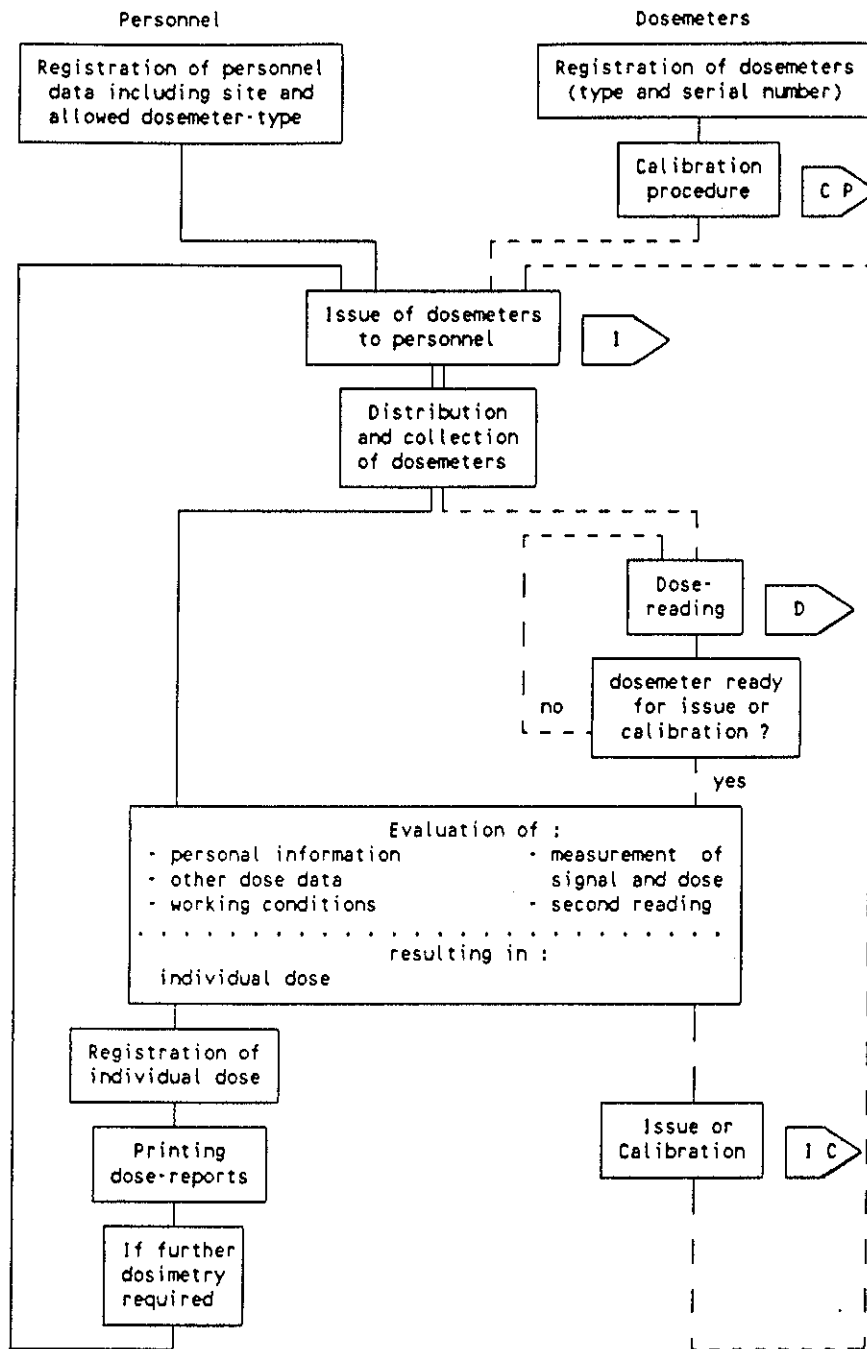


Fig.1 Organisation of dosimetry service

Arrows refer to automated (sub)processes with regard to dosimetry with TLD-cards (see Fig.3.)

## TLD-SYSTEM

Initially 6 commercially available TLD-systems were evaluated. Three systems were put to practical test. We concluded that most systems satisfy the quality requirements for approval of dosimetry service under the radiation protection legislations. However, none of the available system configurations were fully satisfactory with respect to the level of automation concerning organisation, process-control and data-management. With extensive software modifications on our demand we have decided for a system configuration which comprises:

- a Vinten 814 automatic TLD-reader for read-out processing of TLD-cards in batches
- a Vinten Mini 690 manual TLD-reader for read-out processing of extremity dosimeters (chips or tape); because the reader processes TLD-cards as well it can be used as a back-up system for the automatic reader
- Vinten Integrated Record Keeping System and glow curve analysis software for dosimeter handling, read-out processing and raw data management
- SBD/TUE Radiation Protection Management System: a software package for personnel data coordination and personal dose record keeping.

The system configuration is displayed in fig. 2. The vertical lines indicate the coherence between the components; dotted lines refer to optional parts or further development.

Specifications and features of TL-dosimeters cards, automatic TLD-reader and software (organisation, monitoring, process control and data management) can be summarized as follows:

### TL-dosimeters (cards):

- four elements (discs) of  ${}^7\text{LiF}$
- binary hole-code identification, type and serialnumber; type represents the combination of TL-material of four elements
- dose range: 0.05 - 2000 mGy linear response; 2 - 10 Gy supra-linear response
- negligible response to neutrons
- response independency for dose rates up to 1 MGy/sec.
- directional dependency for 60 keV photons and Sr/Y betas less than 15% at angles up to 60°
- energy dependency less than 30% for photon energies from 15 keV to 1.3 MeV
- fading rate less than 5% in 30 days
- accuracy ca. 10% for dose < 1 mGy; 5% for dose > 1 mGy.

### TLD-reader:

- simultaneous reading of 2 elements (2 heaters and 2 photomultipliers)
- automatic batch processing up to 100 cards in 100 minutes for 2 elements per card reading
- hole- and barcoded cards can be mixed in one batch
- different card-types can be mixed in one batch
- the optical system is automatically checked before each reading and automatically calibrated every 15 minutes by means of a light source reading and a dark current measurement
- automatic setting of the designated heating cycles according to card-type
- different heating cycles for each card-type and for each of the four element positions possible.



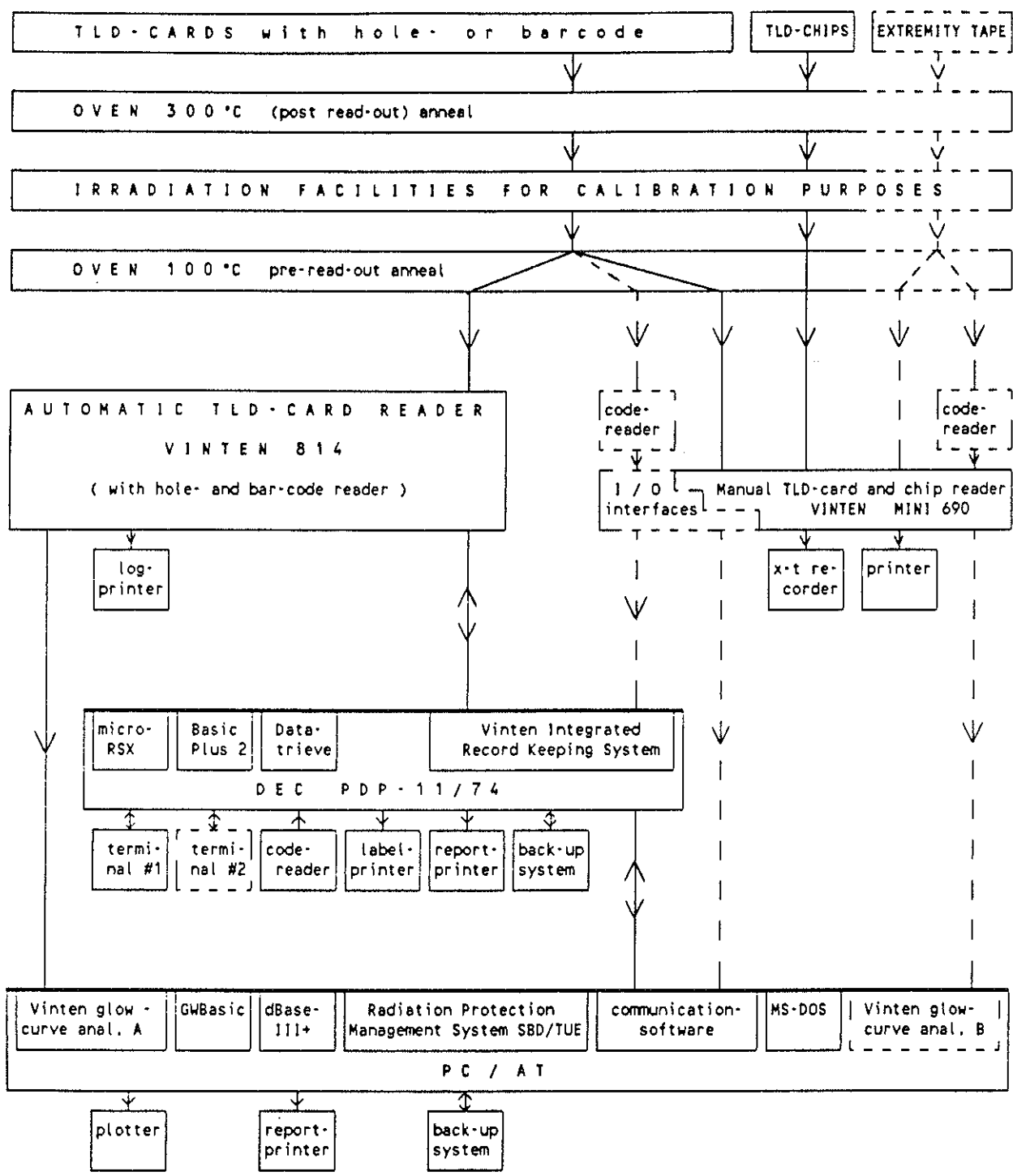


Fig.2 TLD system configuration

**Software outline:**

- registration of customers and work areas (sites)
- registration of personal data including check on site information
- individual card registration and calibration
- storage of date of registration and date of calibration for each card
- storage of calibration factors, background dose and life dose for each element
- checking and matching of card identification, card status, person identification and date of issue; the status indicates whether or not a card is registered, calibrated, ready for issue or already issued
- length of issue period: one month or half a month at choice
- per issued card a label is automatically printed with identification of person, site and card plus expiry date
- possibility to issue more than one dosimeter per person per period
- automatic verification of reader settings before each session
- matching and storage of card identification, glowcurve, raw data and card dose
- matching and storage of card dose, person identification and issue period
- build-in protection against re-issue of cards which are exposed above a preset dose level (verification dose)
- separation and security of personal dose data and dosimetry research data
- different authorisation levels for supervisor, routine operators and researchers (security of files).

Procedures and subprocedures of the TLD-system are shown in the flowcharts (fig. 3). Flowcharts are drawn for one procedure loop. For example, automatic repetition of readings of several cards during one session and multiple issue to all personnel of one site are not included in these schemes.

Specific features of the TLD-reader and the software can be recognised as well in the flowcharts.

**DISCUSSION**

The (sub)processes of TLD handling and data management were tested both separately and in their mutual coherence. Our expectation has been confirmed that such a system cannot be purchased ready to hand. To deal with modifications and problems which arise during testing and implementation an intense co-operation with the designers of the system is necessary. In accordance with our terms of delivery a statement of compliance of the TLD-system with British regulations concerned with an approval of dosimetry service has been obtained. The process of approval by Dutch authorities is in progress.

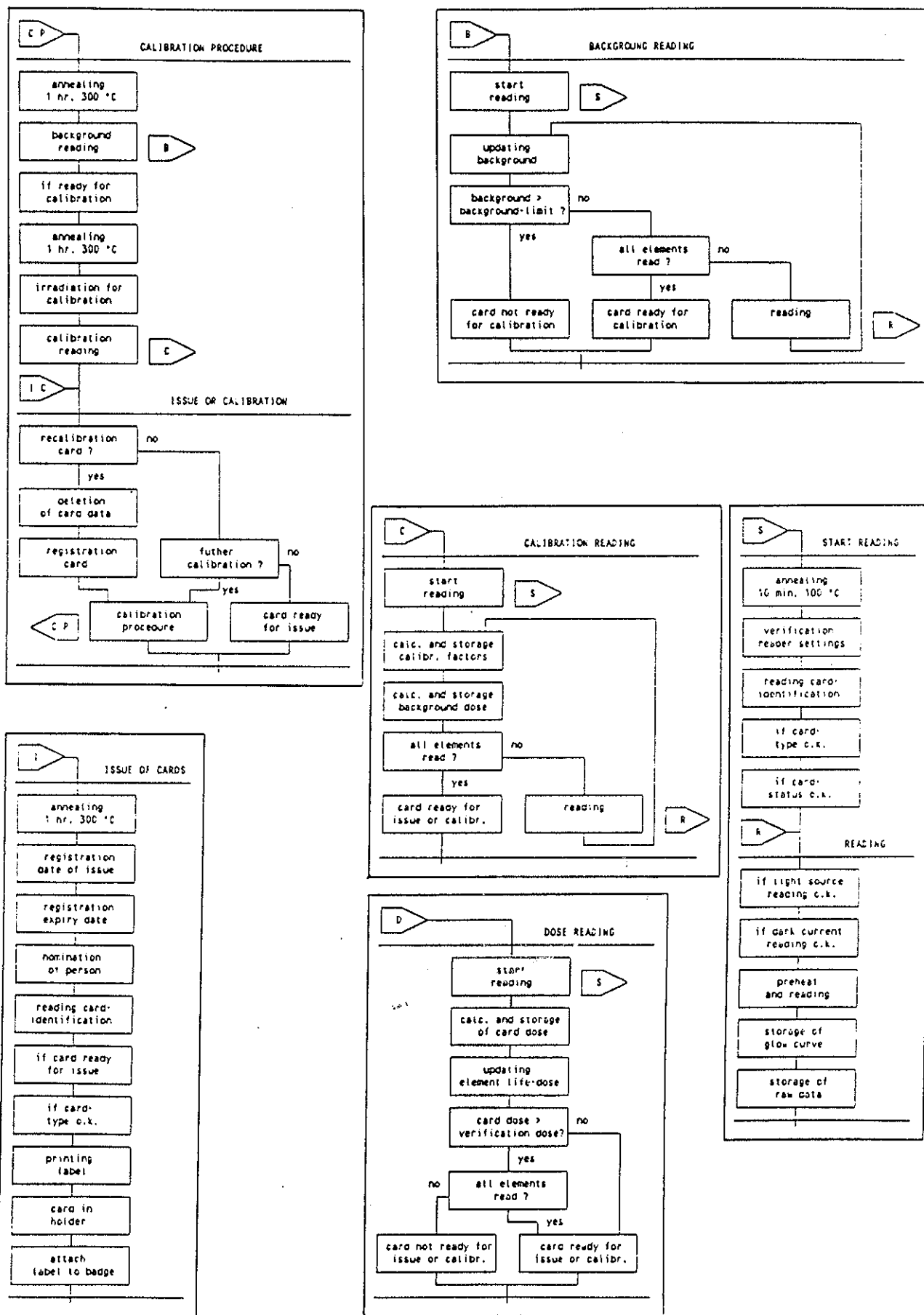


Fig. 3 Flowcharts for TLD-card (sub)processes

ENVIRONMENTAL AND CALAMITY TLD-SYSTEMS AROUND  
DUTCH NUCLEAR POWER STATIONS

L.P.M. van Velzen

Research and Development Division, Reactor Physics and Radiation Protection  
Department, N.V. tot Keuring van Elektrotechnische Materialen, P.O. Box 9035  
6800 ET ARNHEM, The Netherlands

ABSTRACT

In 1981 a research project was initiated at the KEMA department of Environmental Research, concerning a new environmental TLD-system. This project consisted of several parts:

- requirements of the TLD-system
- a comparative study of commercially available TLD-materials
- evaluation of a measuring procedure for a routine monitoring programme.

On the basis of the results of this project, KEMA advised the nuclear power stations to perform their environmental monitoring with a combination of  $\text{CaF}_2$  TLDs (Harshaw's TLD-200) and the automatic TNO TLD-reader. The next step in the development was to turn the laboratory set-up into an operational TLD-system. The development included the design of new TLD-holders, TLD pick-out platforms, a readout table, electronics, automation of the TLD readout cycle, and automation of the data manipulation.

March 1983 the routine environmental monitoring system became operational and on 1 July 1983 officially replaced the existing systems. The environmental calamity TLD-system became operational in July 1984.

INTRODUCTION

The routine environmental monitoring system around the Dutch nuclear power stations contains about 35 measuring points, which are placed upto a distance of 20 km from the power station. As part of the monitoring programme the exposure rate is determined with a TLD-system, that has to meet the following demands:

- the relative standard deviation from the calculated exposure rate must be less than 5%
- the minimum detection limit must be corresponding with a surveillance period of approximately one week
- the stability of the collected data on the monitoring system must allow an accurate determination of the exposure rate during a surveillance period of at least five weeks

- the readout time of all measuring points in one area is not permitted to exceed 8 hours
- the measuring procedure must not be equipment-related.

The demands the calamity TLD-system has to meet are:

- the readout time of all measuring points in one area is not permitted to exceed 2 hours
- the relative standard deviation from the calculated exposure rate must be less than 20%.

#### THE COMPARATIVE STUDY OF TLD-MATERIALS

A special point of interest during this comparative study was the behaviour of different TLD-materials as a function of the measuring time. The combinations compared were:

- |                                      |                                     |
|--------------------------------------|-------------------------------------|
| - LiF (TLD-100)                      | - TNO automatic TLD-reader          |
| - CaF <sub>2</sub> (TLD-200)         | - TNO automatic TLD-reader          |
| - CaSO <sub>4</sub> (TLD-900)        | - TNO automatic TLD-reader          |
| - CaSO <sub>4</sub> :Dy teflon disks | - Teledyne Isotopes TLD 7300 reader |

An ionisation chamber (Reuter-Stokes type RSS-111) was installed at the same measuring point for reference. In this study, one TLD-group consisted of 15 TLDs, divided into three equal subgroups. Each subgroup was subjected to a different radiation treatment.

Subgroup 1 was exposed during the surveillance period only, at the measuring spot. Subgroup 2 was subjected to a reference exposure before the actual surveillance period, while subgroup 3 underwent such an exposure after the actual surveillance period. This was done to estimate the fading from the reference exposure during a surveillance period. Some of the TLD-groups were placed in an aluminium box, whereas others were placed inside a two-millimetre copper sphere. Both box and sphere were placed at 0.8 m above the ground. The gas ionisation chamber was positioned at the same spot and the same height. Figure 1 shows the results of this research. It was evident that the combination of CaF<sub>2</sub> TLD and the TNO automatic TLD-reader was the most promising one.

#### THE MEASURING PROCEDURE FOR THE COMBINATION OF CaF<sub>2</sub> (TLD-200) AND THE TNO AUTOMATIC TLD-READER

The procedure for an environmental TLD-system fulfilling the demands given above is as follows:

- the TLD-group for one spot consists of 14 CaF<sub>2</sub> TLDs, divided into two subgroups of 7 TLDs each

- one subgroup is subjected to a reference exposure both at the beginning and the end of a surveillance period for fading correction, while the other subgroup is exposed at the measuring spot only
- annealing treatment:
  - pre-irradiation anneal 0.5 hour at 300 °C, 1.5 hour at 85° C and 0.5 hour at 20 °C in darkness to cool down
  - pre-reading anneal 1.5 hour at 85° C and 0.5 hour at 20° C in darkness to cool down
- each TLD is read out only once in 11 seconds at a temperature of 275° C
- the background is evaluated by means of one randomly chosen CaF<sub>2</sub> TLD, which is read out many times. The background used is the average of the last 20-40 measurements.

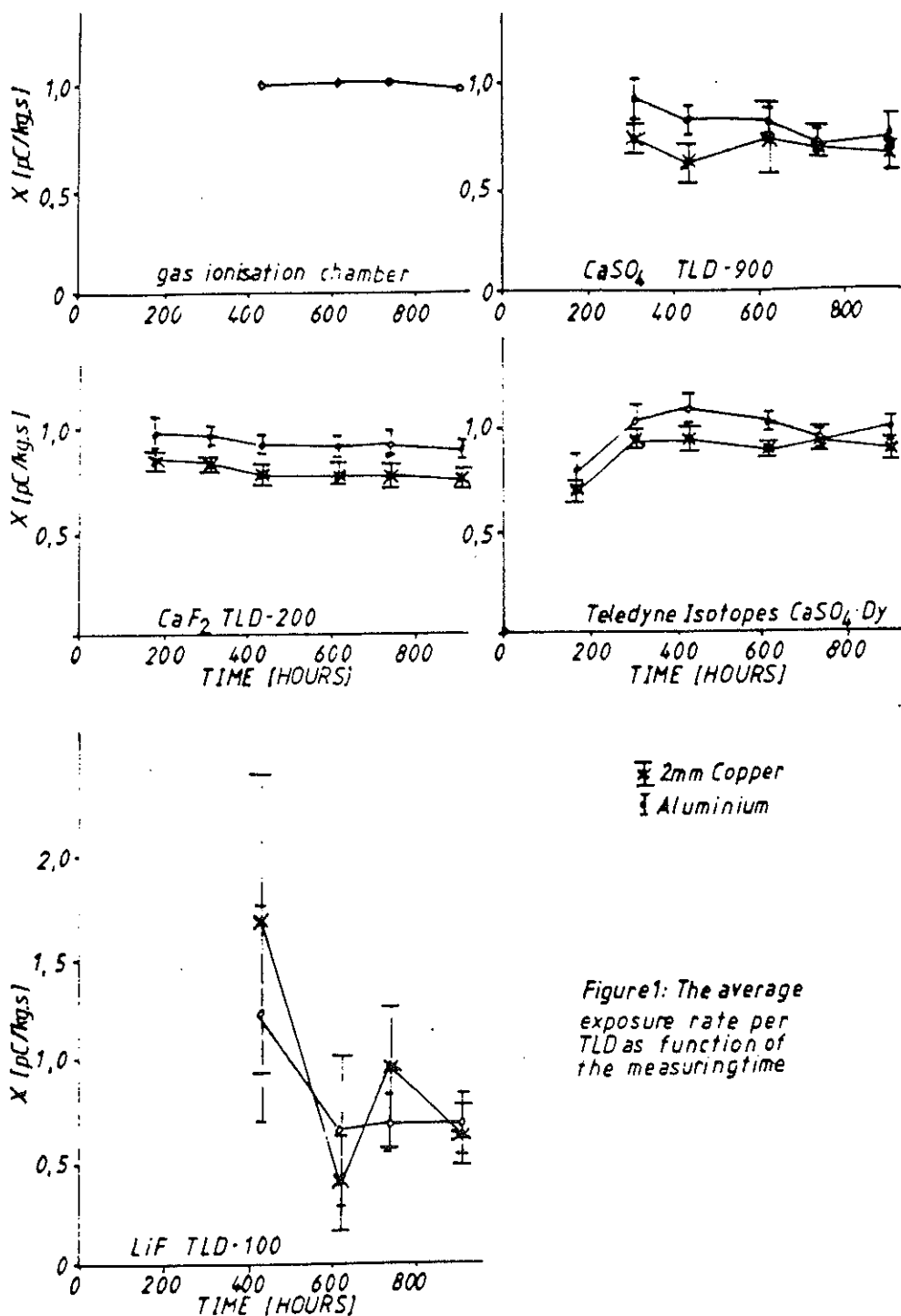


Figure 1: The average exposure rate per TLD as function of the measuring time

- the exposure rate is determined by means of the following formula:

$$\dot{X} = \frac{X_{\text{before}} + X_{\text{after}}}{\bar{D}_{\text{sg2}} - \bar{D}_{\text{sg1}}} \cdot \frac{\bar{D}_{\text{sg1}} - \bar{D}_{\text{bg}}}{t_m} \text{ and}$$

the standard deviation by means of the formula

$$S^2 = \frac{(X_{\text{before}} + X_{\text{after}})^2}{t_m^2 (\bar{D}_{\text{sg2}} - \bar{D}_{\text{sg1}})^4} ((\bar{D}_{\text{sg2}} - \bar{D}_{\text{bg}})^2 S_{\text{sg1}}^2 + (\bar{D}_{\text{sg1}} - \bar{D}_{\text{bg}})^2 S_{\text{sg2}}^2)$$

X is the exposure rate [C kg/s]  $X_{\text{before}}$  and  $X_{\text{after}}$  are the reference exposures [C/kg];  $t_m$  is the exposure time [s];  $\bar{D}_{\text{sg1}}$ ,  $S_{\text{sg1}}$ ,  $\bar{D}_{\text{sg2}}$  and  $S_{\text{sg2}}$  are the averages and standard deviations of the TLD-data from subgroup 1 and 2 [counts] respectively;  $\bar{D}_{\text{bg}}$  is the average of the background [counts].

#### TECHNICAL REALIZATION OF THE NEW ENVIRONMENTAL SYSTEM

The mechanical parts (see Figure 2) like the TLD-holder, the pick-out platforms and the readout table were designed simultaneously and adjusted to each other.

A simplified block diagram of the electronics is shown in Figure 3.

The automation software was developed in cooperation with the KEMA Computer Centre. The automation software consists of 8 programs. These programs include: measurement of the background, the readout of the various environmental areas, calculation of the exposure rate, comparison of the exposure rate last measured with previous data (this program warns the operator if there is a significant difference of 25% between these data), plotting of the measured data exposures, and selecting TLDs in TLD-groups with the statistically most favourable results.

The present hardware and software is capable of reading out the TLD chips with a frequency of more than 120 TLDs per hour and meets all the postulated requirements.

#### CALAMITY DOSIMETERS

The calamity dosimeters are used to obtain an estimation of the local dose rates at a severe reactor accident. Because of the sensitivity and the annealing treatment of the  $\text{CaF}_2$  TLDs they cannot be used as calamity dosimeters. Therefore the calamity dosimeters are personal LiF badges from TNO, with two LiF TLDs (Harshaw's TLD-100) inside. These calamity dosimeters

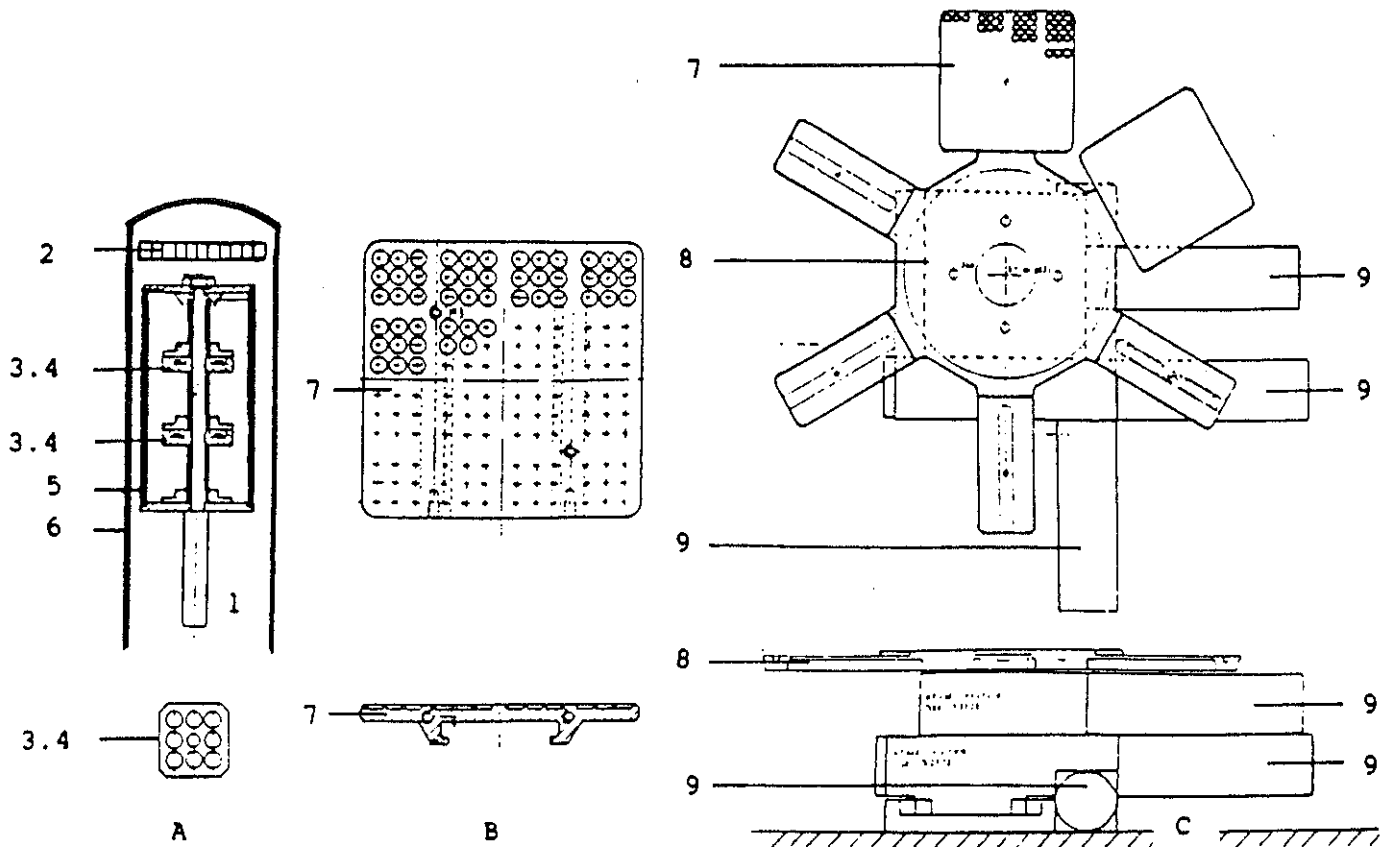


Fig. 2. A The TLD-holder. The calamity TLDs (2) are positioned at the top. Below them are the environmental TLDs (3), which are placed in nylon (4) and surrounded by two-millimetre copper (5). Both TLD-groups are embedded in PVC (6).  
 B The pick-out platforms. The TLDs are placed on these platforms when they have to be annealed or read out.  
 C The readout table (8). The pick-out platforms are placed on the "legs" of the table, so that the TLDs can be accurately positioned under the TLD-reader by stepping motors (9).

are placed above the environmental dosimeters (see Figure 2A). The treatment of these calamity TLDs is very simple. After a surveillance period, they are put on the pick-out platforms which in their turn are placed directly on the readout table. The first readout in eleven seconds at 300°C is the pre-reading anneal as well as the data collection readout. The second readout, with the same settings, is the pre-irradiation anneal. After these two readouts, the

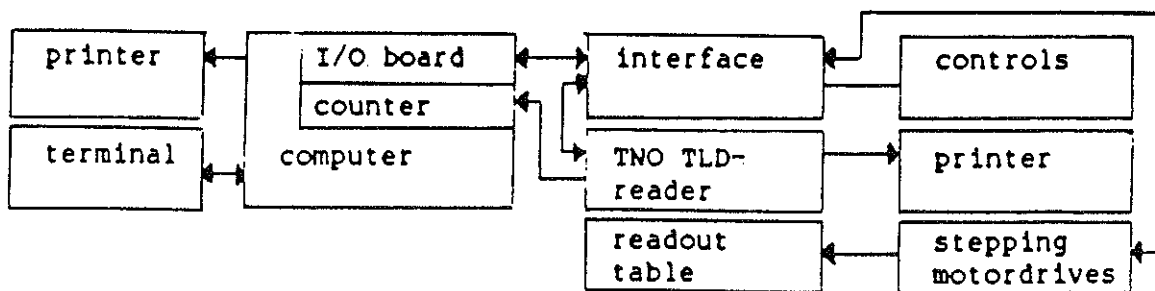


Fig. 3. Simplified blockdiagram of the electronics.



chips are ready to be used again.

EVALUATION

Ever since these TLD-systems have been in use, no exposure data have been lost by a mechanical, electronic or software error. Once, a human error (both

FIG 4A DODEWAARD (15) FROM 15-05-85 TILL 28-01-88

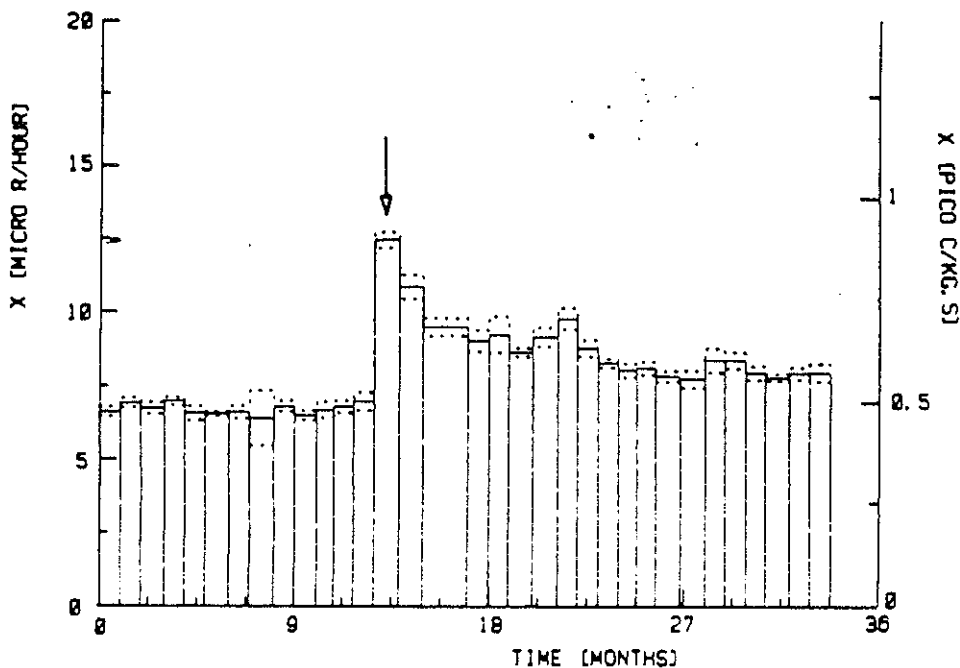


Fig. 4A. Dodewaard (15) from 85-05-15 till 88-01-28

FIG 4B BORSSELE (18) FROM 17-01-84 TILL 16-03-87

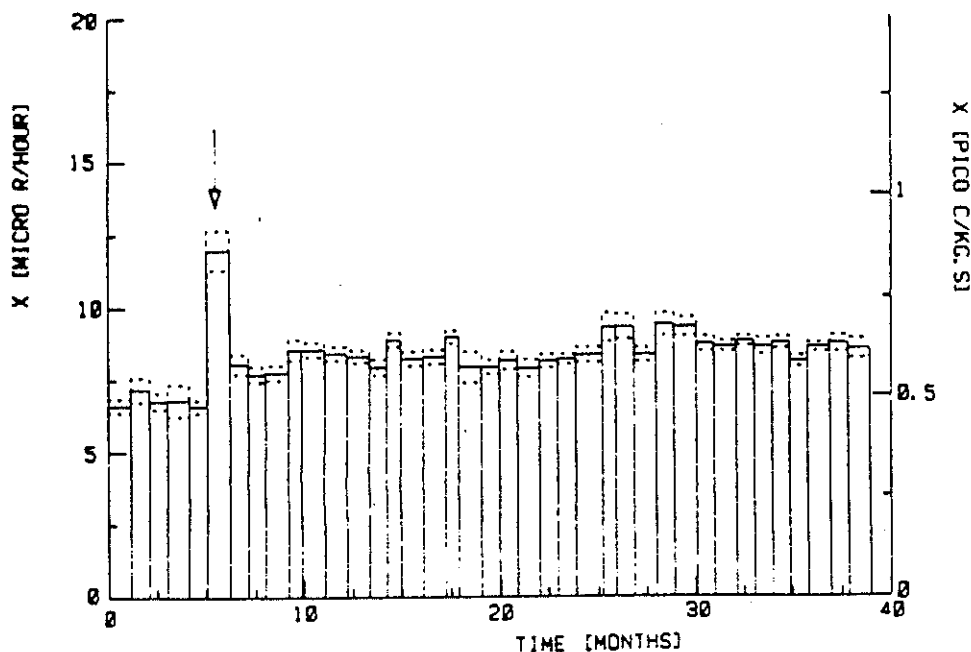


Fig. 4B. Borssele (18) from 84-01-17 till 87-03-16

subgroups were subjected to a reference exposure) caused the standard deviation of the exposure rate to increase from less than 5% to 30% in 16 TLD-groups. In Figure 4, plots are shown of the exposure rate of typical locations of the Dodewaard and Borssele environment.

The increased exposure rate at the Dodewaard location (Figure 4A) is caused by Chernobyl (see month 14). This phenomenon is not observed in Borssele (see month 29 in Figure 4B). The increased exposure rate in month 6 at the Borssele location is due to the use of slugs with a high amount of natural radioactivity for a cycle track near the measuring spot.

#### ACKNOWLEDGEMENT

The author would like to express his gratitude to Mr. C.A.M. Flaar (KEMA Computer Centre) for his cooperation in the development of the automation software.



**Thermoluminescence Dosimetry  
in  
Radiotherapy and Radiobiology**



## EXPERIENCE WITH IN VIVO THERMOLUMINESCENT DOSIMETRY FOR TOTAL BODY IRRADIATION

J. Van Dam and A. Rijnders

University Hospital St. Raphael, Department of Radiotherapy,  
3000 Leuven, Belgium.

### I. INTRODUCTION

Total Body Irradiation (TBI) is used in our centre prior to bone marrow transplantation for treatment of leukaemia. A dose of 8 Gy is delivered in a single fraction midline in the patient, at a dose rate of about  $4\text{cGy}\cdot\text{min}^{-1}$ .

In our set-up the measurement of the dose distribution in the patient relies on in vivo dosimetry. Due to the low dose rate the dosimetry has to be based on a method with sufficient sensitivity. Up to now we have used thermoluminescent detectors (TLD) for these measurements, although semiconductor dosimetry is also commonly used in other centres. This contribution is intended to illustrate the possibilities of the TLD method under the difficult conditions of TBI at low dose rate.

### II. MATERIALS AND METHODS

#### II.1. Thermoluminescent dosimetry

Extruded LiF (Harshaw TLD-100) ribbons of about 3mm x 3mm x 1mm are used. They are read out with a Harshaw system consisting of a model 2000-C TL detector and a model 2000-B automatic integrating picoammeter. The photomultiplier tube is operated at a high voltage of 700V. The heating cycle starts with a fast rise of the temperature to 100°C, which level is maintained during 10s. After this "post irradiation annealing" the temperature increases linearly with time during 30s up to an end temperature of 300°C. During this period the TL signal is integrated and displayed. The "pre irradiation annealing" consists of a heating at 400°C for 2 hours followed by a cooling to 80°C, which temperature is maintained for 24 hours.

With this method a typical standard deviation of  $\pm 3\%$  is obtained under reference conditions, i.e. for a set of dosimeters irradiated simultaneously in a phantom to a dose of 1 Gy. The dosimeters are not

individualized and the spread in response may amount up to  $\pm 10\%$  of the average.

## 11.2. THE TBI METHOD

Our TBI method is derived from the method developed at the Royal Marsden Hospital in Sutton<sup>1</sup> and has been described<sup>2</sup> elsewhere. In summary, patients lying supine are irradiated with two laterally opposed 18MV X-ray beams (Fig.1). They are positioned as close as possible to one of the treatment room walls, which is at a distance of 350cm from the focus. At half-treatment the couch with the patient is turned 180°. As the field size at the level of the wall is only 140 cm x 140 cm, adults have to bend their legs in order to get the whole body within the field. To ensure electronic equilibrium at the level of the skin a 2 cm thick Perspex plate is placed close to the patient's side facing the beam.

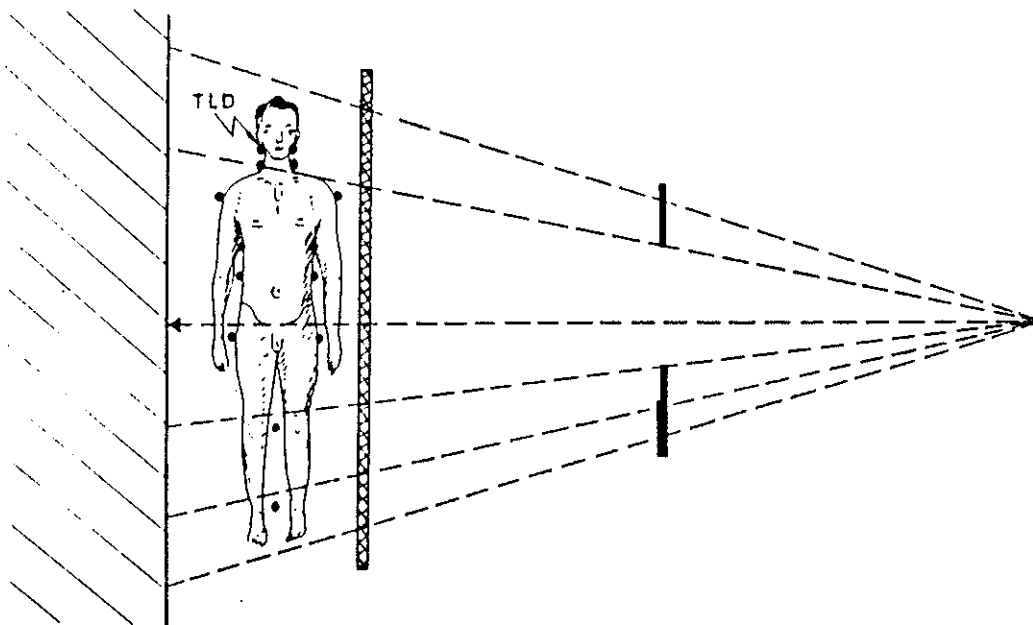


Fig. 1 - Treatment set-up and positions of the TL dosimeters for TBI at low dose rate. Patients are irradiated in supine position with two laterally opposed fields at a focus skin-distance of about 300 cm. Lead compensators are positioned at 150 cm from the focus. A Perspex sheet ensures electronic equilibrium at the entrance side of the beam.

Compensators are positioned at 150 cm from the focus and are aligned in order to compensate for tissue defect at the level of the head and of the lower limbs. They consist of lead sheets with a thickness calculated according to the patient's transversal diameters. In order to achieve a satisfactory dose homogeneity it is necessary in some cases to apply additional polystyrene sheets against the patient at the level of the thorax, pelvis or abdomen.

### II.3. Dosimetric procedures

For TBI applications the TLD's are packed in plastic bags, each containing 4 ribbons, which are taped on the patient's skin. The Perspex plate in front of the patient (see fig. 1) is supposed to provide the necessary electronic equilibrium at the level of the entrance dosimeters, while the bags at the exit are covered with 5 mm Perspex.

About one week before the TBI, a test irradiation up to a dose level of about 5cGy is performed to verify the homogeneity of the dose distribution over the patient's body in cranio-caudal direction. TL dosimeters are applied at the beam entrance and exit side at the level of the ears, neck, shoulder, thorax, abdomen and pelvis and in the middle between the knees and the ankles. The midline doses are calculated as the square root of the product of the measured entrance and exit dose. For the test irradiation the doses received by the TLD range between about 3 and 10 cGy, which is much smaller than for in vivo measurements during the other treatments, where they are typically between 1 and 2 Gy. Nevertheless the standard deviation of the mean remains at the same level (3%) compared to the reference conditions.

During the period between this "test" and the actual TBI, the TL dosimeters are read out and the compensator thicknesses are considered as satisfactory if the midline doses at the different levels investigated do not differ more than  $\pm 10\%$  from their average value. If this condition is not fulfilled, the compensator thickness is adjusted based upon the measured dose deviations.

During the TBI the TLD's are positioned on the patient during the first ten minutes of the irradiation and are irradiated at dose levels between 20 and 70cGy. The dosimeters are read out while the irradiation



continues. As the time needed for reading all dosimeters is of the order of 1 hour, a first quick analysis is performed based on one dosimeter per site, giving results after about fifteen minutes. Despite an obviously relatively large uncertainty, these results are very important as they will show any "dramatic" dose inhomogeneity which, if not immediately corrected, would lead to an unacceptably large dose variation. If the information gained from the complete set of dosimeters still shows some minor problems, the compensators are adapted at half treatment when the patient is turned 180°. At the beginning of this second half of the treatment, the dose distribution is checked a last time. Compensator corrections at this stage of the treatment are however seldom necessary.

### III. RESULTS.

This method was started in 1983 and has been applied for 69 patients. For 30 patients the dose homogeneity was found satisfactory during the test irradiation. For only 50 % of these patients the satisfactory dose distribution was confirmed at TBI, while the other half required compensator thickness adaptation during TBI. For 39 patients the calculated compensator thickness had to be adapted according to the TLD results obtained for the test irradiation. This adaptation resulted in a homogeneous dose distribution during TBI for 26 patients, while for the remaining 13 patients a second adjustment of compensator thickness during TBI was performed.

### IV. DISCUSSION.

The TLD method has allowed us to perform TBI treatments according to the common standards of dosimetry for this kind of application. Despite the relatively small doses delivered to the TLD, the accuracy of the method remains as good as observed under reference conditions.

For 28 patients the results obtained at the test irradiation were not confirmed at TBI. Most likely, however, the reason for these discrepancies is not at the level of dosimetry, but due to unavoidable small differences between test irradiation and TBI concerning patient positioning. Although the patient is more or less immobilized, some minor movements are necessarily allowed which can cause differences in

tissue thickness in front of the exit dosimeter and in body composition (e.g. bowel gas).

The main advantage of TLD for in vivo dosimetry at low dose rate is the absence of any cable around the patient. These cables could indeed hamper patient care when nausea and emesis occur.

On the other hand some drawbacks of TLD in vivo dosimetry for TBI at low dose rate can not be denied when comparing this method to semiconductor dosimetry. The main disadvantage of TLD is its delayed information, which excludes continuous dose monitoring. This is certainly for TBI at low dose rate an important issue. As already mentioned, the patient is not completely immobilized and this could lead to deterioration of the compensator alignment during the course of treatment. A satisfactory dose distribution during the first ten minutes provides in this case no absolute guarantee for the rest of treatment. For this reason we plan to replace, at least partly, the TLD by semiconductors for TBI dosimetry. This does, however, not hold for the test irradiation in which the TLD's are on the patient only one and a half minute. Moreover, the resolution of the Therados DPD-6 semiconductor dosimeter, which is used in our centre, is, with maximum gain factor, equal to  $3 \times 10^{-1}$  cGy per reading unit. For doses as low as those delivered during the test irradiation (see above) this resolution does not allow one to analyse the dose homogeneity with sufficient accuracy. By contrast, the resolution of the TLD-method is, under the conditions specified above, very fine ( $5 \times 10^{-3}$  cGy per reading unit). Also at least two DPD-6 systems, each allowing a total number of 6 simultaneously explored sites, would be necessary to measure all relevant sites, while keeping the patient dose at a satisfactory low level. Although the use of TLD for TBI will be possibly reduced, the method will still maintain its place in the overall dosimetric approach for this kind of treatment.

#### REFERENCES

1. M. Rosenbloom, P.A. Hickling, M. Chow, S. Chittenden, J. Machardy, J. Povall, M. Lewis and A. Barrett, Total body irradiation at the Royal Marsden Hospital Sutton, Meeting of Leiden, May 25-27, 1982, J. Eur. Radiother. 3 (1982) 246-248.

2. A. Rijnders, J. Van Dam and E. van der Schueren, Total body irradiation technique and dosimetry at Leuven, Meeting of Leiden, May 25-27, 1982, J. Eur. Radiother. 3 (1982) 194-195.

## TL - DOSIMETRY IN CLINICAL PRACTICE

D. Bakker, M.A. Crommelin and W.J.F. Dries

Catharina Hospital, Radiotherapy Department,  
Michelangelolaan 2, 5602 ZA Eindhoven, The Netherlands

### INTRODUCTION

At the Radiation Therapy Department of the Catharina Hospital, thermoluminescence dosimetry is used since 1974 for several purposes:

#### A: DOSIMETRIC STUDIES WITH PHANTOMS, e.g.;

Preparation and verification of calculation of absorbed dose before introduction of new irradiation techniques, including the CATHETRON high dose rate after-loading apparatus for gynaecological cancers and the breast sparing treatment with Ir-192 wires and various external beam applications.

#### B: IN-VIVO DOSIMETRY, e.g.;

- 1) Determination of absorbed dose and dose distribution in individual cases where (computer) calculations may not accurate enough because of the restrictions associated with the beam model e.g. with special moulds, or with treatment techniques like electron beam arc therapy.
- 2) Dose measurements at critical organs close to the direct beam in individual patients, e.g. eye lense, gonads.

#### C: RADIATION PROTECTION MEASUREMENTS, e.g.;

Measurement of radiation dose received by personnel involved in preparation of brachytherapy sources and wardroom staff.

This paper is meant as an overview of our materials and methods. A few applications will be illustrated and some results will be presented.

### MATERIALS AND METHODS

#### Equipment:

The equipment consists of a HARSHAW 2000A TL detector, a HARSHAW 2000B integrating picoammeter and a separate oven for annealing. As TLD material HARSHAW TLD-100 LiF ribbons and rods are used.

#### Calibration:

The ribbons and rods have been selected from batches of 100 crystals by means of an iterative process, leading to three sets with increasing standard deviation. The set of ribbons and rods with the smallest standard deviation is mostly used for dosimetric studies with phantoms. A record of

the individual sensitivities and the standard deviation is kept. Optimal calibration accuracy is accomplished by placing the TLD's in a polystyreen phantom mounted on a rotating platform in order to minimize beam flatness deviations.

The linearity of the readings of ribbons and rods is determined in the dose range 0.25-50 Gy. The lower part of this range is typical for fractionated external beam treatment. The data for the high doses may be useful in intra-operative radiotherapy where single doses in the range from 10-20 Gy will be delivered. The results are presented in fig. 1a and 1b, showing supralinear behaviour over the full range for TLD-100 rods, for ribbons only above 4 Gy.

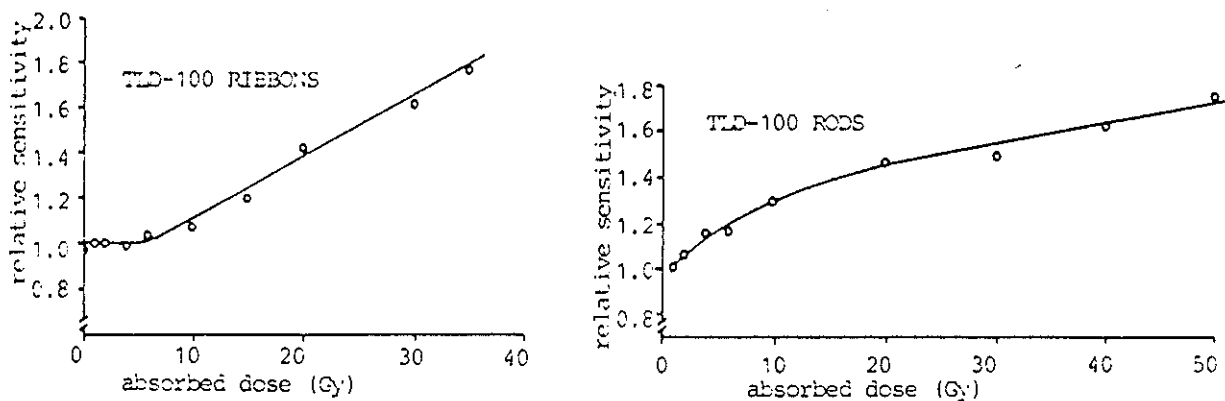


Fig. 1a and 1b. Relative sensitivity as a function of absorbed dose of TLD-100 ribbons and rods. (Sensitivity normalized to 1 for 1 Gy).

Measurements were also carried out to investigate the influence of high doses (>10 Gy) on sensitivity. After irradiation with a high dose, a number of cycles consisting of a sensitivity measurement at the 1 Gy level plus standard annealing, were performed. The results are shown in fig 2a and b.

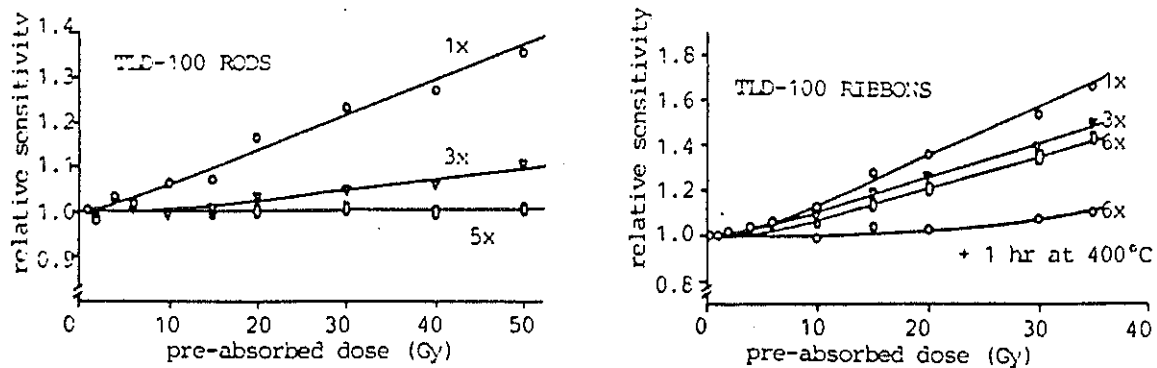


Fig. 2a and 2b. Relative sensitivity (normalized to and measured at 1 Gy) as a function of pre-irradiation dose and number of annealings.

Sensitivity increases significantly after these high doses and returns to the initial value after minimal 5 annealing cycles for rods and after minimal 6 annealing cycles plus one hour at 400°C for ribbons.

#### Measurement procedures:

For phantom measurements TLD rods are commonly used, 4 at each position when possible. For in-vivo applications commonly a group of 4 TLD ribbons, packed in a sealed plastic bag, is used on each position. An extra set of 4 ribbons, packed in a special lucite block guaranteeing full build-up of dose, is irradiated with a calibration dose. After irradiation, the TLD's are kept either for 24 hours at room temperature or for 10 min. at 100°C to reduce the unstable low temperature peaks. The glow curve is integrated between 120°C and 220°C (fig.3). Annealing for the standard external therapy dose range is obtained by heating up to 400°C and a slow cooling period to room temperature during about 10 hours (fig.4). For dose measurements below 0.01 Gy we normally use the TLD's and read-out service of the Radiological Service TNO (ref.1).

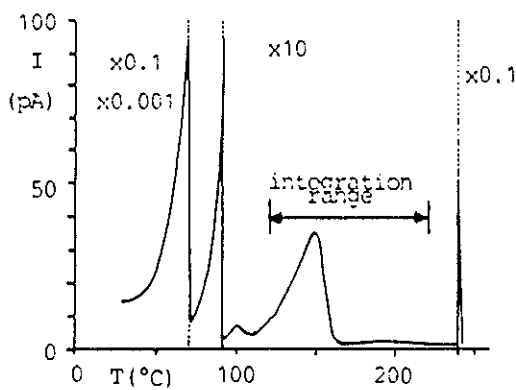


Fig.3. TLD 100 Glow curve and integrating range

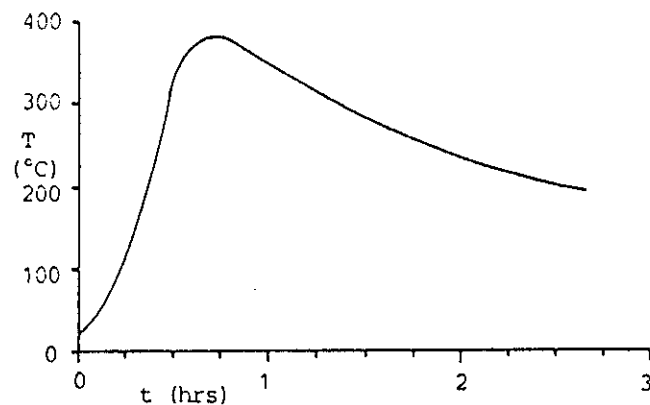


Fig.4. TLD annealing temperature curve

#### A: DOSIMETRIC WITH PHANTOMS FOR BRACHYTHERAPY:

##### Verification of Irradiation Techniques and Calculation Models with TLD'S.

At the introduction of new irradiation techniques or prior to the clinical acceptance of computer calculation models it is necessary to verify the accuracy of the absolute dose and dose distribution. Such studies have been carried out at the introduction of a high dose rate afterloading device (TEM Cathetron) and for interstitial brachytherapy with Cs-137 needles. TLD's are very convenient for this purpose because of their small dimensions, which allows measurements in regions with large dose gradients inhe-

rent to brachytherapy. A recent example of this application is the verification of interstitial irradiation with Ir-192 wires in breast sparing treatment. To verify the dose distribution, TLD rods are positioned at 8 places in a polystyrene phantom (density 1.05 g/cc, fig. 5a) around a single 77 mm long Ir-192 wire (4.44 GBq/m). Another phantom with 7 Ir-192 wires in a configuration which resembles the clinical situation is used to measure the dose in two midplane points (fig 5b). The results are corrected for supralinearity. A comparison was performed with the Philips OSS brachytherapy program. All results agreed within 2%.

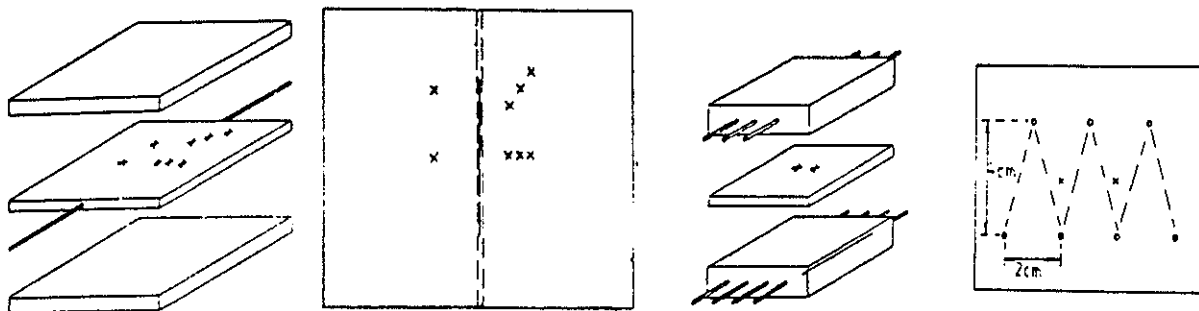


Fig. 5a and 5b. Phantoms used for verification of Ir-192 interstitial therapy dosimetry.

## B: IN-VIVO DOSIMETRY:

### 1) Individual Verification of Dose and Dose Distribution

Breast cancer patients with local recurrence undergo irradiation of the chest wall (ref.2). To reduce the dose to the underlying lung tissue rotation therapy with electrons of 6 to 10 MeV is frequently used at the Catharina Hospital. To compensate for variations in the thickness of the chest wall a customized bolus of tissue equivalent material is constructed, based on thickness information from serial CT scans. Compensation for variations in body contour requires a variable slit electron beam collimator which, amongst other reasons, makes computer calculations not yet adequate to determine dose and dose distribution. Therefore, before starting the patient irradiation sessions, phantom measurements with TLD's and films are performed to find optimal settings of treatment parameters, i.e. collimator width, horizontal table rotation, position of isocentre, gantry rotation speed, etc. During the first treatment session these settings are checked with in-vivo TLD-measurements.

## B: IN-VIVO DOSIMETRY:

### 2) Individual Critical Organ Dose and Target Dose Measurements with TLD'S

As a routine procedure, all teletherapy treatments are prepared and checked

with a simulator and dose distributions are calculated on the Philips OSS system. However, in clinical practice an additional measurement is sometimes requested, especially in the first treatment session, for several reasons, e.g:

- Due to a very irregular geometry (e.g. nose, ear) or the use of bolus material or irregular field blocking, calculations may not be accurate enough, especially in the case of electron beams.
- The dose calculation model does not take into account the effect of Compton electrons from a tray. This is relevant in the case of inverted-Y field irradiations, where the dose on the male gonads has to be minimized (ref.3).
- It is not always clear whether critical organs like gonads or eye lenses are adequately kept outside the treatment portal. Occasionally the target volume can be very close to the eye lens.

The absorbed dose in the eye lens is estimated from sealed TLD ribbons on the lid of the closed eye. For gonad measurements, sealed TLD's are placed on the scrotum and an extra set is packed in 2 cm thick Lucite to filter out the contribution of the Compton electrons.

In our clinic, these TLD measurements are done since 1975 and recently the stockpile of individual reports is put into a database management system to see whether useful information could be extracted from a systematical analysis. Because the decision criteria to request a verification measurement have not been constant and uniform, one must be cautious to draw statistical conclusions from this evaluation. Another disturbing factor is the fact that the total dose to an organ cannot be derived from a measurement in one treatment session because sometimes, after a certain target dose is reached, the field size is reduced. However, some figures might be informative:

- In total 420 times the dose to one or more locations on the patient was measured, 156 on the eye lens(es), 123 on the testes and 227 times the target dose was verified.
- These 227 target dose measurements were performed for 27 total body irradiations, 85 electron arc therapies, the remainder for stationary electron fields.
- 18% of the critical organ dose measurements showed a dose > 8% of the target dose. In these cases it might be worthwhile to reconsider the treatment setup. In most therapies this level results in a total absorbed dose which is still below the tolerance dose for eye lens and gonads (ref.4).



- During a certain period, testis dose measurements were done systematically in inverted-Y field treatments. Fig 6 shows a frequency histogram of the extrapolated total testis dose. In this figure, three classes are indicated, according to Hahn et al (ref 5). Patients in class A (0.25-0.75 Gy) show recovery after temporary sterility within 18 months. In class B (0.75-1.5 Gy) after 12-24 months of sterility recovery is reported after a total period of 24-30 months. Patients with testis dose > 2 Gy (class C) are reported to remain sterile for more than 4 years.

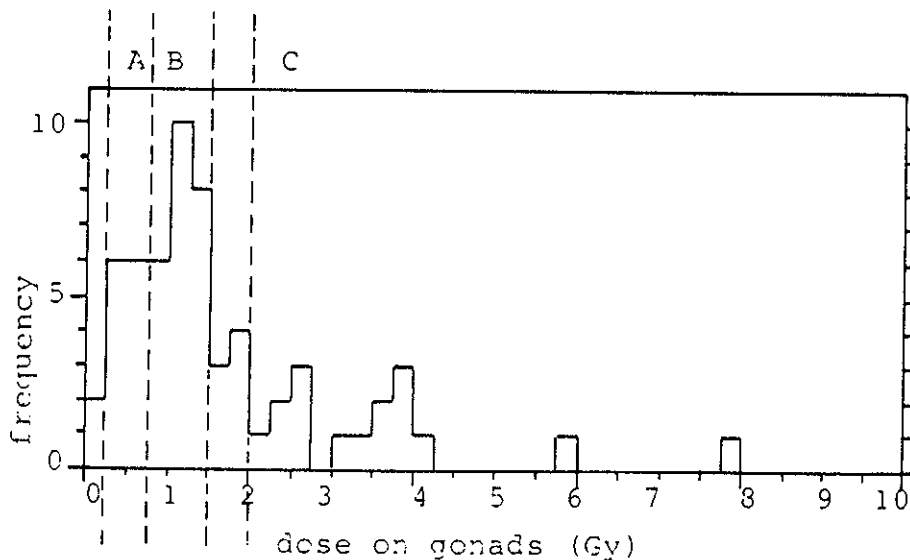


Fig. 6. Frequency histogram of extrapolated total testis dose

### C: RADIATION PROTECTION MEASUREMENTS

In order to evaluate the radiation dose to personnel, involved in the application of Ir-192 wire for breast sparing treatment, we measured the dose to the fingers of the technician and of the radiotherapist, respectively while preparing the sources and while applying the sources to the patient. Using standard protection measures like lead shields etc, an average application leads to a finger dose of 0.7 mSv for the technician and of 0.6 mSv for the radiotherapist. This means that with the present frequency of about 70 applications per year finger doses are less than 10% of the dose limit. Similar measurements were done on the wardroom staff.

### CONCLUSIONS

Our experience in using thermoluminescence dosimetry shows that it is a very useful method for calibration and verification procedures in brachytherapy. In teletherapy and in radiation protection of personnel and patients TLD's can be applied next to other dosimetry methods.

#### ACKNOWLEDGEMENTS

The authors are greatly indebted to W. Theunissen, C. Kersten, S. Somers, A. Heys, L. Wolters for their contribution to the measurements.

#### REFERENCES

1. The TNO TLD Individual Monitoring Service: Concepts and Methodology, Proceedings TLD Symposium, march 1988.
2. M.A. Crommelin, C.W.M. Kersten, D. Bakker, Electron beam arc therapy in breast cancer, IV Mediterranean Conference on Medical and Biological Engineering (sept 1986, Sevilla, Spain)
3. M.A. Crommelin, D. Bakker, Planning for radiation therapy with irregular fields, Medicamundi 24 (1979) 98.
4. ICRP-41 (1984,) Non-stochastic effects of ionizing radiation, vol. 14 no. 3 (Pergamon Press, Oxford, UK)
5. E.W. Hahn, W. Schlegel, L. Simpson, M. Batata, Dose response recovery of spermatogenesis in cancer patients following incidental testicular radiation, Eighth International Congress of Radiation Research (july 1987, Edinburgh, UK)



APPLICATION OF TLD FOR DETERMINATIONS OF DOSE DISTRIBUTIONS  
FOR PHOTON IRRADIATIONS IN RADIOBIOLOGY

J. Zoetelief and N.J.P. de Wit

Radiobiological Institute TNO, P.O. Box 5815, 2280 HV Rijswijk, The Netherlands

INTRODUCTION

To predict the responses of irradiated biological specimens, it is essential to determine the energy dissipation with a sufficient degree of accuracy and precision. Investigations in radiobiology have demonstrated that differences of 10 per cent in absorbed dose can produce clearly observable variations in biological response. It has been suggested that an accuracy of  $\pm 5$  per cent and a precision of  $\pm 2$  per cent (one standard deviation) is required for the determination of absorbed dose in radiobiological studies<sup>1</sup>. The irradiation of a target volume (e.g., tissue, organ or animal) should be uniform. The condition for uniform irradiation is that the inevitable variation in absorbed dose throughout the volume of interest should be small enough to prevent a significant effect on the biological response considered. The criterion for uniform irradiation is a maximum ratio of 1.10 in the absorbed doses in the target volume but preferably less than 1.05<sup>2</sup>. For partial body irradiations, the absorbed dose in other essential organs should be as small as practically possible, certainly restricted to levels which do not interfere with the projected course of the experiment. Advantageous features of thermoluminescent (TL) dosimeters are their small size and their applicability over a wide dose range. Their small size makes them particularly suitable for studying the dose distribution within small animals (e.g., mice and rats). Examples of dose distributions measured with TLD are given for partial and whole body irradiation of rats in radiobiological studies and compared with the results of the use of ionization chambers.

PRINCIPLES OF DOSIMETRY USING TLD

The TL dosimeters used for the experiments are LiF:Mg,Ti (TLD-100, Harshaw) rods with a diameter of 1 mm and a length of 6 mm. A pre-reading anneal of 1 hour at 100°C was applied; the pre-irradiation annealing was generally carried out in the TLD reader (Harshaw 2000D) up to 350°C.

If  $R_i$ ,  $B_i$ ,  $R_{ci}$  and  $B_{ci}$  are the results of four readouts (R refers to reading, B to background and index c to the calibration situation) of the i-th dosimeter from a set, the dose,  $D_i$ , at the position of dosimeter i, is given by:

$$D_i = (R_i - B_i) / S_i$$

where  $S_i$  is the calibration factor of the individual dosimeter i derived from comparison with a calibrated ionization chamber under secondary charged particle equilibrium for both TL dosimeters and the ionization chamber.

#### EXAMPLES OF PARTIAL BODY IRRADIATIONS

For studies on the entry of the prothymocyte into the thymus after irradiation and bone marrow transplantation<sup>3</sup> several types of irradiations of mice were carried out with 6 MV X rays produced with a Philips MEL SL75 linear accelerator. Mice were irradiated with or without thymus shielding (10 cm high cylindrical bar with a diameter of 12 mm) and on the thymus only (a 10 cm thick lead block with a aperture of 23 mm diameter). For the irradiations with thymus shielding, measurements were made with TLD rods with their longitudinal axis in the beam direction inside a polymethylmethacrylate (PMMA) mouse phantom to which a 10 mm thick PMMA build-up layer was added. The results are shown in Table 1 for various shielding diameters.

Table 1: Relative doses  $D_r(l)$  determined with TLD rods at 8 mm depth in a PMMA mouse phantom irradiated with thymus shieldings (10 cm thick) of different diameters (d) for 6 MV X rays where l (in mm) is the distance to the central shielding axis. The doses are given relative to the unshielded situation.

| shielding diameter (mm) | $D_r(0)$ | $D_r(2)$ | $D_r(5)$ | $D_r(6)$ | $D_r(9)$ |
|-------------------------|----------|----------|----------|----------|----------|
| 12                      | 0.061    | 0.068    | 0.195    | 0.214    | 1.002    |
| 16                      | 0.038    | 0.040    | 0.047    | 0.057    | 0.195    |
| 20                      | 0.033    | 0.033    | 0.038    | 0.050    | 0.109    |
| 20*                     | 0.047    | 0.049    | 0.054    | 0.058    | 0.133    |

\* For irradiation with 12 cm x 14 cm field instead of 4 cm x 14 cm.

It can be concluded from Table 1 that the doses behind the shielding increase with decreasing shielding diameter, with increasing distance l to the central shielding axis and with increasing field size.

For studies on volume effects of spinal cord tolerance of rats after CNS-irradiation, dose measurements were made inside a (20 mm x 25 mm x 59 mm) PMMA phantom with TLD-100 rods and an 0.2 cm<sup>3</sup> Baldwin-Farmer ionization chamber. The phantom simulates the neck of a rat. Irradiations with 6MV X rays were carried out with a field length (perpendicular to the spinal cord) of 5 cm and field widths varying from 2 to 15 mm. The TLD rods were placed with their longitudinal axis parallel to the length axis of the field at different depths. The doses at different field width (s) and depth (d) and distance to the centre of the field (a) (see Table 2) are normalized to the doses at 15 mm field width, 5 mm depth in the centre of the field, D(15,5,0).

Table 2: Relative doses determined with TLD-100 rods at depth (d) inside a PMMA phantom (20 mm x 25 mm x 59 mm) irradiated with 6 MV X-ray fields of various widths (s) and a length of 50 mm.

| s<br>(mm) | d<br>(mm) | a<br>distance to<br>field centre<br>(mm) | D(s,d,a)<br>D(15,5,0) | D(s,d,a)<br>D(s,5,0) |
|-----------|-----------|--|-----------------------|----------------------|
| 2         | 0         | 0  | 0.75±0.03             | 1.07±0.05            |
| 2         | 5         | 0  | 0.70±0.03             | 1                    |
| 2         | 10        | 0  | 0.68±0.03             | 0.98±0.04            |
| 2         | 15        | 0  | 0.63±0.03             | 0.90±0.04            |
| 2         | 5         | 6.5                                      | -                     | 0.026±0.002          |
| 5         | 5         | 0  | 0.93±0.03             | 1                    |
| 5         | 15        | 0  | 0.87±0.03             | 0.95±0.03            |
| 5         | 5         | 6.5                                      | -                     | 0.069±0.002          |
| 10        | 5         | 0  | 1.00±0.03             | 1                    |
| 10        | 15        | 0  | 0.95±0.03             | 0.95±0.03            |
| 10        | 5         | 6.5                                      | -                     | 0.137±0.004          |
| 15        | 0         | 0  | 0.98±0.03             | 0.98±0.03            |
| 15        | 5         | 0  | 1                     | 1                    |
| 15        | 15        | 0  | 0.95±0.03             | 0.95±0.03            |
| 15        | 5         | 6.5                                      | -                     | 0.92±0.03            |

To facilitate the depth dose comparison at different field widths and the relative dose in the shielded area, also the values for D(s,d,a)/D(s,5,0) are given. It can be concluded that the depth dose distribution is steepest

for the 2 mm field width. For field widths of 5, 10 and 15 mm the depth dose distributions differ not significantly. There is a significant dependence of the dose in the centre of the field at 5 mm depth on field size for field widths up to 10 mm. The differences between field widths of 10 and 15 mm are not significant. The doses behind the shielding vary with distance to the edge. Within the largest field the variation is about 6 per cent.

The absolute dose determination was made at 10 mm depth with the 0.2 cm<sup>3</sup> ionization chamber, which showed previously good agreement with in vivo dosimetry carried out with TLD rods placed in a vinyl tube inserted in the spinal canal of a sacrificed rat<sup>5</sup>.

#### WHOLE BODY IRRADIATION OF RATS

To investigate the influence of phantom shape, dose measurements were made in rectangular and cylindrical phantoms of similar size irradiated uni- and bilaterally with 300 kV X rays (HVL, 3.2 mm Cu). The distance between the centre of phantoms and the source was 1.5 m. Dose measurements made with an ionization chamber in the central circular/square plane of the phantoms in absence of side or back scatter material showed maximum to minimum dose ratios ( $\hat{D}/\check{D}$ ) of about 1.9 and 1.1 for uni- and bilateral irradiation, respectively. In addition, dose decreases in excess of 10 per cent were observed toward the distal ends of the phantoms. Dose deviations are also to be expected near the surface and at extremities of real animals, but this can not be measured with ionization chambers.

Therefore, measurements were carried out with TLD in real shape rat phantoms for uni- and bilateral irradiation with 300 kV rays on the sides of the animal phantom as shown in Figure 1 and for irradiation on the top of the phantom under full back scatter conditions as shown in Figure 2. For the unilateral and bilateral irradiation on the sides of the real shape phantoms maximum to minimum dose ratios ( $\hat{D}/\check{D}$ ) in the trunk were found of about 2.5 and 1.25, respectively, which is considerably larger than comparable values for rectangular and cylindrical phantoms.

For the unilateral irradiation under full scatter conditions a  $\hat{D}/\check{D}$  value of about 1.26 was found. The doses in the extremities are only about 5 per cent higher than the dose in the centre of the phantom. The use of TLD provides the possibility to realistically compare bilateral irradiation with unilateral irradiation under full scatter conditions.

CONCLUSIONS

- Because of their small size TL detectors can provide essential information on doses for small field sizes or behind small shieldings.
- Employing TLD, dose mapping in small realistic animal phantoms is possible and is providing interesting information.

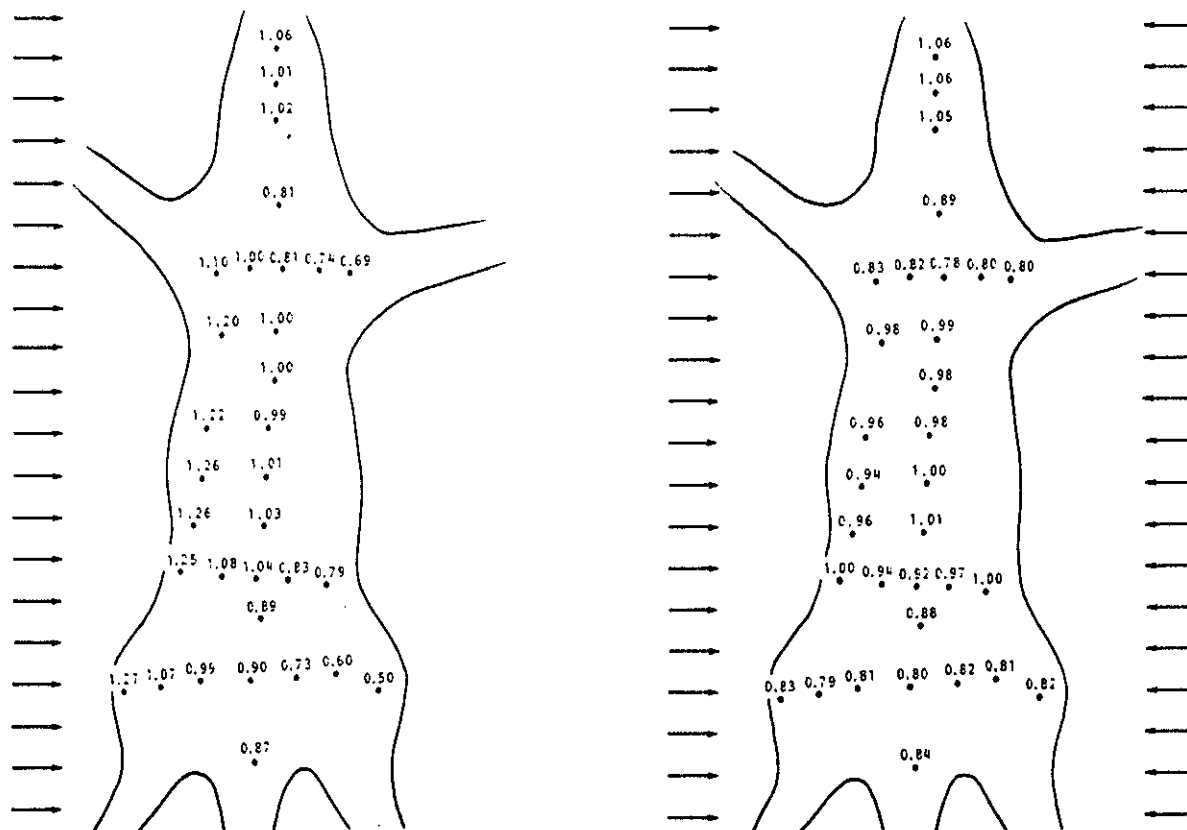


Fig. 1. Relative dose distributions measured with TL detectors for uni- and bilateral irradiation with 300 kV X rays (HVL, 3.2 mm Cu) on the sides of a rat phantom under low scatter conditions.



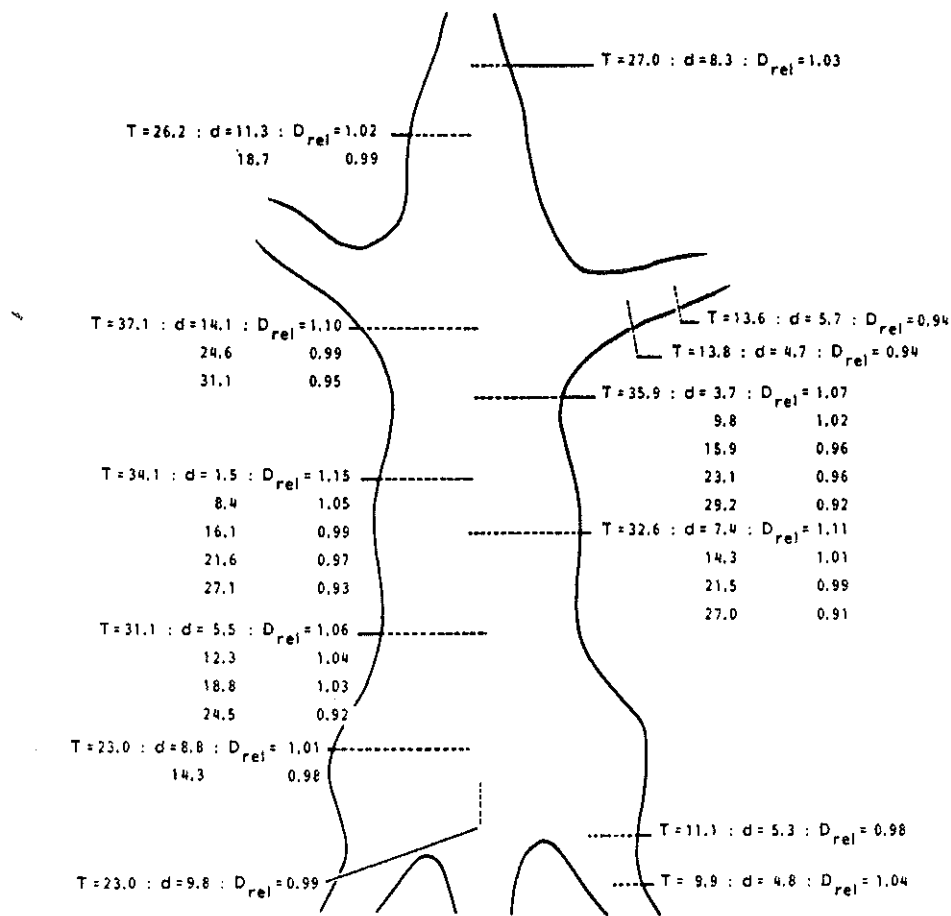


Fig. 2. Relative dose distribution measured with TLD detectors for unilateral irradiation with 300 kV X rays on the top of a rat phantom under full back scatter conditions.

REFERENCES

1. J.J. Broerse and B.J. Mijnheer. Uncertainties in basic physical data for neutron dosimetry in biology and medicine. In: Proc. VIIIème Congress International de la Société Française de Radioprotection, Saclay, France (1978) 641-659.
2. ICRU (International Commission on Radiation Units and Measurements), Quantitative Concepts and Dosimetry in Radiobiology. Report 30, ICRU Publications, Bethesda, Maryland, USA, 1979.
3. A.H. Mulder, J.W.M. Visser, J. Zoetelief and D.W. van Bekkum. The entry of the prothymocyte into the thymus after lethal irradiation and bone marrow transplantation: II. Time of entry. Thymus 11 (1988) 29-41.
4. A.J. van der Kogel, J.J. Fawcett and J. Zoetelief. Effect of volume and localization on spinal cord tolerance (To be published).
5. A.J. van der Kogel. Some dosimetric and radiobiological aspects of partial body irradiation for late effect studies in rodents. In: EULEP protocol for X-ray dosimetry (J. Zoetelief, J.J. Broerse, and R.W. Davies, eds.). Commission of the European Communities, EUR 9507, 1985, 81-87.
6. R.W. Davies and J. Zoetelief. Animal phantoms for radiobiological dosimetry. In: *ibid*, 45-51.

RESPONSE OF  $^7\text{LiF}$  THERMOLUMINESCENT DOSIMETERS TO CLINICAL NEUTRON BEAMS WITH ENERGIES RANGING FROM  $d(14)+\text{Be}$  to  $p(75)+\text{Be}$

S. Vynckier a), B. Hocini b) and A. Wambersie a)

a. UCL- Cliniques Universitaires St-Luc, 1200 Bruxelles, Belgium.

b. Laboratoire de Dosimétrie, Haut Commissariat à la Recherche, 2. Bd Frantz Fanon - B.P. 1017, Alger, Algeria

INTRODUCTION

Thermoluminescent dosimeters are still most appropriate detectors for in-vivo dosimetry in radiotherapy due to their reproducibility and sensitivity, their small size and their independence from electronic devices during irradiation. The aim of this paper is to study the variation of the relative sensitivity ( $k_U$ ) of Lithium-7 Fluoride (TLD700) as a function of the neutron energy and the depth of irradiation in a phantom :

$$k_U = \frac{\text{Sensitivity of the TLD to neutrons}}{\text{Sensitivity of the TLD to Co-60 photons}}$$

The determination of the  $k_U$ -value of these TLD's requires the knowledge of the gamma contribution ( $D_G$ ) to the total absorbed dose ( $D_N + D_G$ ) at the point of interest. In a mixed neutron + gamma field, the gamma component is obtained by the two detector method. This method, recommended by the ICRU <sup>2</sup> and the ECNEU protocol <sup>1</sup>, is based on the responses of a tissue-equivalent ionization chamber and a less neutron-sensitive detector (GM-counter).

EXPERIMENTAL PROCEDURES

The TLD material used for this study was  $^7\text{LiF}$  from Harshaw (LiF:Mg:Ti chips of  $3 \times 3 \times 0.8 \text{ mm}^3$ ). A total of 144 chips were divided into 16 sets of 9 chips each. All points reported, consist of data obtained from at least 1 set of 9 TLD's. Each detector was identified and put in a labeled compartement between aluminium plates, used for handling and annealing. The reading was carried out using a Harshaw 2000 reader in the temperature range from  $100^\circ\text{C}$  to  $300^\circ\text{C}$ . The annealing of the TLD's, prior to each irradiation, consisted in a heat treatment at  $400^\circ\text{C}$  for 2 hours followed by  $80^\circ\text{C}$  for 20 hours <sup>4</sup>.

The gamma calibration was performed using a Cobalt-60 treatment source. The sets of 9 chips were irradiated separately in a polystyrene phantom at a depth of 5mm; doses of 1Gy were delivered. One set of 9 TLD's was irradiated with gamma's only, each time the others received

neutron doses. In this way, no difference in the variation of the neutron- and  $\gamma$ - sensitivity with accumulation in time of neutron- and gamma doses respectively was observed.

The neutron irradiations were carried out at the neutron therapy facility of Louvain-la-Neuve<sup>7</sup> using the d(20)+Be, d(50)+Be, p(34)+Be, p(45)+Be, p(65)+Be and the p(75)+Be neutrons and at the facility of Gent<sup>5</sup> using d(14.5)+Be neutrons. These irradiations were also performed as a function of depth in the phantom, different doses from 0.5 to 4Gy were delivered. Total absorbed doses were determined following the ECNEU protocol<sup>1</sup>.

## RESULTS

### a. The gamma-component

Figure 1 illustrates the variation of the gamma-component for all beams as a function of depth in a polystyrene phantom for a 10cm x 10cm field size. These data are obtained from Vynckier et al<sup>8</sup>. At the entrance,  $D_G$  is equal to about 5% or less. A rapid increase with depth is observed for the small energies (e.g. d(14.5) + Be) whereas for the higher energies (e.g. p(65) + Be) the gamma component remains small (less than 8%) and shows less variation with depth.

### b. supralinearity

Supralinearity is observed for these TLD's for gamma doses higher than 1.5 Gy. For neutrons, supralinearity was investigated for both extreme neutron energies. Doses from 0.2 to 3 Gy and from 0.1 to 2 Gy were given for the d(14.5)+be and the p(65)+Be neutrons respectively. Up to these doses nearly no supralinearity effect was observed.

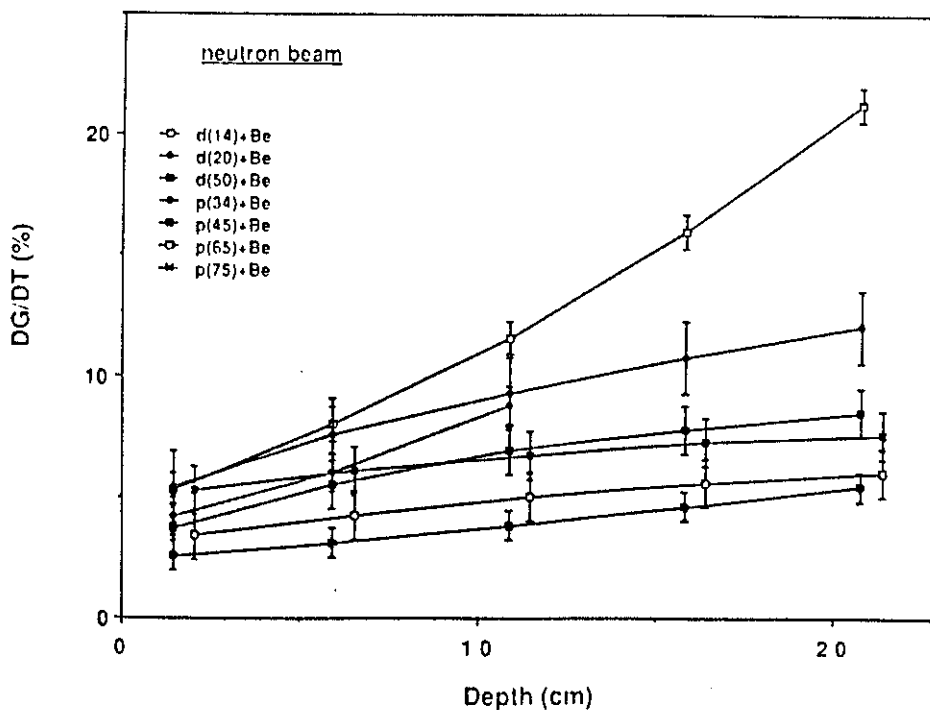


Fig 1 : Variation of the gamma component as a function of the depth in a polystyrene phantom for different clinical neutron beams (10cm x 10cm field size).

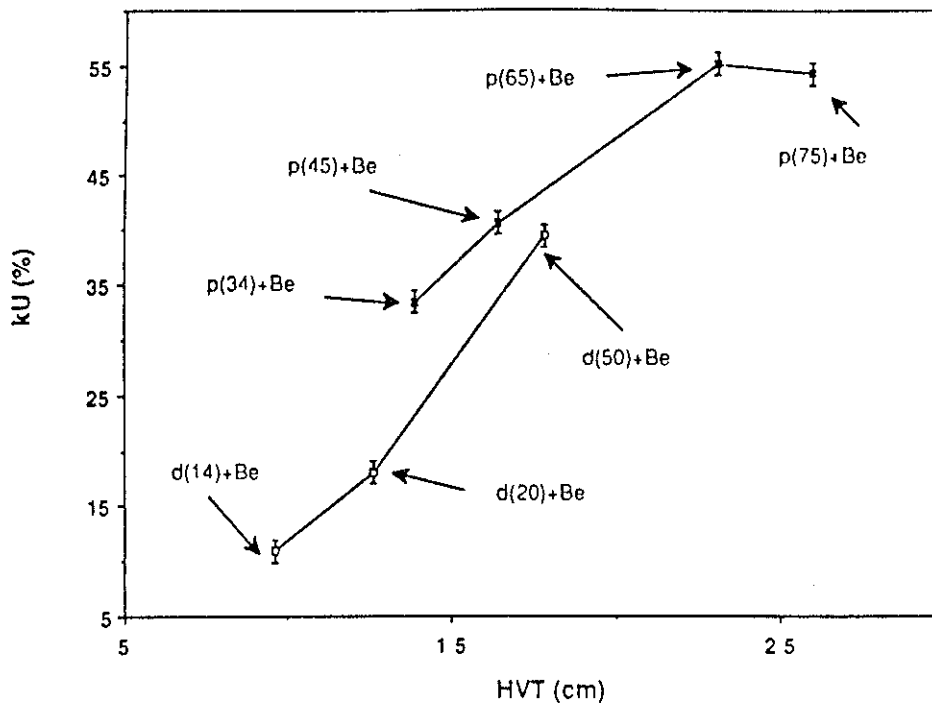


Fig. 2 : Variation of the  $k_U$  value of TLD700 as a function of the HVT (at a depth of 2cm and a 10cm x 10cm field size).

c. Variation as a function of energy

The relative sensitivity  $k_U$  of the TLD700 is shown in figure 2 as a function of the HVT (Half Value Thickness) of the different neutron beams. This HVT is known to be a good parameter for presenting the mean neutron energy of a neutron beam whose neutron energy spectrum is not known<sup>9</sup>.

At the depth of dose maximum the  $k_U$ -value increases rapidly with the HVT, hence with neutron energy. Indeed, its value varies from 10.5% for the d(14.5)+Be neutron beam to 57% for the p(65)+Be beam at which energy it seems to level off.

d. Variation as a function of depth in a phantom

The neutron energy spectrum might vary slightly with depth in a phantom. Therefore a variation of the  $k_U$  value with depth can be expected. This value increases significantly with depth for neutron beams produced from protons (fig.3) : e.g. it varies by 10% when the depth increases from 2 cm to 20 cm for the p(45)+Be neutrons. This variation is much less for neutrons produced from deuterons.

DISCUSSION AND CONCLUSIONS

The present results for the d(14.5)+Be neutron beam are in good agreement with published

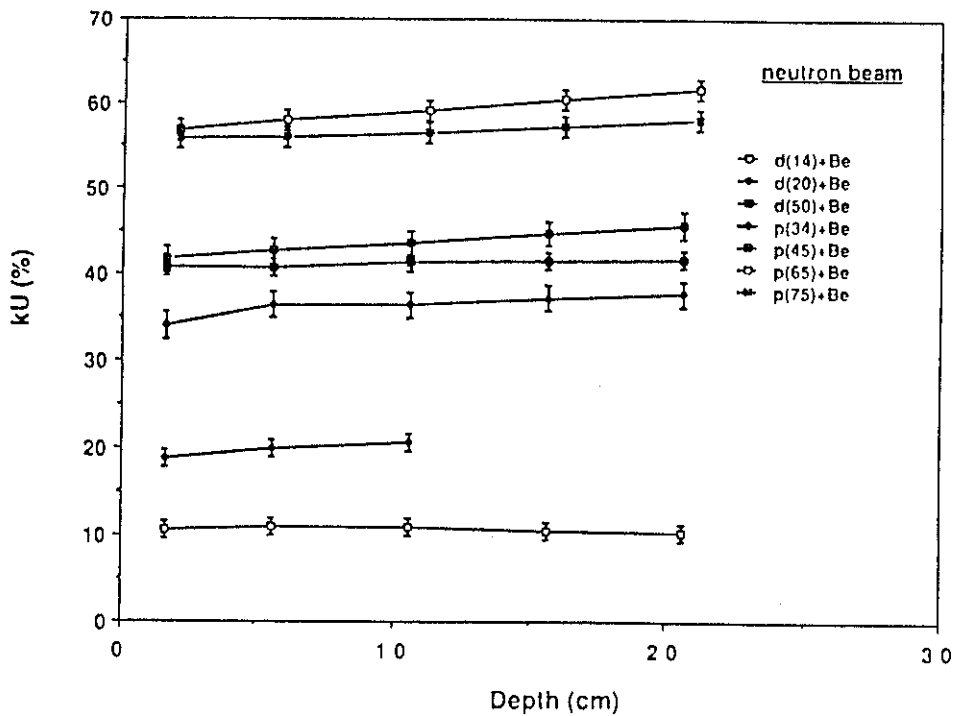


Fig. 3 : Variation of the  $k_U$  value of TLD700 as a function of the depth in a polystyrene phantom (10cm x 10cm field size).

values<sup>10,6,3</sup>. Small differences are to be attributed to differences in the irradiation conditions and to differences in Lithium-6 concentration in the TLD700. This shows the importance to performe such a study with a single set of TLD. At higher energies no data are available in the literature.

Our results show that these detectors can be used in therapy under well-established conditions. Due to their small  $k_U$  value LiF-7 detectors allow the determination of the gamma component for low neutron energy beams (e.g. d(14.5)+Be) by means of a two detector method. At high neutron energies we showed that the gamma component is small and that the  $k_U$  value is relatively important. This means these detectors are appropriate for the measurement of the neutron dose or the total absorbed dose when the  $\gamma$ -component is known. However, for accurate measurements, it is advisable to take into account the variation of  $k_U$  with depth.

**ACKNOWLEDGEMENTS**

The authors wish to thank Dr. K. Strijckmans of the Gent university for offering the possibility to make use of their neutron beam and for the perfect cooperation.

**REFERENCES**

1. Broerse J.J., Mijnheer B.J. and Williams J.R., " European protocol for neutron dosimetry for external beam therapy", Br. J. Radiol., 1981, 54, 882.
2. ICRU report n° 26 " Neutron dosimetry for biology and medicine", ICRU Washington, 1977.
3. Mc Ginley P.H., "Response of LiF to fast neutrons", Health Phys., 1972, 23, 105.
4. Mc Kinley A.F., "Thermoluminescence dosimetry" Medical Physics handbook 7, Ed. A. Hilger Bristol, 1981.

5. Strijckmans K., Mortier R. and Fache P. "The isocentric neutron therapy facility of the university of Gent" *J. Eur. Radiother.*, 1984, 5, 243.
6. Tochilin E., Goldstein N. and Miller J.P., "Berillium oxide as a thermo-luminescence dosimeter", *Health Phys.*, 1969, 16, 1.
7. Vynckier S., Pihet P., Flémal J.M., Meulders J.P. and Wambersie A. "Improvement of a p(65)+Be neutron beam for therapy at Cyclone, Louvain-la-Neuve" *Phys. Med. Biol.*, 1983, 28, 685.
8. Vynckier S., Pihet P., Marquebreucq S. and Wambersie A., "The gamma component in clinical neutron beams of different energy", *Br. J. Radiol.*, 1987, 60, 314.
9. Wambersie A., Bewley D.K. and Lalanne C.M., "Prospects for the application of fast neutrons in cancer therapy." *Bull. Cancer (Paris)*, 1986, 73, 546.
10. Wingate C.L., Tochilin E. and Goldstein N., "Response of LiF to neutrons and charged particles", in *Proc. Int. Conf. Luminescence dosimetry. Conf- 650637 U.S. Atomic Energy Commission, Stanford Univerisity*, 1965, p 421.



DOSIMETRY IN A MIXED (14.8 MeV NEUTRON, GAMMA) RADIATION FIELD  
WITH CaF<sub>2</sub>:Tm (TLD-300)

J.B. Dielhof<sup>a)</sup>, A.J.J. Bos<sup>a)</sup>, J. Zoetelief<sup>b)</sup>, J.J. Broerse<sup>b)</sup>

- a. Interfaculty Reactor Institute, Delft University of Technology,  
Mekelweg 15, NL 2629 JB Delft  
b. Radiobiological Institute TNO, P.O. Box 5815, NL 2280 HV Rijswijk

INTRODUCTION

The relative biological effectiveness of fast neutrons differs considerably from that of gamma radiation. Therefore in a mixed (n,γ) radiation field it is important to determine the separate contributions of the neutrons and gamma rays to the total absorbed dose. The usual technique comprises two detectors, one neutron insensitive and the other having equal sensitivity to neutrons and photons. From the signals of the two detectors the neutron and gamma doses can be derived<sup>1</sup>.

A disadvantage of this technique is the need for two separate measurements. Moreover, the spatial resolution is in current practice relatively small since the detectors usually involved are relatively large. The spatial resolution can be improved by applying the same technique with a small neutron sensitive and neutron insensitive thermoluminescent dosimeters (TLD's). Even a single dosimeter can be applied since some thermoluminescent (TL) materials show glow curves where the different peaks exhibit a different dependence on the LET of the radiation. This property allows determination of both gamma and neutron dose in a mixed (n,γ) radiation field with the so-called two-peak method<sup>2,3</sup>. However, the neutron sensitivity of TL-materials depends on many factors<sup>4</sup> which must be known before reliable dose determinations can be made.

The TL-material CaF<sub>2</sub>:Tm (TLD-300) shows a glow curve with several separate peaks. Two of these peaks show a great difference in neutron sensitivity<sup>5</sup>, which makes application of the two-peak method possible. Schraube<sup>6</sup> stated that with this method at high neutron energies, i.e. 15 MeV, photon to neutron discrimination is possible up to a photon to neutron dose ratio of about 1. According to Rassow et al.<sup>3</sup>, however, the two-peak method used in a mixed (14.8 MeV n,γ) radiation field with CaF<sub>2</sub>:Tm (TLD-300) was not applicable for clinical dosimetry due to great uncertainties of the TL-signals. The object of this study is to determine the relative neutron and gamma ray sensitivities of the glow peaks of CaF<sub>2</sub>:Tm (TLD-300) and to



study the applicability and limitations of the two-peak method with  $\text{CaF}_2:\text{Tm}$  (TLD-300) in a mixed (14.8 MeV neutron, gamma) radiation field.

METHODS

The normalized response of a TL-dosemeter to a type of radiation  $j$  is defined as:

$$M_{ij} = \frac{R_{ij}}{R_{ic}/D_c} \quad (1)$$

where  $R_{ij}$  and  $R_{ic}$  are peak areas of peak  $i$  in the glow curve for a type of radiation  $j$  and a  $^{60}\text{Co}$  gamma ray calibration irradiation respectively, and  $D_c$  is the  $^{60}\text{Co}$  gamma ray calibration dose. According to ICRU-26<sup>1</sup> the normalized TL-response in a mixed  $(n,\gamma)$  radiation field  $M_{iM}$  can be described by:

$$M_{iM} = M_{iN} + M_{iG} \quad (2)$$

$$= k(i)D_N + h(i)D_G \quad (3)$$

where  $k(i)$  and  $h(i)$  are the relative neutron and gamma ray sensitivities for peak  $i$  respectively, and  $D_N$  and  $D_G$  the absorbed neutron and gamma doses respectively. Generally  $k(i)$  and  $h(i)$  are denoted as  $k_U$  and  $h_U$  for neutron insensitive peaks (detectors) and as  $k_T$  and  $h_T$  for neutron sensitive peaks (detectors). This notation is not used here, because it is not a priori known whether a peak is sensitive or insensitive to neutrons. For a TL-material with two peaks, with one peak neutron sensitive and the other neutron insensitive, one gets two equations with two unknowns  $D_N$  and  $D_G$ . In this way it is possible to determine separately the absorbed neutron and gamma dose in a mixed  $(n,\gamma)$  radiation field with one detector.

To derive the relative neutron and gamma ray sensitivities, equation (3) is rewritten as:

$$\frac{M_{iM}}{D_T} = k(i) + (h(i) - k(i)) \frac{D_G}{D_T} \quad \text{with } D_T = D_N + D_G \quad (4)$$

By determination of  $M_{iM}/D_T$  for various values of  $D_G/D_T$  a linear relationship results.  $k(i)$  and  $h(i)$  can be derived from the slopes and intercepts with the ordinate of straight lines fitted to the data.

### EXPERIMENTAL TECHNIQUES

The TL-material used in this study was CaF<sub>2</sub>:Tm (TLD-300), purchased from Harshaw Chemical Company (Ohio, USA; ribbons 3.2x3.2x0.9 mm<sup>3</sup>). At the start of the investigation all the ribbons possessed a history of small irradiation doses. Before each irradiation the ribbons were annealed in a specially designed microprocessor controlled annealing oven (Norhof, Vianen, The Netherlands) for 1 hour at 400 ± 1 °C followed by a fast cooling (360 °C.min<sup>-1</sup>). The oven demonstrates highly reproducible annealing cycles (in heating and cooling).

The 14.8 MeV neutron irradiations were performed at the TNO-facility described by Zoetelief et al.<sup>7</sup>. The gamma ray fraction of the total kerma measured in air was (6.8 ± 0.7)%. Dosimetry was carried out with an Exradin T-2 tissue equivalent ionization chamber with a reproducibility of ± 2%. For the calibration and additional gamma ray irradiations a 37 GBq (1 Ci) <sup>60</sup>Co gamma ray irradiation facility at IRI has been used. The absorbed dose in tissue has been determined with a calibrated 30 cm<sup>3</sup> air equivalent ionization chamber (PTW, type M 23361 accuracy ± 0.5%) employing an exposure to absorbed dose conversion factor of 9.62 mGy.R<sup>-1</sup>.

A group of 50 CaF<sub>2</sub>:Tm (TLD-300) ribbons was divided into subgroups of 4 ribbons. Every subgroup has been exposed to a test irradiation with 14.8 MeV neutrons (10.0 mGy), preceded by an additional <sup>60</sup>Co gamma ray irradiation with doses varying from 0 to 41.2 mGy i.e. a D<sub>G</sub>/D<sub>T</sub> variation (taking into account the gamma ray contribution of the neutron beam) from 6.8% to 82%. Every ribbon was calibrated individually with <sup>60</sup>Co gamma radiation (10.0 mGy). All irradiations were performed in an A-150 plastic (tissue equivalent) container with 4 mm material in front of and behind the ribbon.

Irradiated TL-materials were read out with a modified microprocessor controlled Harshaw 2000 TL reader described elsewhere<sup>8</sup>. The reader is equipped with a bialkali photocathode photomultiplier tube (no 9757B, EMI Electron tubes, Middlesex, England) and an infrared filter with a maximum transmission range of 350 - 650 nm (type KG-1, Spindler u. Hoyer, Göttingen, FRG). The reading was performed with a heating cycle of 39 s at 312 K followed by heating during 321 s at a linear temperature increase rate of 1.0 K.s<sup>-1</sup>. Glow curves were recorded by sampling the digitized PM-current and planchet temperature every 0.75 s. Each ribbon was read out twice. The second readout is considered to be the reader background and subtracted from the first one. The glow curves were analyzed with a curve fitting program for thermally activated processes<sup>9</sup>. In the program a linear least-square minimization procedure is used to determine simultaneously the actual parameters (peak

area, activation energy and frequency factor) of all peaks in the glow-curve.

### RESULTS AND DISCUSSION

A typical glow curve of  $\text{CaF}_2:\text{Tm}$  (TLD-300) after irradiation with 14.8 MeV neutrons and the results of the fitting procedure are shown in figure 1. The best fit was obtained assuming for peaks 3, 4 and 5 first order and for peaks 2 and 6 second order processes. For all peaks, except for peak 2, a very small residue was obtained. The process order for peak 2, especially in cases with low  $D_G/D_T$ , seems neither first nor second. Further investigation with regard to the fitting of this peak is necessary. The standard deviation of the fitted activation energy of peak 5 of all 50 measurements made with

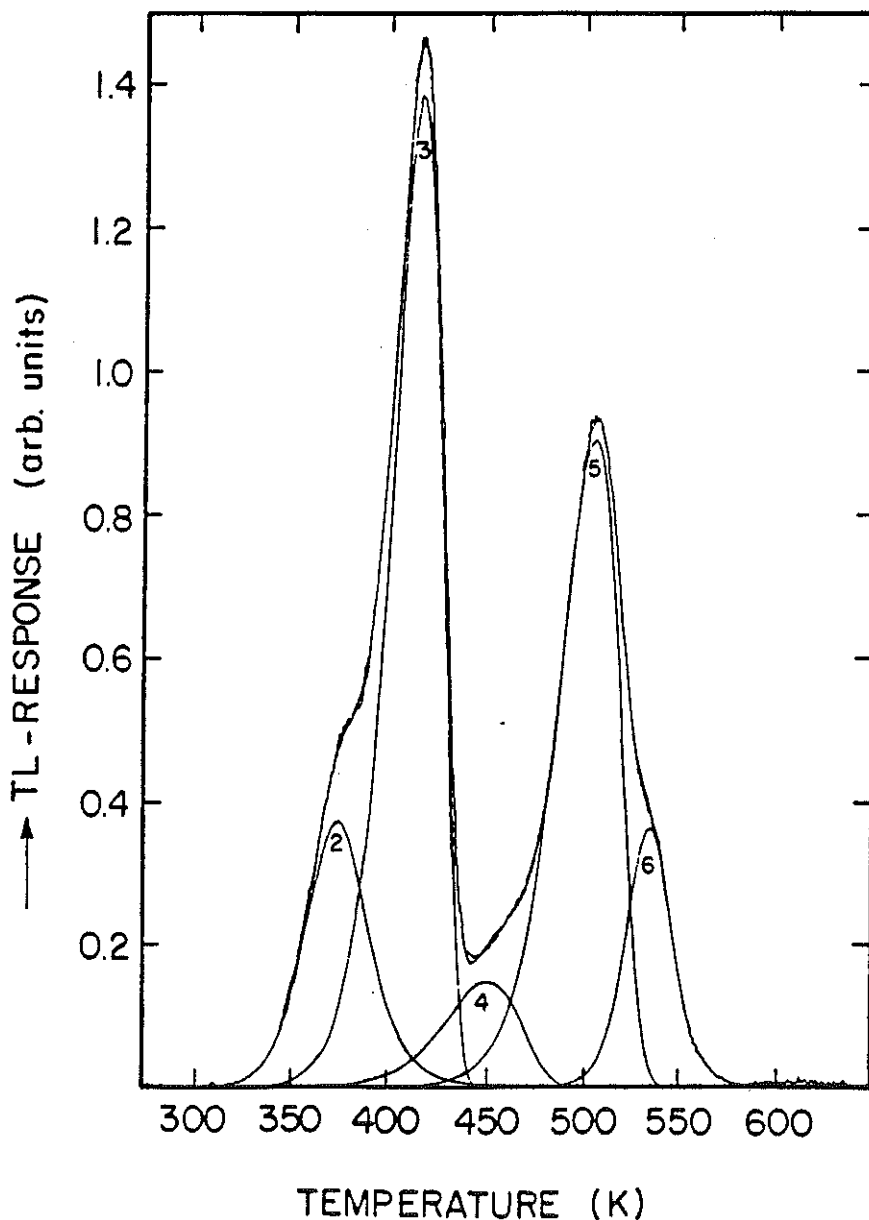


Fig. 1.  
Glow curve and results of the fitting procedure for  $\text{CaF}_2:\text{Tm}$  (TLD-300) after an irradiation with 9.3 mGy 14.8 MeV neutrons and 4.0 mGy gamma rays.

different values of  $D_G/D_T$ , was 1.7%. This illustrates the internal consistency of the fitting procedure. However, the comparable value for peak 3 was 6.5%, due to the less good fit of peak 2.

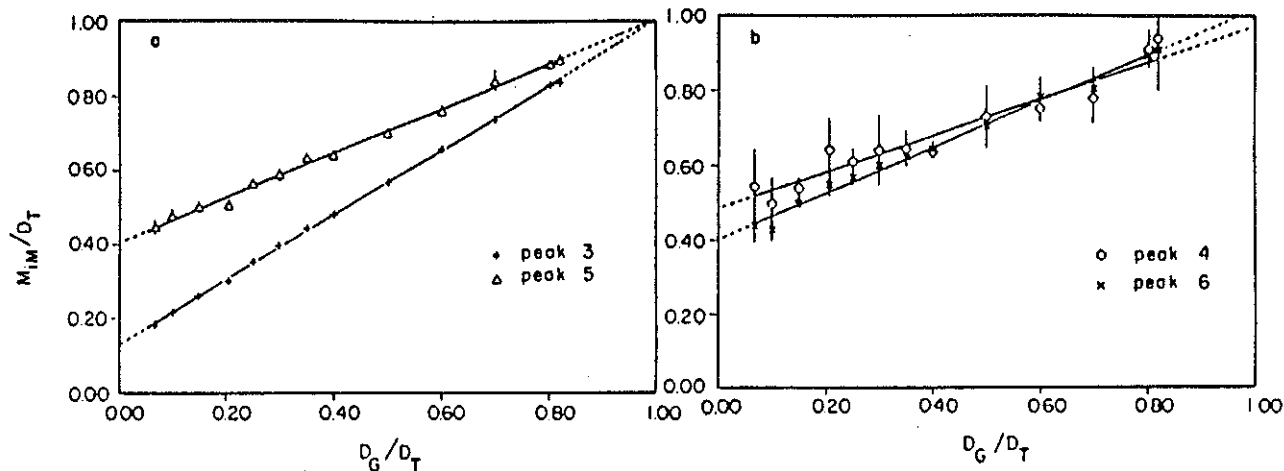


Fig. 2.

Normalized TL-response as a function of the relative absorbed gamma dose of CaF<sub>2</sub>:Tm (TLD-300) for (a) peak 3 and 5 and (b) for peaks 4 and 6. The straight lines are the result of a linear regression. The points are averages of four measurements with error bars of  $\pm$  one standard deviation.

Figures 2a and 2b show the normalized TL-response as a function of the relative absorbed gamma dose of peaks 3 and 5 and peaks 4 and 6, respectively. Table 1 summarizes the resulting relative neutron and gamma ray sensitivities with their standard deviation. The sensitivities of peak 2 are not calculated because of fading of this peak (a half life of  $16 \pm 1$  h when stored at room temperature was deduced) in the course of the experiments. An experiment in which the sequence of additional gamma ray and neutron irradiations was reversed demonstrated no changes in the glow curves and sensitivities derived. This implies that the readings due to gamma and neutron doses are additive.

Variation of  $D_G/D_T$  from 6.8% to 82% changes the peak area ratio of peak 5 and 3 ( $R_{5M}/R_{3M}$ ) from  $1.28 \pm 0.02$  to  $0.56 \pm 0.01$ . The neutron sensitivities of these main peaks of CaF<sub>2</sub>:Tm (TLD-300) differ by a factor 3.2 (see table 1). Therefore, peaks 3 and 5 are the most appropriate peaks for the two-peak method. Since peaks 4, 5 and 6 show, within the experimental error (see table 1), the same relative neutron sensitivities the sum of the three peaks can also be used as a neutron sensitive signal. The accurate determination of peak 3 (the gamma ray sensitive signal) is influenced by the overlap from peak 2. By waiting 48 h before readout, thus allowing peak 2 to fade, a more accurate value of the area of peak 3 can be obtained. In is case the peak

height instead of area can be used as well. In an earlier study, using peak heights, the same  $k$  values for peaks 3 and 5 were found<sup>5</sup>.

The relative gamma ray sensitivities ( $h(i)$ ) found for peaks 3, 4, 5 and 6 are all equal to 1. This result is expected since both the additional dose and the calibration dose were due to from  $^{60}\text{Co}$  gamma rays and the energy of the photons in the 14.8 MeV neutron beam is comparable to the energy of  $^{60}\text{Co}$  gamma rays.

Table 1. The relative neutron ( $k(i)$ ) and gamma ray ( $h(i)$ ) sensitivities of glow curve peaks of  $\text{CaF}_2:\text{Tm}$  (TLD-300) in A-150 container (4 mm in front and behind of the ribbons)

| peak nr. $i$ | $k(i)$          | $h(i)$            |
|--------------|-----------------|-------------------|
| 3            | $0.13 \pm 0.01$ | $1.003 \pm 0.004$ |
| 4            | $0.48 \pm 0.07$ | $0.97 \pm 0.04$   |
| 5            | $0.41 \pm 0.02$ | $1.01 \pm 0.01$   |
| 6            | $0.40 \pm 0.02$ | $1.02 \pm 0.03$   |

A study on the accuracy of the calculated values of  $D_N$  and  $D_G$  using the two-peak method based on the measured sensitivities and TL-response has been carried out. It appears that the uncertainty in  $D_N$  is approximately 10% if  $D_G/D_T < 0.5$ . The same applies for  $D_G$  if  $D_G/D_T > 0.2$ . The main contribution to the uncertainty originates from the error in the  $k$  values. Reduction of this error will improve the accuracy in  $D_N$  and  $D_G$  proportionally. Above  $D_G/D_T = 0.5$  the uncertainty in  $D_N$  increases rapidly. The same holds for  $D_G$  when  $D_G/D_T < 0.2$ .

A systematic error will be introduced when the neutron energy in the phantom cannot be considered constant, since for lower neutron energies the relative neutron sensitivity will be lower<sup>5</sup>. Another error will be introduced when the gamma ray contribution has low energy components since the relative gamma ray sensitivity will be greater than 1 for low energy photons.

### CONCLUSIONS

Dosimetry in a mono energetic mixed (14.8 MeV  $n, \gamma$ ) radiation field in air is possible with  $\text{CaF}_2:\text{Tm}$  (TLD-300) using peak 3 in the glow curve of the TL-material as the neutron insensitive and peak 5 as the neutron sensitive signal. When TLD-300 is used in a tissue equivalent container these peaks differ in neutron sensitivity by a factor 3.2. Complicated peak fitting procedures appear unnecessary provided that proper use is made of the fading

of peak 2. More simple methods such as determination of peak height or light integration between certain temperature limits give the same results.

The accuracy in the determination of the neutron and gamma doses strongly depends on the gamma ray contribution to the total dose. The uncertainty in the neutron dose is approximately 10% if  $D_G/D_T < 0.5$ . The uncertainty in the gamma dose is approximately 10% if  $D_G/D_T > 0.2$ . Outside the mentioned regions the uncertainty increases strongly.

It should be noted that these conclusions are only valid for measurements performed in air. The use of this method for dose determinations in a phantom irradiated by a 14.8 MeV neutron beam will be limited due to the strong variation of  $k(i)$  with the neutron energy.

#### REFERENCES

1. ICRU (International Commission on Radiation Units and Measurements), Neutron Dosimetry for Biology and Medicine, Report 26, ICRU Publication, Washington, USA, 1977
2. M. Apostolova, G. Burger, D. Combecher, H. Eckerl, and P. Kneschaurek, The use of TLD-detectors for reactor mixed field dosimetry, Commission of the European Communities, Radiation Protection, EUR 9762 EN volume II, 817-827. Proceedings Fifth Symposium on Neutron Dosimetry, Munich/Neuherberg, September 1984
3. J. Rassow, J.J. Broerse, R. Duehr, F.W. Hensley, S. Marquebreucq, K. Olthoff-Muenter, A.S. Pradhan, A. Temme, S. Vynckier, and J. Zoetelief, Spectral dependence of response coefficients and applicability of the two-peak TLD method in mixed neutron-photon radiation fields, Commission of the European Communities, Radiation Protection, EUR 9762 EN volume II 783-794. Proceedings Fifth Symposium on Neutron Dosimetry, Munich/Neuherberg, September 1984
4. J.A.B. Gibson, The relative Tissue Kerma Sensitivity of Thermoluminescent Materials to Neutrons, Radiat. Prot. Dosim. 15 (4) (1986) 253-266
5. J.B. Dielhof, A.J.J. Bos, J. Zoetelief and J.J. Broerse, Sensitivity of CaF<sub>2</sub> Thermoluminescent Materials to Fast Neutrons, Radiat. Prot. Dosim. (in press)
6. H. Schraube and E. Weitzenegger, Response of CaF<sub>2</sub>:Tm (TLD-300) to monoenergetic fast neutrons, Commission of the European Communities, Radiation Protection, EUR 9762 EN volume II 805-815. Proceedings Fifth Symposium on Neutron Dosimetry, Munich/Neuherberg, September 1984
7. J. Zoetelief, A.C. Engels, C.J. Bouts and J.J. Broerse, Experimental Arrangement and Monitoring at TNO, In: European Neutron Dosimetry Inter-comparison Project (ENDIP), Results and Evaluation., J.J. Broerse, G. Burger and M. Coppola eds., Commission of the European Communities, Radiation Protection, EUR 6004 EN, (1978) 32-43
8. M.H. van Wijngaarden, J. Plaisier and A.J.J. Bos, A Microprocessor Controlled Thermoluminescence Dosemeter Reader for Routine Use and Research, Radiat. Prot. Dosim. 11(3) (1985) 179-183
9. J.E. Hoogenboom, W. de Vries, J.B. Dielhof and A.J.J. Bos, Computerized analysis of glow curves from thermally activated processes, J. Appl. Physics 64 (6) (1988) 3193-3200



TLD USING LiF POWDER APPLIED IN RADIOTHERAPY:  
PRACTICAL ASPECTS AND RESULTS.

J.P.A. Marijnissen and B. Göbel.

Dr Daniel den Hoed Cancer Centre,  
Groene Hilledijk 301, 3075 EA Rotterdam, The Netherlands.

INTRODUCTION

Small underdosage of the radiation delivered to a tumour volume may dramatically decrease the tumour control probability. On the other hand small overdosage in the surrounding normal tissue may cause severe damage. Margins with respect to the dose as well as to the geometry are often small. These problems are frequently encountered in interstitial radiotherapy (brachytherapy) and in external radiotherapy with adjacent field treatments using photon and/or electron beams. TLD is applied to check dose and dose distributions in vivo and in phantom studies to verify and/or optimize treatments. The main advantage of TLD in these applications is its small detector volume of only a few mm<sup>3</sup>. LiF 700 powder is chosen because of the possibility to match the dimensions of the TLD detector volume to the spatial resolution required for dose verifications in radiotherapy. Furthermore the use of TLD powder is rather easy in practice, because bookkeeping arising with solid TLD dosimeters (chips, discs, rods, etc.) with various sensitivity is not necessary. Moreover, LiF powder encapsulated in polyethelene tubing is insensitive to mechanical damage compared to solid TLD dosimeters, which is an advance in clinical dosimetry (e.g. intracavity dosimetry).

In this paper, the precision of TLD with LiF 700 powder at radiotherapy dose levels (0.1 - 15 Gy) is evaluated.

MATERIALS AND METHODS

Almost all data presented in this paper have been obtained for Harshaw 1KTU and B701 LiF 700 batches which have been in use over a period of at least 10 years. Recently Vinten LiF 700 powder from batch 118 (160-012p) has also been evaluated. The thermoluminescence of the LiF powder is measured with a Pitman model 654 TLD-reader, equipped with a research heating control module. This heating control module allows for an independent adjustment of the temperature and duration of preheating, read-out and internal annealing. In addition the heating rate and cooling rate can be chosen. Via a 654/SA Linear Ratemeter the heating profile and glow curve can be recorded simultaneously with an x,y-t recorder. Glow curve analysis during linear heating facilitates an accurate tuning of the read-out cycle to the actual TL-properties of the TL-materials.



Internal annealing in the TLD-reader is not applied for TL-powders. Annealing of LiF powder is always performed in the Pitman model 622/B annealing facility. Usually 2.5 gram LiF is annealed in a sealed stainless steel container placed in an anodized aluminium block ( 9.5 x 7.5 x 5 cm), flanked by two blocks of the same size. The annealing cycle involves a high temperature annealing of 1.5 hours at 400°C, natural cooling in the oven to 80°C, followed by a low temperature annealing at 80°C for 16 hours and subsequent natural cooling down to room temperature. The large heat capacity of blocks and oven ensures a uniform temperature distribution throughout the LiF and slow cooling down to room temperature. After annealing the powder is well shaken to spread out homogeneously a possibly variation over the sample.

For a single TLD read-out  $6 \pm 1$  mg powder is used which is uniformly spread over the 25 mm<sup>3</sup> area of the type M-tray (heating planchet) of the reader. This amount is dispensed by a home made dispenser. For common use the LiF is encapsulated in polyethelene tubing of 0.25 mm wall thickness and 1.0 or 1.6 mm inner diameter. Typical dimensions of the sensitive part of single read-out LiF capsules are  $\phi$  1.0 x 5.5 mm or  $\phi$  1.6 x 2.2 mm. The total lengths of the capsules are 11 and 8 mm respectively, nylon end stops included. Capsules containing more read-out samples can easily be composed. Either the powder is encapsuled in bulk or nylon spacers are introduced to maintain separate read-outs. Using the dispenser the amount of powder from bulk capsules is divided in individual read-out samples of  $6 \pm 1$  mg. For each TLD read-out the mass of the LiF powder together with the planchet is determined by a Mettler M5 analytical balance. The actual mass of the LiF is calculated by subtracting the mass of the planchet (192 mg) from the total mass. One LiF powder read-out takes 60-90 seconds, including the spreading of the powder over the planchet and the weighing.

The results presented in this paper are obtained using a multi plateau TLD-read-out cycle, viz. a preheating of 134°C for 16 seconds followed by a read temperature of 235°C for 16 seconds. The pre read-out heating at 134°C - 16 seconds effectively suppresses the effect of fading. Usually the LiF is read-out the day after irradiation. Read-out directly after irradiation results in a  $2 \pm 1$  per cent higher response. A time lapse of about 4 hours to one week yields no significant difference in response. The present temperature and timing makes the light yield only slightly sensitive to the read-out temperature. A difference of  $\pm 3^\circ\text{C}$  affects the TL light yield by about  $\pm 1-2$  per cent.

After each annealing the LiF is calibrated in a 4 MV photon beam against a 0.6 cm<sup>3</sup> thimble ion chamber in a perspex phantom. The capsules are located at the effective measuring point of the ion chamber.

**RESULTS**

The precision of the TLD procedure has been evaluated by read-out of 8-9 LiF samples, taken from capsules irradiated under calibration conditions. The histogram in figure 1 shows the results for a person having much experience in TLD work.

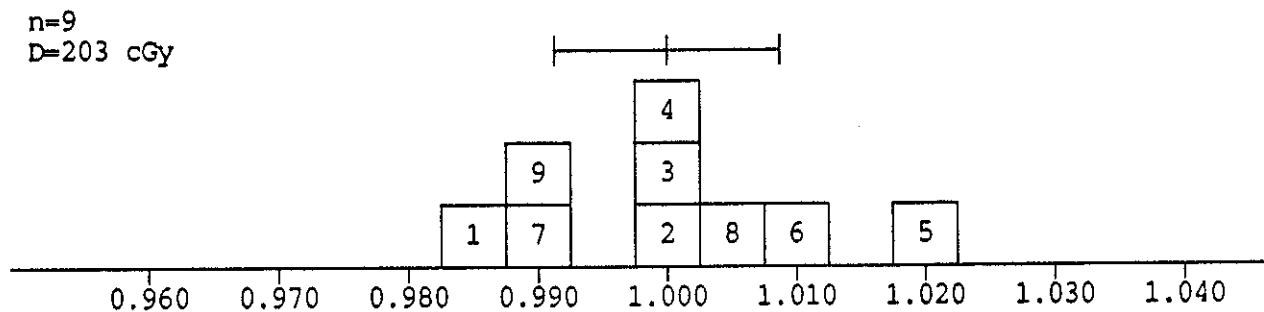


Fig. 1. Results of TLD read-outs. The bar gives the 95% confidence limits of the mean measured dose. Numbers indicate the sequence of the read-outs.

It should be noticed that these results include all random errors due to variations in sensitivity of each LiF grain, sensitivity of the TLD reader, weighing, etc.. The mean dose calculated from these measurements is 2.03 Gy, although the dose obtained from the ionization chamber is 2.01 Gy. A systematic error of about 1 per cent may be due to converting TL yield per unit mass to dose.

The actual mass of the LiF during read-out does not affect the detected light yield per unit of mass (fig. 2). It was anticipated that differences in the mass of LiF easily lead to different responses per unit of mass due to self absorption of the fluorescent light, scattering, inhomogeneous heat contact, etc.. These effects appeared to be negligible in the mass range of 6 ± 1 mg.

To convert response per unit mass to dose, a dose-response curve has been established over the dose range 0.1 to 100 Gy. However, the usual dose range for most TLD applications in radiotherapy is 0.1 to 15 Gy. A measure for the supralinearity is defined as the supralinearity ratio :

$$F_s = \frac{R/D \{ D_x \}}{R/D \{ D=1 \}} \tag{1}$$

where R = response per unit dose, D = dose in Gy, D<sub>x</sub> = dose for which the supralinearity is calculated relative to the response to a dose of 1 Gy.

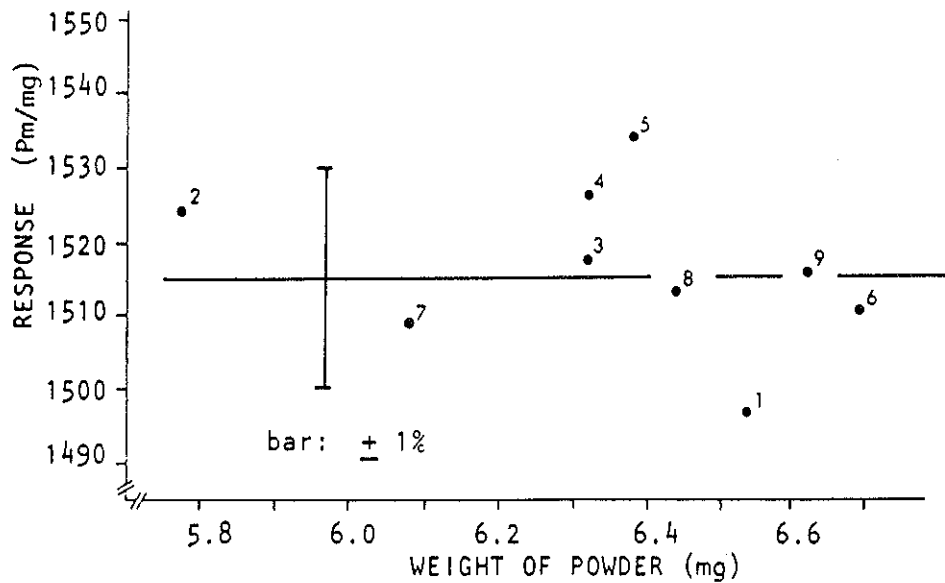


Fig. 2. Response in Pm/mg versus the weight of powder. The unit Pm stands for "Pitman", an apparatus bound arbitrary unit for response.

This ratio  $F_s$  is plotted in figure 3 for the 0.1 - 15 Gy dose range. From figure 3 the phenomenon of supralinearity is obvious. The dose response relationship is accurately described over the 0.1 to 70 Gy dose range by:

$$F_s(D) = aD + b \tag{2}$$

which can be rewritten, using (1) to:

$$R(D) = (aD^2 + bD) * R \{D=1 \text{ Gy}\} \tag{3}$$

Thus the response appears to be a quadratic function of the dose. The response to dose formula, which is of interest to calculate the dose from the measured response, is the inverse function of (3) and is obtained easily by simple algebra.

After each annealing the supralinearity  $F_s$  is measured at a dose of 10 Gy. For the Harshaw LiF 700 batches the value  $F_s$  is  $1.21 \pm 0.01$  and the Vinten batch tends to  $1.18 \pm 0.01$ . The supralinearity appears to be constant when the annealing procedure is highly reproducible. Annealing in the Vinten oven has proven to be highly reproducible. The sensitivity of the LiF after annealing may vary by about  $\pm 2$  per cent. Therefore calibration at a single test dose (reference test dose is 1 Gy) should be sufficient. But because the supralinearity is highly dependent on the annealing procedure, at least one additional test dose (i.e. 10 Gy) is required as a check on the supralinearity.

Retrospectively, a calibration at only one test dose at 1 Gy would never have lead to an error exceeding  $\pm 2$  per cent over the 0.1 to 15 Gy dose range.

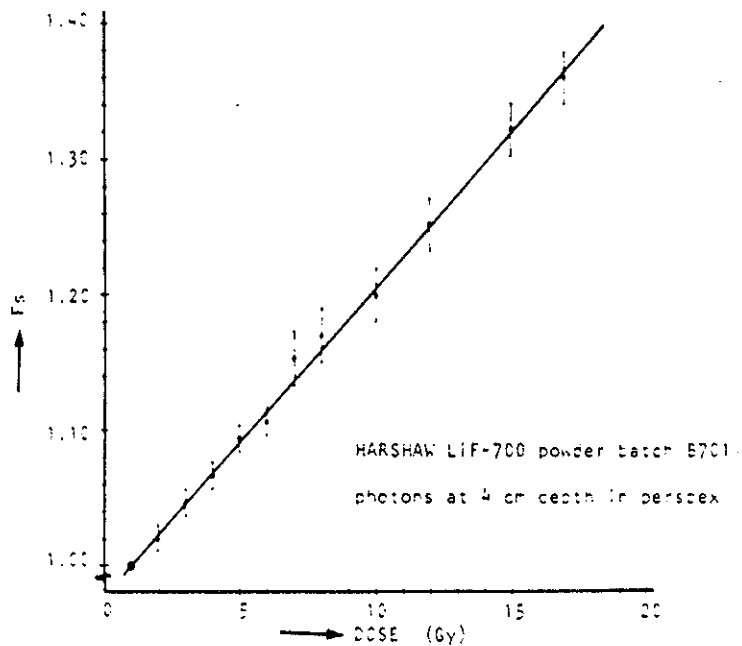


Fig. 3. The ratio  $F_s$  (eq.3) plotted versus dose. Supralinearity is already obvious at the radiotherapy dose level.

### DISCUSSION

The use of powder has several advantages over solid TLD dosimeters. At first sight the use of powder for TLD seems laborious due to weighing of the powder: an accurate analytical balance is required as well as a TLD-reader which is ergonomically suitable for reading TLD powder. But then, after annealing of e.g. 2.5 gram powder approximately 400 readings with the same sensitivity and calibration constants are available. There is no selecting and bookkeeping of individual TLD dosimeters with respect to their sensitivity. Dimensions of the TLD capsule are easily adapted to the experimental conditions, e.g. in case of steep dose gradients and/or directional dependence and in case of adjacent field treatments. The minimal LiF detector volume is only  $4 \pm 0.5 \text{ mm}^3$ , which allows high spatial resolution. The overall uncertainty in a single read-out by an experienced user is  $\pm 1-2$  per cent (95 % confidence limits), estimated from experiments similar to figure 1. The systematic error in the response to dose conversion is estimated to be 1 per cent for the 4 MV photon reference beam. Supralinearity and sensitivity to high energy photons and electrons with respect to Co-60 are discussed elsewhere in these proceedings<sup>1</sup>.

Extended measurements on the dose response relationship (0.1 - 100 Gy) have indicated that the quadratic dose response function (3) is accurate over a dose

range of 0.1 - 70 Gy. Above 70 Gy the measure of supralinearity slightly decreases and equation (3) is not longer valid.

It should be realized that supralinearity is highly dependent on the annealing procedure. Formerly a rapid cooling down from the high temperature annealing to room temperature was applied for the 1KTU batch. Although this yielded a 25 % higher sensitivity, this procedure is not acceptable because the sensitivity altered by  $\pm 12$  % after subsequent annealings and the observed supralinearity ratios varied between 1.16 to 1.29, compared with  $1.21 \pm 0.01$  for the present annealing procedure (1.5 hours at 400°C, natural cooling in the oven to 80°C, followed by 80°C for 16 hours and subsequent natural cooling down to room temperature). After rapid cooling down also a slight decrease (several per cent) in sensitivity during a post anneal period of 1-2 months was observed. With the present annealing procedure the supralinearity ratio  $F_s$  remains stable after repeated annealing procedures. Changes of sensitivity in the post anneal period were never observed.

#### CONCLUSION

The use of LiF 700 powder has proven to be a reliable and accurate method for dosimetry in radiotherapy. Reliability is significantly influenced by the annealing procedure. The dose response relationship is supralinear. A correction for this phenomenon is required. The dose-response relationship is accurately described by a quadratic function over a 0.1 - 70 Gy dose range. The small volume of the LiF capsules and the accurate response to dose conversion over a broad dose range, makes the LiF powder also suitable for in vivo dose verification in single high dose treatments e.g. in brachytherapy.

#### REFERENCE

1. J.P.A. Marijnissen and B. Göbel, Supralinearity and dependence on energy of LiF 700 powder for photons and electrons., Proceedings TLD-symposium Bilthoven, The Netherlands, 1988.

EIGHTEEN MONTHS OF CLINICAL TLD-DOSIMETRY: EQUIPMENT, CALIBRATION- AND ANNEALING PROCEDURES, REPRODUCTIBILITY AND APPLICATIONS IN RADIOTHERAPY.

R. Van Loon, B. Schaeken, L. Coppens, M. Van Lancker and C. Goor

Departement Radiotherapie, Akademisch Ziekenhuis, Vrije Universiteit Brussel  
Laarbeeklaan 101, B-1090 Brussel, Belgium

INTRODUCTION

It is the aim of a radiotherapy session to deliver throughout the treatment volume the prescribed dose. All authorities agree on the fact that a precision better than 5% in the dose delivery is needed. This requires a quality assurance program verifying every step in the treatment procedure. One must be concerned about the calibration procedures of the treatment facility, the acquisition of the patient data, the correct setting of the parameters of the treatment unit, dose distribution calculation and finally direct measurement in situ of the dose delivered to the patient in treatment conditions.

The recent development of small and reliable semiconductor dosimeters announced a possible "in-vivo" use that could give a real time dose determination, avoiding the cumbersome read-out and anneal procedures of TLD's. However, recent experience [1] shows that multiple factors can increase the uncertainty on the dose determination with semiconductors. Consequently TLD remains a most valuable aid for the ultimate verification of the dose delivered to the patient.

The purpose of this study was to assess if a not specialized laboratory could obtain with commercial equipments a reproducible and accurate dose determination in both reference and clinical conditions.

MATERIALS AND METHODS.

1. Thermoluminescent dosimeters.

The dosimeters used are Mg and Ti doped  $^7\text{LiF}$  chips (4.5mm diameter, 0.8mm thick: Vinten 160-052).

The isotopic abundance of  $^7\text{Li}$  is better than 99.95% and the mean atomic number is 8.14. The chips investigated belonged to one single batch. The read-out peak luminescence is at  $\lambda_m = 400\text{nm}$ . Preliminary investigations also have been done on  $\text{Li}_2\text{B}_4\text{O}_7$  disks and  $^7\text{LiF}$  rods.

2. TLD-reader.

A Vinten TOLEDO 654D universal thermoluminescent dosimeter reader was used. The heating is by thermal contact of the dosimeter with a heating "finger". The temperature of the heating element is controlled to better than  $1^\circ\text{C}$  by means of a feed-back circuit. Pure nitrogen was flowed at  $500\text{ cm}^3/\text{min}$ . The reader is equipped with an automatic sample changer Vinten 233.

The heating cycles are fully programmable: preheat and anneal zones can be switched in and out, time and temperatures are freely adjustable, linear and "ramp-and-hold" heating cycles may be programmed and read zone heating rate and anneal zone cooling rate can be adjusted

Glow curve investigation of the  $^7\text{LiF}$  chips (160-052) resulted in the following optimal procedure. Preheat: 22s at  $120^\circ\text{C}$ ; reading cycle: total time 20s with a ramp of  $20^\circ\text{C}/\text{s}$  to a temperature of  $260^\circ\text{C}$ ; no anneal cycle (external annealing).

### 3. Annealing facility.

Since constant sensitivity of the thermoluminescent material requires a reproducible annealing cycle, it was decided to use an external programmable annealing facility (Vinten 622E). This facility allows two stage annealing up to 400°C with time settings between 0.1 and 99.9 hours.

The final settings for chips annealing are 1 h at 400°C followed by 16h at 80°C; no control is available for the cooling down to 80°C (natural cooling down).

### 4. Calibration facility.

The calibration is done in a 8 MV (nominal) photon beam of a linear accelerator (Philips SL75/20).

The chips are irradiated at maximum build-up in a compact polystyrene phantom. The dosimeters exactly fit in a grid of holes (spacing 1 cm) were. The polystyrene phantom is irradiated with a square field of side 20cm at a source phantom distance of 100cm. Field flatness was better than 1 %. Calibration was done against an ionization chamber (0.6 cm<sup>3</sup>, NE2571) with Farmer electrometer, at maximum build-up in water under identical irradiation conditions. Doses stated are obtained from the NPL calibration in exposure at Co<sup>60</sup> according to the HPA protocol [2].

### PROBLEMS ENCOUNTERED.

Three types of dosimeters have been investigated: lithiumfluoride rods of 1mm diameter (LiF700), Li<sub>2</sub>B<sub>4</sub>O<sub>7</sub> chips (Vinten 160-051) and <sup>7</sup>LiF chips (Vinten 160-052).

The rods have been eliminated after a few calibration cycles: deformation of the rods took place in the reader causing bad contact with the heater and resulting in bad reproducibility.

The reproducibility of the Li<sub>2</sub>B<sub>4</sub>O<sub>7</sub> chips was not as expected: a mean standard deviation of 6-7% was obtained for 5 readings of 20 chips (Fig. 1).

By recording glow curves systematically, it was noticed that the preheating and reading times had to be increased with respect to those recommended by Vinten. Light output for Li<sub>2</sub>B<sub>4</sub>O<sub>7</sub>:Mn was low, mainly due to the fact that the spectral peak of the glow curve is about 600nm (Li<sub>2</sub>B<sub>4</sub>O<sub>7</sub>:Mn) [3] whereas the quantum efficiency of the photomultiplier tube peaks at 400nm, better suited for LiF.

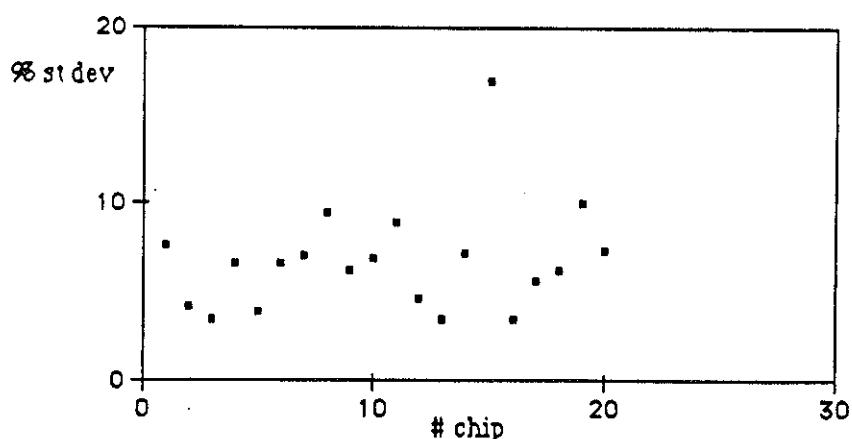


Fig. 1. Standard deviations of 20 lithiumborate chips - 5 readings.

Irradiation of LiF chips with a dose of 2.00Gy lead to a an unexpected result, when the Vinten prescribed anneal cycle (1h at 300°C, followed by 16h at 80°C, natural cooling to 80°C) [4] was used: a sensitivity

increase of about 10 % after each exposure (Fig.2). A constant sensitivity is obtained when annealing is done at 400°C

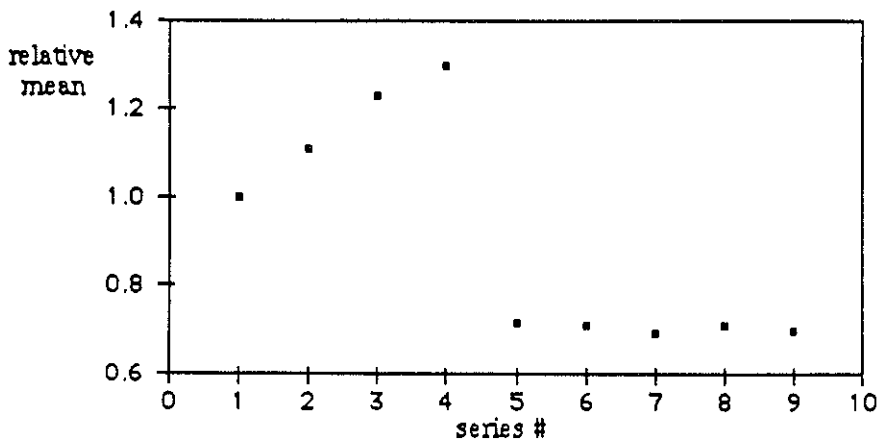


Fig. 2. Relative mean of read-out of 20 LiF chips irradiated with 2.16 Gy. Irradiation 1-4 was after annealing at 300°C, irradiations 5-9 after annealing at 400°C.

Some irregularities in reading were observed, due to a lack of contact between heating system and heating tray. After correction of the mechanism by Vinten, no problems were encountered with the heating system. It has to be mentioned that this problem can occur when different shapes of dosimeters are used. Positioning of the TLD-dosimeter in the center of the tray is critical for obtaining reproducible readings. With the automatic sampler changer it happens that the chip shifts towards the edge of the tray during transport, giving a lower reading. This has been prevented by using a tray with an inner ring. A new type of tray with a circular rim with an inner diameter equal to the chip diameter is under examination.

RESULTS (Physics)

Reproducibility.

A test of reproducibility was performed on the TLD-dosimeters Vinten 160-052, and the batch clearly separated in two categories: "good" ones with standard deviation of about 2% and others above the level of 5-6% (Fig. 3).

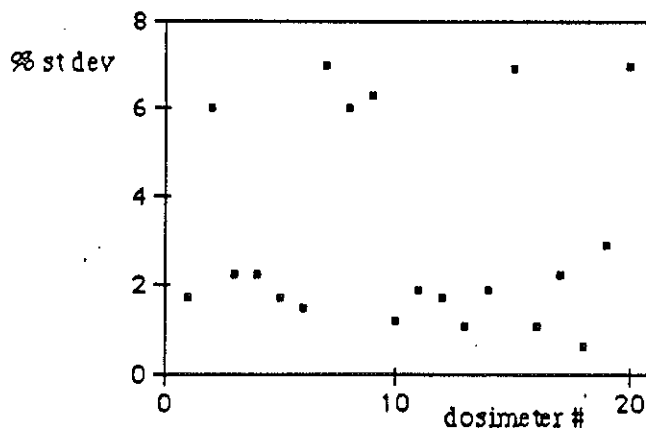


Fig. 3. Reproducibility test. Percentage standard deviation on 5 readings. Dose: 2 Gy. Separation into two distinct categories.



Read-Out efficiency.

A second read-out performed immediately after the normal read-out, gave second read-out values of 0.1 to 0.5% of the former.

Supralinearity.

After selection on reproducibility, we irradiated <sup>7</sup>LiF dosimeters with doses of 1,2,4,8, and 16 Gy. Sensitivity clearly increases with dose, and the departure from linearity is significant above 2Gy (Table 1. and Fig.4.).

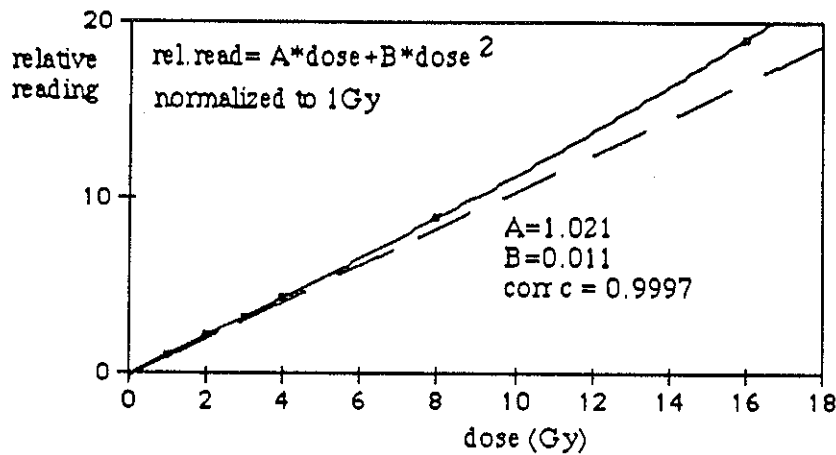


Fig. 4. Relative reading of <sup>7</sup>LiF dosimeters. Quadratic fit. Mean of 25 dosimeters, 3 readings.

Table 1. Relative readings in function of dose.

| dose (Gy) | relative reading |
|-----------|------------------|
| 1         | 1.000            |
| 2         | 2.075            |
| 3         | 3.211            |
| 4         | 4.234            |
| 8         | 8.848            |
| 16        | 19.071           |

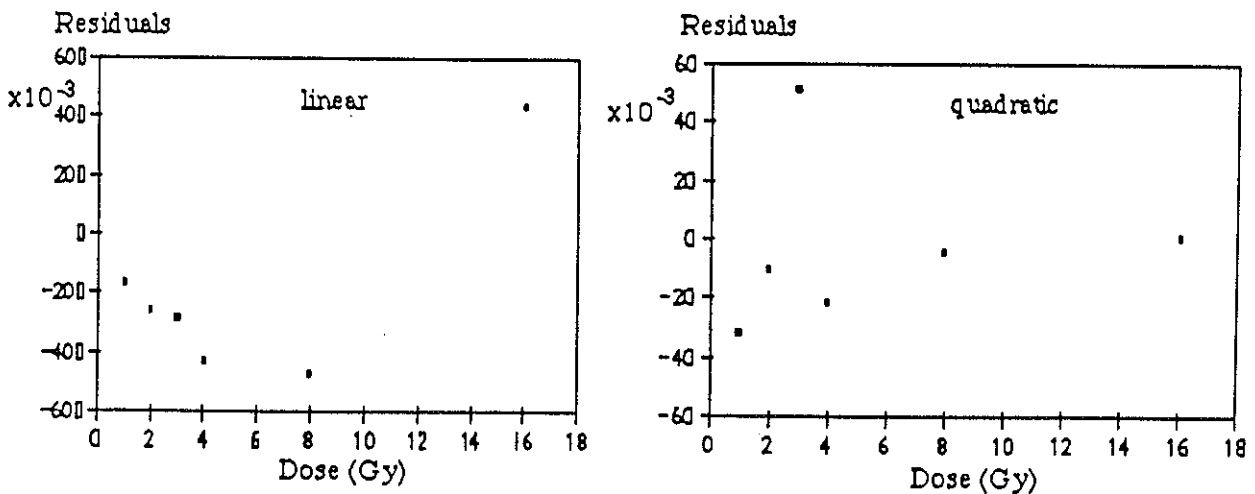


Fig.5. Plot of residuals after a linear and a quadratic fit, without constant. Doses from 1 up to 16 Gy.

The relative reading were fitted with a linear and a quadratic function (without constant) and a plot of the residuals (Fig.5.) shows a better representation with the latter, although errors in reproducibility of the individual chips will be of the same magnitude as the errors of the fit. But Table 1. clearly shows that a linear extrapolation towards high doses is not allowed.

Stability.

It is well known that TLD-dosimeters are very sensitive to the history of irradiation and annealing. One of the possible applications of TLD's is to accumulate the daily dose to a patient during 10 or 20 sessions. We investigated this possibility by irradiating <sup>7</sup>LiF dosimeters on 8 successive weekdays with a dose of 2.00Gy, and reading the dosimeter after the complete session. The results were again unpredictable: the dose expected was 16Gy, but the use of the calibration curve of Fig. 4. leads to a dose of 15.1Gy. Recalibration at 2Gy confirmed the change in sensitivity due to high dose irradiation (up to a total dose of 220Gy): sensitivity decreased to 0.849 of the initial value.

RESULTS (Clinical)

Most often TLD's are use in clinical routine for verification of treatment conditions. Following their small size, they can be positioned nearly everywhere.

Notwithstanding the increasing sophistication of treatment planning systems, situations remain wherein these machines cannot inform us. This is the case when values of treatment parameters are chosen outside the range were the calculation model is valid.

A flagrant example is irradiation at unusual focus-skin distances, e.g. for total body irradiation (500cm). During such treatments TLD's are fixed to the skin of the patient, at corresponding entrance and exit points (the entrance-TLD being covered with plexi till maximum build-up). Knowledge of the thickness of the patient between these points allows one to calculate the dose  $D_{mid}$  at midplane from the doses  $D_{ant}$  and  $D_{post}$  measured at entrance and exit <sup>5]</sup>. Correction factors C defined as  $C = 2 D_{mid} / (D_{ant} + D_{post})$  have been measured with an ionization chamber and TLD: agreement is better than 5% (Table 2).

Table 2. Correction factor  $C = 2 D_{mid} / (D_{ant} + D_{post})$  with TLD and with ionisation chamber.

| thickness(cm) | C[TLD] | C[ion] | C[TLD]/C[ion] |
|---------------|--------|--------|---------------|
| 5             | 1.024  | 1.024  | 1.000         |
| 9             | 1.043  | 1.037  | 1.006         |
| 13            | 1.092  | 1.041  | 1.050         |
| 17            | 1.044  | 1.038  | 1.006         |
| 21            | 1.078  | 1.028  | 1.049         |

It is often difficult in treatment planning systems to determine accurately the dose at points at shallow depths (<0.5cm). If superficial regions ( e.g. lymph nodes ) have to be treated, bolus thickness has to be chosen experimentally with TLD, to find a good compromise between lymph node dose and skin sparing. Repeated measurements on patients in treatment conditions (ENT tumors) indicated that a bolus thickness of .5 cm is ideal for most applications.

Example: two opposing lateral beams on the neck. Distance between entrance points is 12 cm.

FSD: 100 cm. Energy: 8 MV. Midline fraction size: 200 cGy.

| bolus thickness (cm) | "skin" doses (cGy)<br>(mean of 4 TLD) |
|----------------------|---------------------------------------|
| 0.0                  | 166                                   |
| 0.5                  | 203                                   |
| 1.0                  | 223                                   |

It appears clearly that the use of 1 cm bolus would overdose the skin by more than 10 %.

We use TLD dosimeters, in particular, for measurements of the dose on the eye, by fixing them on plastic eye-caps. If suitably protected against moisture, they can even be used in mouth and rectum (e.g. during intracavitary applications).

### CONCLUSIONS.

We succeeded in the control of main physical parameters to use the LiF chips with a reproducibility of the order of 2%, sufficient for clinical applications. Their use is appreciated by the physicians. However a drawback is still the time consuming read-out procedure. We work presently on the automatization of the acquisition of glow curves and readings.

### ACKNOWLEDGMENTS.

We thank Mr. G. Catto from Vinten for the assistance during the set-up period.

<sup>1</sup> A. Noel, P. Aletti, B. Romary, Contrôle de qualité des diodes avant leur mise en service, Recueil des Communications, SFPH XXVIe Congrès Virtel, Juin 1987.

<sup>2</sup> HPA protocol, Phys. Med. Biol. 28, 1097 (1983).

<sup>3</sup> G. Portal, "Présentation de matériaux R.T.L.", dans La Dosimétrie par Thermoluminescence, Enseignement Postuniversitaire, Soc. Franç. Ohyus. d'Hôpital, Rennes, avril 1986, p. 72.

<sup>4</sup> Vinten Instrumentation Systems, Dosimeter material information no 5.

<sup>5</sup> S. Naudy, "Etude de la dosimétrie par thermoluminescence et des jonctions a semiconducteurs: application a la dosimetrie des irradiations du corps entier en vue de greffe de moelle osseuse", Thèse, Toulouse 1981.

LIST OF PARTICIPANTS

A.H.L. Aalbers  
RVM/LSO  
Postbus 1  
3720 BA Bilthoven

S.Y. Acram  
Neth. Institute for Radiation Techn.  
Postbus 1359  
1000 BS Amsterdam

W.J. Altena  
Hoogovens IJmuiden B.V.  
Postbus 10.000  
1970 CA IJmuiden

H. Baan  
Urenco Ned.Op. B.V.  
Drienemansweg 1  
7601 PZ Almelo

L.J. Battum  
Rotterdamsch Radiotherapeutisch  
Instituut  
Groene Hilledijk 301  
3075 EA Rotterdam

H. Boersma  
Acad. Centrum Tandheelkunde  
Amsterdam V.U.  
Louwesweg 1  
1066 AE Amsterdam

F.A.I. Busscher  
Radiologische Dienst TNO  
Postbus 9034  
6800 ES Arnhem

L. Coppens  
Vrije Universiteit Acad. Ziekenhuis  
Laarbeeklaan 101  
B-1090 Brussel/België

J.P. Deworm  
Inst. Studiecentrum voor Kernenergie  
Boeretang 200  
2400 Mol/België

R. van Dongen  
Rijksinstituut voor de  
Volksgezondheid en Milieuhygiëne  
Postbus 1  
3720 BA Bilthoven

W. Dries  
Catharina Ziekenhuis  
Michelangelolaan 2  
5602 ZA Eindhoven

R. van Aalst  
Centr. Lab. Bloedtransfusiedienst  
Plesmanlaan 125  
1066 CX Amsterdam

J.J.H. Alderhout  
Landbouw Universiteit  
Diedenweg 18  
6703 GW Wageningen

J.C. van der Baan  
Mallinckrodt Diagnostica B.V.  
Westerduinweg 3  
1755 ZG Petten

D. Bakker  
Catharina Ziekenhuis  
5602 ZA Eindhoven

H.W.J. Bierhuizen  
Dr. Bernard Verbeeten Instituut  
Brugstraat 10  
5042 SB Tilburg

A.J.J. Bos  
Interfacultair Reactor Instituut  
Mekelweg 15  
2629 JB Delft

G. Catto  
Vinten Instruments Ltd.  
Jessamy Road/Weybridge  
Surrey KT 13 8LE/U.K.

J. van Dam  
Universitair Ziekenhuis St. Rafaël  
Capucijnenvoer 35  
3000 Leuven/België

J.B. Dielhof  
Interfacultair Reactor Instituut  
Mekelweg 15  
2629 JB Delft

F.E. van Doorne  
Intechmij B.V.  
Postbus 187  
1110 AD Diemen

J.H. Duijsings  
Stralingsbeschermingsdienst Univer-  
siteit van Nijmegen  
Toernooiveld 1  
6525 ED Nijmegen

J.W. Edel  
Hoechst Holland N.V.  
Postbus 65  
4380 AB Vlissingen

A.J.M. Gerritsen  
Academisch Ziekenhuis  
Postbus 9600  
2300 RC Leiden

B. Göbel  
Rotterdamsch Radiotherapeutisch Inst.  
Groene Hilledijk 301  
3075 EA Rotterdam

J.T.G.M. Hemelaar  
Stralingsbeschermingsdienst  
Technische Universiteit Eindhoven  
Postbus 513  
5600 MB Eindhoven

M.S. Henkelman  
Rotterdamsch Radiotherapeutisch Inst.  
Groene Hilledijk 301  
3075 EA Rotterdam

S. Heukelom  
Antonie van Leeuwenhoekhuis  
Plesmanlaan 121  
1066 CX Amsterdam

P.J. van der Jagt  
Dienst Veiligheid en Milieu V.U.  
Postbus 7161  
1007 MC Amsterdam

R.G.C. Janssen  
Röntgen Technische Dienst B.V.  
Delftweg 144  
3046 NC Rotterdam

L.S. Jonker  
Ziekenhuis Leyenburg, MEO Fysica  
Leyweg 275  
2545 CH 's-Gravenhage

H.W. Julius  
Radiologische Dienst TNO  
Postbus 9034  
6800 ES Arnhem

A.S. Keverling Buisman  
Energie Centrum Nederland  
Postbus 1  
1755 ZG Petten

S.J. Feenstra  
RIF  
Borniastraat 4a  
8934 AD Leeuwarden

P.H. van der Giessen  
Dr. Bernard Verbeeten Instituut  
Burgstraat 10  
5042 SB Tilburg

Mw. N. de Haan  
Dienst Veiligheid en Milieu V.U.  
Postbus 7161  
1007 MC Amsterdam

D. Hengst  
Academisch Medisch Centrum  
Meibergdreef 9  
1105 AZ Amsterdam

J. Hermans  
Acad. Ziekenhuis St. Jan  
Rudtushove 10  
8000 Brugge/België

Mw. W.A. Hummel  
Radiobiologisch Instituut TNO  
Lange Kleiweg 151  
2288 GJ Rijswijk

J. Jans  
Mallinckrodt Diagnostica B.V.  
Westerduinweg 3  
1755 ZG Petten

T. Janssen  
Arnhems Radiotherapeutisch Instituut  
Wagnerlaan 55  
6815 AD Arnhem

R.A. Jonkers  
Röntgen Technische Dienst B.V.  
Delftweg 44  
3046 NC Rotterdam

G.J. Kemerink  
Radiodiagnostiek/Nucl. Geneesk. AZM  
Postbus 1918  
6201 BX Maastricht

P.J.H. Kicken  
Technische Universiteit Eindhoven  
Postbus 513  
5600 MB Eindhoven

E.W. de Kler  
Intertechmij B.V.  
Postbus 187  
1110 AD Diemen

J.G. Koomen  
PZEM Kerncentrale Borssele  
Poelendaelesingel 10  
4330 AA Middelburg

P. de Lange  
Nederlands Kanker Instituut  
Plesmanlaan 121  
1066 CX Amsterdam

H.P. Leenhouts  
Rijksinstituut voor de Volks-  
gezondheid en Milieuhygiëne/LSO  
Postbus 1  
3720 BA Bilthoven

J.A.G. Lemmens  
Landré & Glinderman GmbH  
Elsenheimerstrasse 4a  
8000 München/B.R.D.

J. Lindeijer  
Mallinckrodt Diagnostica B.V.  
Westerduinweg 3  
1755 ZG Petten

A.C. Loman  
Rijksinstituut voor de  
Volksgezondheid en Miliehygiëne/LSO  
Postbus 1  
3720 BA Bilthoven

P.W.F. Louwrier  
NIKHEF-K  
Postbus 4395  
1009 AJ Amsterdam

Mw. J. Maat  
Arnhems Radiotherapeutisch Instituut  
Wagnerlaan 55  
6815 AD Arnhem

J.P.A. Marijnissen  
Dr. Daniël den Hoed Kliniek  
Groene Hilledijk 301  
3075 EA Rotterdam

P. Mourik  
Directie Materieel  
Koninklijke Luchtmacht  
Postbus 20703  
2500 ES Den Haag

C. Koedooder  
A.M.C., afd. Radiotherapie  
Meibergdreef 9  
1105 AZ Amsterdam

L.L. Kossakowski  
Groot Ziekengasthuis  
Postbus 90153  
5200 ME 's-Hertogenbosch

H. Lanson  
Antonie van Leeuwenhoekhuis  
Plesmanlaan 121  
1066 CX Amsterdam

A. de Leeuw  
Universiteit van Nijmegen  
Stralingsbeschermingsdienst  
Toernooiveld 1  
6525 ED Nijmegen

C.J. Leurs  
PZEM  
Poelendaelesingel 10  
4335 JA Middelburg

V. Lippens  
Kerncentrale Doel  
Scheldemolenstraat  
2791 Beveren Doel/België

R.E. van Loon  
Vrije Universiteit Acad.Ziekenhuis  
Laarbeeklaan 10  
B-1090 Brussel/België

J.H.W. Maasen  
Bedrijfs-geneeskundige Dienst R.U.  
Boerhaavelaan 3a  
2334 EB Leiden

L. Maes  
Inst.Studiecentrum voor Kernenergie  
Boeretang 200  
2400 Mol/België

L.H. van Mierlo  
Kerncentrale Dodewaard  
Waalbandijk 112a  
6669 MG Dodewaard

H. Nieuwenhuyse  
Organon International B.V.  
Postbus 20  
5340 BH Oss

G.W. Oplaat  
Philips Ned. B.V.  
Groep Ziekenhuizen VB2-15  
Boschdijk 525

J. Reitsma  
Universiteit Twente  
Postbus 217  
7500 AE Enschede

L.M.M. Rodenrijs  
Röntgenafd. Reinier de Graaf  
Gasthuis Delft  
privé: Kaag 5  
2636 CV Schipluiden

Mw. A. Roos  
Biochemisch Laboratorium R.U.  
Wassenaarseweg 64  
2333 AL Leiden

H.J. Serdijn  
Medisch Centrum Alkmaar  
Wilhelminalaan 12  
1815 JD Alkmaar

F.M. Sijtsma  
R.U. Utrecht (BGZ)  
Heidelberglaan 8  
3584 CS Utrecht

M. Steggerda  
Antonie van Leeuwenhoekhuis  
Plesmanlaan 121  
1066 CX Amsterdam

T. Tee  
Academisch Medisch Centrum  
Meibergdreef 9  
1105 AZ Amsterdam

L.P.M. van Velzen  
N.V. KEMA  
Postbus 9035  
6800 ET Arnhem

J.L.M. Venselaar  
Dr. Bernard Verbeeten Instituut  
Brugstraat 10  
5042 SB Tilburg

A.M.T.I. Vermeulen  
Directoraat Generaal van de  
Arbeid, afd Stralingshygiëne  
Balen van Andelplein 2  
2273 KH Voorburg

H. Pauw  
Philips/Arbeidsbescherming ECY-4  
Willemstraat 22a  
5600 MD Eindhoven

A.H.J. Renders  
Groot Ziekengasthuis afd. Nucl. Gen.  
Postbus 90153  
5200 ME 's-Hertogenbosch

L. Rombouts  
Kerncentrale Doel  
Scheldemolenstraat  
2791 Beveren Doel/België

P. Schonken  
K.U. Leuven  
Haelwijnlaan 12  
3060 Bertum/België

A.V. Siemelink  
R.B.B. vestiging Acad. Ziekenhuis  
Catharijnesingel 101  
3500 CG Utrecht

J. van der Steen  
KEMA  
Postbus 9035  
6800 ET Arnhem

P.F. van der Stelt  
ACTA, Afd. Tandheelkundige Radiologie  
Louwesweg 1  
1066 EA Amsterdam

Mw. X.L. Velders  
ACTA, Afd. Tandheelkundige Radiologie  
Louwesweg 1  
1066 EA Amsterdam

H.W. Venema  
Lab. Medische Fysica/Afd. Radiodiagnostiek AMC  
Meibergdreef 15  
1105 AZ Amsterdam

C.W. Verhoef  
Radiologische Dienst TNO  
Postbus 9034  
6800 ES Arnhem

H.H.A. Vis  
Intechmij B.V.  
Postbus 187  
1110 AD Diemen

R. Viveen  
Dr. Daniël den Hoed Kliniek  
Postbus 5201  
3008 AE Rotterdam

L. van Vliet  
Directoraat Generaal van de Arbeid/  
Arbeidsgezondheidskunde  
Postbus 69  
2270 MA Voorburg

H.M.L. van Voorst  
Universiteit van Amsterdam  
Mignonpad 9  
3816 ES Amersfoort

R.J. de Vos  
R.T.I.L.  
Henri Dunantstraat 5  
6419 PC Heerlen

W. de Vries  
Interfacultair Reactor Instituut  
Mekelweg 15  
2629 JB Delft

S. Vynckier  
Clinique Universitaire St. Luc  
Avenue Hippocrate 10  
1200 Brussel/België

Mw. G.A. v.d. Wagt  
Erasmus Universiteit (SBD EE100)  
Postbus 1738  
3000 DR Rotterdam

C. de Wagter  
Kliniek Radiotherapie en Kerne-  
De Pintelaan 185  
B-9000 Gent/België

J. Wallart  
Organon International B.V./SBD  
Postbus 20  
5340 BH Oss

J. Weeda  
IRS - J.A. Cohen Instituut  
Rijnsburgerweg 86  
2333 AD Leiden

C.F. Westerman  
Westeinde Ziekenhuis  
Postbus 432  
2501 CK Den Haag

K.M. Wimmers  
Min. van Defensie/DMGD  
Rozeveldlaan 53  
2241 NS Wassenaar

J.G.J. van Winsen  
SZW, DGA, afd. Stralingshygiëne  
Postbus 69  
2270 MB Voorburg

N.P.J. de Wit  
Radiobiologisch Instituut TNO  
Lange Kleiweg 151  
2288 GJ Rijswijk

C. Wittenbernds  
Nederlandse Philips Bedrijven  
Willemstraat 22a, gebouw ECY-1  
5600 MD Eindhoven

E.L.M.J. van Wonderen  
N.V. KEMA  
Postbus 9035  
6800 ET Arnhem

J. Zoetelief  
Radiobiologisch Instituut TNO  
Postbus 5815  
2280 HV Rijswijk



## Technical Exhibitors

Canberra Positronika B.V.  
De heer J. Kasten  
Postbus 1145  
5602 BC Eindhoven

Veenstra Instrumenten  
De heer T. IJbema  
Schaapstreek 5  
9463 PE Eext  
tel.: 05926-1203

Pechiney World Trade  
De heer W. Broekman  
Postbus 7917  
1008 AC Amsterdam

Intequip Nucleair B.V.  
Ing. J.G. Hagelen  
Amstelveenseweg 145  
1075 VZ Amsterdam

Intechmij B.V.  
De heer H.H.A. Vis  
Postbus 187  
1110 AD Diemen  
tel.: 020-5696611

**Index of authors**

|                          |                |
|--------------------------|----------------|
| Aalbers, A.H.L.          | 71             |
| Bader, F.J.M.            | 71             |
| Bakker, D.               | 101            |
| Bos, A.J.J.              | 5, 31, 43, 121 |
| Broerse, J.J.            | 121            |
| Busscher, F.             | 51             |
| Coppens, L.              | 135            |
| Crommelin, M.A.          | 101            |
| Dam, J.,                 | 95             |
| Dielhof, J.B.            | 31, 43, 121    |
| Dries, W.J.F.            | 101            |
| Göbel, B.                | 25, 129        |
| Goor, C.                 | 135            |
| Hemelaar, J.T.G.M.       | 79             |
| Hocini, B.               | 115            |
| Hoogenboom, J.E.         | 31             |
| Huyskens, Chr.           | 79             |
| Julius, H.W.             | 51             |
| Keverling Buisman, A.S.  | 65             |
| Kicken, P.J.H.           | 79             |
| Kuile C.R. ter.          | 71             |
| Lancker, M. Van          | 135            |
| Loon, R. van             | 135            |
| Lunenburg, A.P.P.A. van. | 71             |
| Marijnissen, J.P.A.      | 25, 129        |
| Mijnheer, B.J.           | 17             |
| Pauw, H.                 | 61             |
| Preston, H.              | 37             |
| Rijnders, A.             | 95             |
| Schaeken, B.             | 135            |
| Velzen, L.P.M.           | 85             |
| Verhoef, C.W.            | 51             |
| Vries, W. de.            | 31             |
| Vynckier, S.             | 115            |
| Wambersie, A.            | 115            |
| Weeda, J.                | 17             |
| Wit, N.J.P. de           | 109            |
| Wittenbernds, C.J.H.     | 51             |
| Zoetelief, J.            | 109, 121       |

